12-2010

Nonlinear Model Predictive Control and Dynamic Real Time Optimization for Large-scale Processes

Rui Huang
Carnegie Mellon University

Nonlinear Model Predictive Control and Dynamic Real Time Optimization for Large-scale Processes

Submitted in partial fulfillment of the requirements for

for the degree of

Doctor of Philosophy

in

Chemical Engineering

Rui Huang

B.S., Control Science and Engineering, Zhejiang University

M.S., Control Science and Engineering, Zhejiang University

Carnegie Mellon University

Pittsburgh, PA

December, 2010

Acknowledgments

I am extremely blessed by the opportunities that allow me to finish my PhD study and write this dissertation. I consider myself very fortunate to work with Prof. Lorenz T. Biegler. I would like to thank him for his patience and guidance not just in research but also in general which helped me to be where I am today. His enthusiasm, devotion, vast knowledge and ability to focus on the fundamental problems set up a great role model for me. I am also in debt to Prof. Sachin Patwardhan from the Department of Chemical Engineering in IIT Bombay, with whom I coauthored several research articles and had many intriguing discussions on model predictive control and state estimation. I would also like to express my gratitude to Prof. Ignacio Grossmann, Prof. Nikolaos Sahinidis, Prof. Erik Ydstie and all the faculty and staff in the Department of Chemical Engineering at Carnegie Mellon University for their support during my study.

My thanks go to the National Energy Technology Laboratory (NETL) for the financial support of my PhD work. My committee members Prof. Biegler, Prof. Ydstie, Prof. Sahinidis and Prof. Messner deserve my special thanks for their advices and suggestions. I would also like to thank the entire Biegler group for the positive working environment. I specifically thank Dr. Carl Laird and Dr. Victor Zavala for enlightening conversations on interior point methods and advanced step algorithm.

I could not be where I am now without the unconditional love, support and encouragement from my father and mother. Juan has been there for me in the most difficult time and made my journey in the past six years enjoyable. My gratitude to them is undescribable.

Abstract

This dissertation addresses some of the theoretical and practical issues in optimized operations in the process industry. The current state-of-art is to decompose the optimization into the so-called two-layered structure, including real time optimization (RTO) and advanced control. Due to model discrepancy and inconsistent time scales in different layers, this structure may render suboptimal solutions. Therefore, the dynamic real time optimization (D-RTO) or economically-oriented nonlinear model predictive control (NMPC) that directly optimizes the economic performance based on first-principle dynamic models of processes has become an emerging technology. However, the integration of the first-principle dynamic models is likely to introduce large scale optimization problems, which need to be solved online. The associated computational delay may be cumbersome for the online applications.

We first derive a first-principle dynamic model for an industrial air separation unit (ASU). The recently developed advanced step method is used to solve both set-point tracking and economically-oriented NMPC online. It shows that set-point tracking NMPC based on the first-principle model has superior performance against that with linear data-driven model. In addition, the economically-oriented NMPC generates around 6% cost reduction compared to set-point tracking NMPC. Moreover the advanced step method reduces the online computational delay by two orders of magnitude.

Then we deal with a realistic set-point tracking control scenario that requires achieving offset-free behavior in the presence of plant-model mismatch. Moreover, a state estimator is used to reconstruct the plant states from outputs. We propose two formulations using

NMPC and moving horizon estimation (MHE) and we show both approaches are offset-free at steady state. Moreover, the analysis can be extended to NMPC coupled with other nonlinear observers. This strategy is implemented on the ASU process.

After that, we study the robust stability of output-feedback NMPC in the presence of plant-model mismatch. The Extended Kalman Filter (EKF), which is a widely-used technology in industry is chosen as the state estimator. First we analyze the stability of the estimation error and a separation-principle-like result indicates that the stability result is the same as the closed-loop case. We further study the impact of this estimation error on the robust stability of the NMPC.

Finally, nominal stability is analyzed for the D-RTO, i.e. economically-oriented NMPC, for cyclic processes. Moreover, two economically-oriented NMPC formulations with guaranteed nominal stability are proposed. They ensure the system converges to the optimal cyclic steady state.

Contents

List of Figures

Chapter 1

Introduction

In this chapter, we present the overall context and objectives of the research problem in this dissertation. The current challenges in optimized operation in the process industry are addressed by the so-called hierarchical sctructure. Special focus is given to dynamic real-time optimization or economically-oriented nonlinear model predictive control. Finally background information and terminology used in this dissertation are introduced.

1.1 Current Practices in Hierarchical Operation

The operation of a chemical process involves a large number of decisions which are normally distributed into the so-called hierarchy planning and operations structure as shown in Fig. 1.1. This structure has been summarized in many text books [75, 73]. The planning layer focuses on economic forecast and providing production goals. It addresses questions like what products to make, which feed-stocks to buy and how much to produce and to buy, respectively. It predicts the economical disturbance such as product demands and prices of feed-stocks to optimize the future policy of production. The time horizon in the planning layer is rather long, typically in months or weeks. Scheduling addresses the timing of actions and events necessary to execute the chosen plan. It answers the questions like how to arrange the manufacturing sequence and when to start a certain process. The major focus here is the feasibility of the operation. The time span in the scheduling is typically

in weeks or days. In addition, the planning and scheduling entities also provide parameters of the cost functions (for example prices of products, raw materials, energy costs) and constraints (for example amount of raw material, production time). Currently, the planning and scheduling calculations are obtained systematically using various mixed integer programming formulations [16]. To avoid computational complexity, this layer treats the process as a black-box model by using rough estimates of its operation.

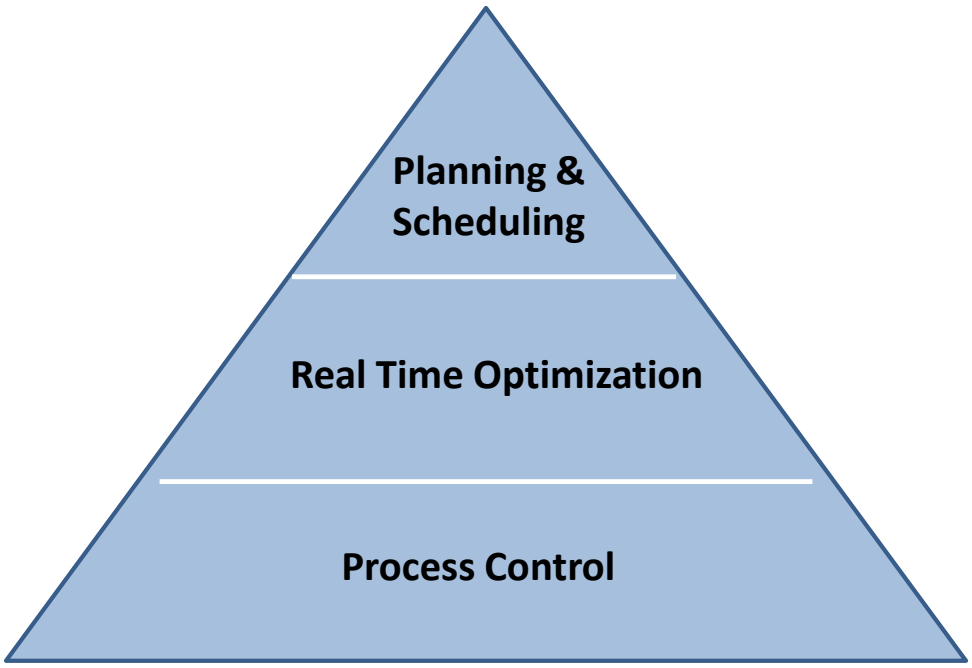

Figure 1.1: Illustration of the hierarchical operation.

These business decisions are communicated to the two-layered process operation level consisting of real-time optimization (RTO) and advanced control. This two-layered structure is illustrated in Fig. 1.2. RTO is concerned with implementing business decisions and production schedules in real time based on a first-principle steady state model of the plant. It optimizes the profit of the plant and seeks additional profit based on real-time data reconciliation and parameter estimation. The reconciled plant data are used to compute a new

set of model parameters so that the model represents the plant as accurately as possible at the current operating point. Then the set-point is progressively refined using the new model parameters to optimize an economic cost function while satisfying the constraints. Since the optimization is performed online, RTO provides a mechanism to react to changes and reject long term (days or hours) disturbances. RTO is normally solved using Nonlinear Programming (NLP). With advances in computer power and NLP algorithm, current RTO technology can solve problems with 1 million variables and generate multi-million dollar annual profits [14]. Nevertheless, RTO does not manipulate any dynamic degrees of freedom in the process. It assumes that the lower-level advanced controller is able to adjust the inputs to keep the process at the desired set-points at all times.

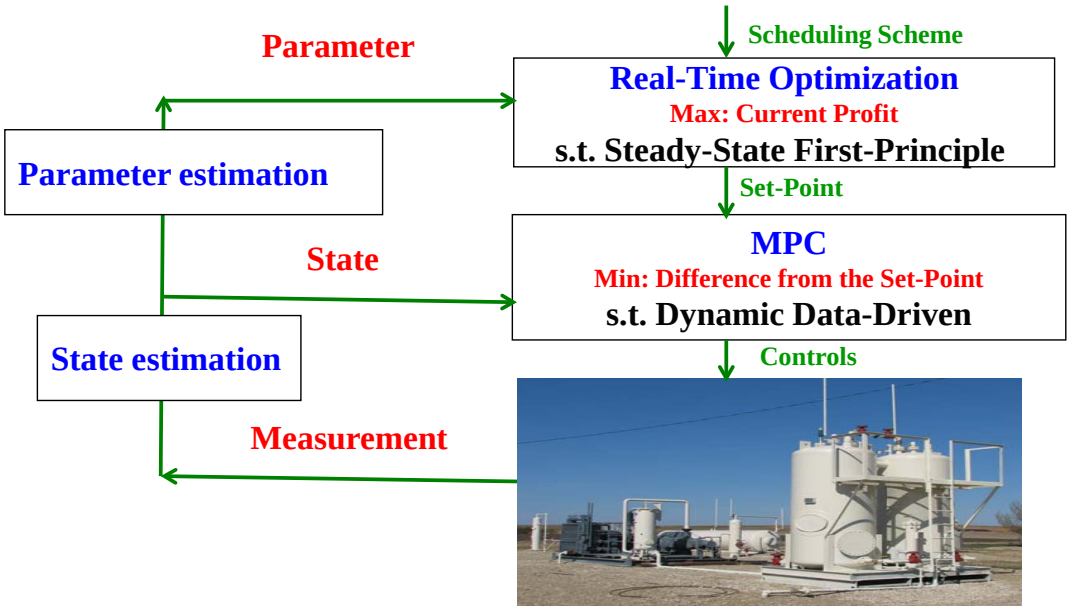

Figure 1.2: Illustration of RTO and advanced control structure.

These set-points are filtered by a supervisory system that usually includes the plant operators; and forwarded to the advanced control layer. Up to the 1970s, the dominating industrial practice was to use PID controllers. The PID controller is able to keep its out-

put at the desired set-point and reject short-term disturbances. However, it is difficult to tune and decouple the PID controller for multi-input-multi-output (MIMO) systems. The current dominant practice in the process industry is to use model predictive control (MPC) [89, 82] as the advanced controller. It uses a dynamic model of the process to predict the future dynamic behavior over a time horizon (hours or minutes). Therefore, it is possible to compute the optimal control actions to minimize transition time and the deviation of the output from the target. It is termed as set-point tracking MPC in this dissertation. The main advantages of the set-point tracking MPC are that it handles MIMO system naturally using model prediction and it is able to impose constraints. In addition, since MPC is based on the feedback idea, state estimation which reconstructs the plant state from the output is necessary for the implementation of MPC.

Currently, most set-point tracking MPC controllers still use dynamic input-output data-driven models identified from process step responses. This leads to a crucial limitation that the set-points calculated from RTO are often inconsistent and unreachable when viewed from the dynamic layer. This is because of the discrepancies between the models used for steady-state optimization and dynamic regulation. It has been pointed out by many researchers [33, 102] that the models in different layers are inconsistent. In particular, the steady-state gains are different. In addition, RTO does not fully utilize the degrees of freedom in the dynamic layer which may yield suboptimal set-point. The two layers have different time scales so that the optimization in RTO layer is inevitably delayed [27]. Moreover, if the process is operated over a wide range of conditions, a fixed model identified at a steady-state is usually not sufficient to have the predictability to cover the operating range.

Recently, nonlinear model predictive control (NMPC), which is based on the first-principle dynamic model of a process, has been applied widely and generated many economic benefits, especially for processes with frequent transitions [8]. However, it also brings important

computational issues. The data-driven dynamic models are usually manageable computationally since they are posed in a relatively small state space, while the first-principle dynamic models usually involve differential algebraic equations (DAE) that describe the momentum of processes. It has been shown that the computational complexity associated with online solving the DAE-constraint optimization problems may deteriorate the performance or destroy the stability of NMPC [35, 100].

On the other hand, the process dynamics controlled by the set-point tracking (N)MPC do not have the economical information in the objective function as in the conventional two-layered structure. Hence it may not be economically optimal for the controller to minimize the transition time in some cases [93].

1.2 D-RTO or Economically-Oriented NMPC

Motivated by these observations, the concept of a dynamic real time optimization (D-RTO) is introduced [40, 58]. This strategy is illustrated in Fig. 1.3. Instead of decomposing the optimization into steady state optimization and dynamic regulation, D-RTO directly optimizes the economical performance of a process over a prediction horizon and calculates the control actions. This formulation is essentially solving an NMPC problem with an economically-oriented objective function based on first-principle dynamic models. It is termed economically-oriented NMPC throughout this dissertation. Here the economical objective is translated into process control objectives, which is the goal of a control structure synthesis first stated by Morari et al. [83]. As a result, the two-layered structure is merged into a centralized decision-making and control layer. Therefore the problems associated with the two-layered operation structure discussed in Section 1.1 disappear.

In the last few years, many researchers have contributed to refine the D-RTO or economically-

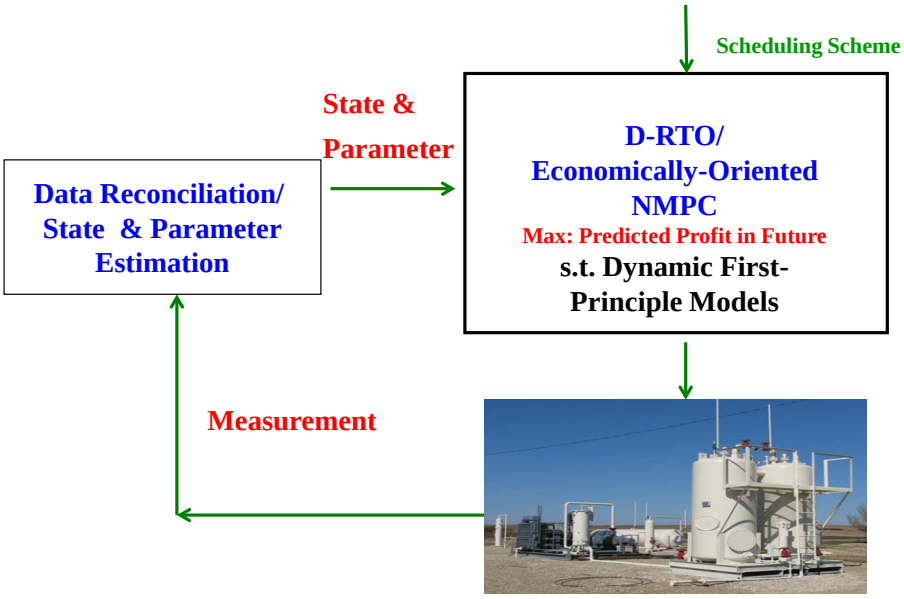

Figure 1.3: Illustration of D-RTO or Economically-Oriented NMPC.

oriented NMPC formulations to improve the economical performance. Zanin et al. [113] proposed a formulation and solution strategy and implemented them on a fluidized bed catalytic cracker. Adetola and Guay [1] proposed an MPC design approach that integrates RTO and MPC together. Angeli and Rawlings [4] proposed a receding horizon controller to optimize constrained nonlinear plants. Würth et al. [111] proposed an infinite-horizon formulation for economically-oriented NMPC. Moreover, Krstić and Wang [64] addressed the closed-loop stability of the general extremum seeking approach with economic performance. Diehl et al. [30] also analyzed the nominal stability property of a general economically-oriented NMPC formulation assuming strong duality.

1.3 Research Problem Statement

Although both the current state-of-art two-layered structure (shown in Fig. 1.2) and the emerging centralized D-RTO or economically-oriented NMPC (shown in Fig. 1.3) have been heavily studied in the literature, there are still many open issues. In particular theoretical questions like stability and offset-free properties need to be addressed. Moreover, the usage of first-principle dynamic models introduces computational complexity associated with the optimization which may be cumbersome for online applications.

The objective of this dissertation is to identify some of the theoretical issues related to both operation schemes, and propose strategies to improve their performance. Moreover, the recently developed advanced step algorithm [115] is incorporated into proposed strategies to reduce the online computational delay. The specific tasks we focus on are set-point tracking NMPC in the two-layered structure, state and parameter estimation and centralized economically-oriented NMPC or D-RTO formulations.

1.4 Thesis Outline

This dissertation is organized as the following.

Chapter 2 presents NMPC formulations, notations and basic definitions and serves as a literature review for the following chapters.

Chapter 3 discusses the solution strategies for DAE-constrained dynamic optimization problems. A simultaneous method, orthogonal collocation on finite elements, is used in this dissertation, which will convert the optimization problem to a large scale Nonlinear Programming (NLP). IPOPT algorithm is used to solve this NLP. Moreover, two moving-horizon-based applications, NMPC and moving horizon estimation (MHE) are introduced

and the sensitivity-based advanced step algorithm is formulated for both the NMPC (asNMPC) and MHE (asMHE) to reduce the online computational delay.

Chapter 4 presents simulation studies using the asNMPC to control a large scale air separation unit. Both set-point tracking NMPC and economically-oriented NMPC are used. For the economically-oriented NMPC controller, a moving-horizon-based ARIMA modeling strategy is proposed to forecast the future real-time price information from a utility company. Moreover, multi-scenario formulation is introduced to deal with uncertainties in electricity price information. In all the simulations, advanced step algorithm is used to reduce the online computational delay.

Chapter 5 deals with more realistic control scenarios where the plant state is not fully measured and critical control performances need to be retained in the presence of plant-model mismatch. Two formulations such as state-output disturbance and parameter estimation based on MHE are proposed. Both of them can be shown to yield offset-free behavior.

Chapter 6 studies the robust stability of the set-point tracking NMPC with an observer in the presence of plant-model mismatch. The Extended Kalman Filter (EKF) is chosen as the observer due to its popularity in industry. Given observability, we analyze the dynamic behavior of the estimation error, and we further show the impact of this error on the robust stability property of NMPC.

Chapter 7 demonstrates the nominal stability of the economically-oriented NMPC or D-RTO, based on the assumption that all the states are measured. Since the commonly used Lyapunov framework to analyze the stability can not be applied directly to the economically-oriented NMPC, we introduce a transformed system for which a Lyapunov function is easy to find. Moreover, two formulations of economically-oriented NMPC with guaranteed nominal stability are proposed.

Chapter 8 concludes the dissertation and presents recommendations for future work.

Chapter 2

Literature Review

In this chapter, we introduce the MPC problem formulation and review previous work that appears in the literature. In particular, we focus on real time NMPC strategies, stability of set-point tracking NMPC and economically-oriented NMPC. Moreover, some notations used in this dissertation are defined.

2.1 MPC Problem Formulation

We consider a general discrete time nonlinear system as the plant

$$x_{k+1} = f(x_k, u_k),\ x_k \in \mathbb{X},\ u_k \in \mathbb{U}, \tag{2.1}$$

where $x_k \in \mathbb{R}^{n_x}$ and $u_k \in \mathbb{R}^{n_u}$ are the plant state and control action at time step k.

Given the the plant model (2.1), a general MPC formulation can be described as the following

$$\begin{aligned} & \min && \sum_{i=0}^{N-1} l(z_i, v_i) \\ \text{s.t} \quad & z_{i+1} &=& \bar{f}(z_i, v_i), \quad i = 0, \ldots, N-1 \\ & z_0 &=& x_k, \\ & z_i &\in& \mathbb{X},\ v_i \in \mathbb{U} \end{aligned} \tag{2.2}$$

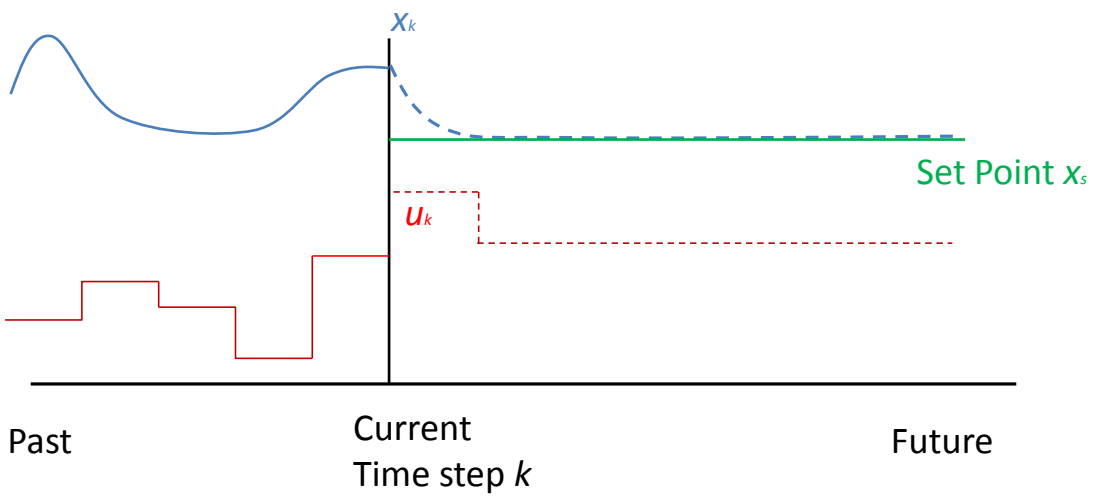

Figure 2.1: Illustration of Model Predictive Control.

where N is the horizon length, x_k is the initial condition which is the plant state at time step k. To differentiate from the actual plant state x and control u, we use z and v as the predicted state and control in the MPC formulation. $\bar{f}(\cdot,\cdot)$ is the model equation representing the plant (2.1), which is usually a linear function $(Az_i + Bv_i)$ in industrial MPC applications. $l(\cdot,\cdot)$ is the objective function. For the set-point tracking NMPC, $l(\cdot,\cdot)$ is a quadratic term $(|z_i - x_s|^2)$ that minimizes the difference between the predicted state and the set-point.

The MPC controller is implemented in a moving horizon framework as shown in Fig. 2.1. At current time step k, the plant state x_k is used as the initial condition and the optimization problem (2.2) is solved on a horizon N. However, only the first calculated control action is implemented, i.e. $u_k = v_0$. At the next time step $k+1$, we move the time frame one step ahead and the problem (2.2) is solved with the new plant state x_{k+1} as the initial condition. As a result, this requires the MPC controller to obtain a solution as fast as possible.

Depending on different modeling and solution strategies, there are many variations of linear MPC. For instance, engineers at Shell Oil developed the so-called dynamic matrix con-

trol (DMC) [27] that uses linear step response models and a quadratic objective function. DMC solves the optimization problem (2.2) without constraints as the solution to a least-squares problem. Furthermore, Shell engineers developed QDMC [37] by posing the DMC problem as a quadratic programming (QP) problem in which constraints appear explicitly. Then in the following years, more and more variations of the MPC controllers [76, 112] were proposed to improve the performance of the original DMC controller. Some of the formulations are based on linear impulse response models. More detailed review can be found in [89].

Generally, linear MPC uses a small linear data-driven model to represent the plant. Thus it has the advantage of solving a small optimization problem, which can be done fast enough at each time step in order to be implemented in the moving horizon framework. On the other hand, linear MPC also suffers from drawbacks such as plant-model mismatch so that the model is only valid around an operating point.

In this dissertation, we are interested in NMPC controllers that directly use the first-principle dynamic model of the plant, i.e. $\bar{f}(\cdot,\cdot) = f(\cdot,\cdot)$ in the formulation (2.2). It has the advantages that the model is valid over a wide range of operating conditions and can be extended to the D-RTO as discussed in Chapter 1.

2.2 Real Time NMPC Strategies

As mentioned in Chapter 1, performance deterioration of NMPC and stability loss due to computationally delays have been noted by [100, 35]. To address this issue, real time NMPC strategies such as neighboring extremals, explicit schemes, Newton-type controllers and NLP sensitivity-based controllers have been studied.

Neighboring extremals [23] solve a full solution of the optimal control problem off-line using indirect methods and perform a full iteration online to find the approximated optimal solution. As a result, it inherits the disadvantages associated with the indirect method which are briefly summarized in Chapter 3.

Explicit schemes [10] compute the control sets off-line by enumerating all the possible states or their approximations. Then online control actions are chosen from these sets based on where the state lies. These methods have been applied on the fast systems where the state space is relatively small [38, 10], but posing difficulties when applied to large scale systems due to the exponential growth in computational complexity of off-line enumeration.

The Newton-type controller was proposed by Li and Biegler [70] and has been developed by many other researchers [31, 29, 86]. It performs a single full Newton step of NMPC (2.2) online to allow a quick return of control action. The Newton-type controllers have shown good performance to reject the fast disturbance quickly. However, since the full Newton-step is just a linearization at steady state, it can not guarantee to work in the presence of strong nonlinearity, varying operating point or even large disturbance.

NLP sensitivity-based controllers [115, 57, 24] aim to overcome the drawbacks posed by the Newton-type controllers. Similar to the neighboring extremals scheme, the control action is approximated around a continuously updated reference solution. However, the NLP sensitivity-based controllers use direct methods to solve the optimal control problem. The advantages of the direct method are briefly discussed in Chapter 3. In particular, Zavala and Biegler [115] proposed an NLP sensitivity-based NMPC named advanced step NMPC (asNMPC), which is used throughout this dissertation. It solves the optimization problem (2.2) between sampling times $k-1$ and k to constantly update the reference trajectory and calculates the control action by a single Newton step at time step k to obtain fast solution. As a result, it significantly reduces the computational delay online. In our experience,

the computational delay is reduced by at least two orders of magnitude using asNMPC which is reported in Chapter 4. The detailed asNMPC algorithm is discussed in Chapter 3. Moreover, it has been shown that asNMPC inherits the same nominal stability as NMPC and suffers a little loss of robustness due to the introduced NLP sensitivity error [115].

2.3 Stability of set-point tracking NMPC

One of the key questions in NMPC is whether the NMPC formulation leads to stability of the closed-loop system. The finite-horizon formulation is of particular interest because it is computationally manageable. The stability of system without disturbances is called *nominal* stability, while the stability of system in the presence of disturbance is termed *robust* stability. In this section, we first present the notations and basic definitions used in the stability analysis in this dissertation and summarize the existing results in the literature for both nominal and robust stability. In addition, one can also find the detailed discussion in the overview papers [78, 72], and a new NMPC book [95].

2.3.1 Notations and Basic Definitions

Let $\mathbb{R}, \mathbb{R}_{\geq 0}$, $\mathbb{Z}$ and $\mathbb{Z}_{\geq 0}$ denote real, non-negative real, integer and non-negative integer numbers, respectively. Given $n \in \mathbb{Z}_{\geq 0}$, an arbitrary norm of a vector $x \in \mathbb{R}^n$ is denoted as $|x|$. Given a positive semidefinite matrix W, the weighted norm of x is given by $|x|_W := \sqrt{x^T W x}$. Given a signal $w \in \mathbb{R}^n$, then at time step $k \in \mathbb{Z}_{\geq 0}$ it is denoted by w_k and the signal sequence is denoted by $\{w_k\} \triangleq \{w_1, w_2, \ldots, w_k\}$. For a given sequence $\{w_k\}$, we denote $\|w\|_k \triangleq \sup_{0 \leq j \leq k}\{|w_j|\},\ j \in \mathbb{Z}_{\geq 0}$. In the sequel, the index k is sometimes dropped if the cardinality of the sequence is inferred from the context. A function $f : \mathbb{R} \to \mathbb{R}$ is said to be

$\mathscr{C}^1$ function if its derivative $f'(\cdot)$ exists and is continuous. A function $\tau : \mathbb{R}_{\geq 0} \to \mathbb{R}_{\geq 0}$ is of class $\mathscr{K}$ (or a $\mathscr{K}$-function) if it is continuous, strictly monotone increasing and $\tau(0) = 0$. A function $\tau : \mathbb{R}_{\geq 0} \to \mathbb{R}_{\geq 0}$ is of class $\mathscr{K}_\infty$ if it is a $\mathscr{K}$-function and $\tau(s) \to +\infty$ as $s \to +\infty$. A function $\tau : \mathbb{R}_{\geq 0} \times \mathbb{Z}_{\geq 0} \to \mathbb{R}_{\geq 0}$ is of class $\mathscr{K}\mathscr{L}$ if, for fixed $k \in \mathbb{Z}_{\geq 0}$, $\tau(\cdot, k)$ is of class $\mathscr{K}$, and for each fixed $s \in \mathbb{R}_{\geq 0}$, $\tau(s, \cdot)$ is decreasing and $\tau(s,k) \to 0$ as $k \to +\infty$. Consider $\tau_1(\cdot)$ and $\tau_2(\cdot)$ as $\mathscr{K}$-functions, then $\tau_1 \circ \tau_2(\cdot) \triangleq \tau_1(\tau_2(\cdot))$ denotes the function composition, besides $\tau_1^j(\cdot)$ denotes the j-th composition of $\tau_1(\cdot)$. Given compact sets $A \subset \mathbb{R}^a$ and $B \subset \mathbb{R}^b$, function $f(x,y) : \mathbb{R}^a \times \mathbb{R}^b \to \mathbb{R}^c$ is said to be uniformly continuous in x for all $x \in A$ and $y \in B$ if for all $\varepsilon > 0$, a $\delta(\varepsilon) > 0$ exists such that $|f(x_1, y) - f(x_2, y)| \leq \varepsilon$ for all $x_1,\ x_2 \in A$ with $|x_1 - x_2| \leq \delta(\varepsilon)$ and for all $y \in B$.

Lemma 1 *[92] The space of $\mathscr{K}$-functions is closed under addition, composition and positive scalar multiplication.*

Lemma 2 *[72] If $f(x,y) : \mathbb{R}^a \times \mathbb{R}^b \to \mathbb{R}^c$ is a uniformly continuous function in both $x \in A \subset \mathbb{R}^a$ and $y \in B \subset \mathbb{R}^b$, then there exist $\mathscr{K}$-functions $\tau_1(\cdot)$ and $\tau_2(\cdot)$ such that*

$$\begin{aligned} |f(x_1, y_1) - f(x_2, y_2)| \quad &\leq \quad \tau_1(|x_1 - x_2|) + \tau_2(|y_1 - y_2|), \\ &\qquad \forall x_1,\ x_2 \in A,\ y_1\ y_2 \in B. \end{aligned}$$

Definition 1 *Consider an autonomous system where x_k is the state*

$$x_{k+1} = f(x_k), \tag{2.3}$$

System (2.3) *is said to be locally nominally stable if there exists a positive constant e_1 and a $\mathscr{K}\mathscr{L}$-function $\beta(\cdot,\cdot)$ such that*

$$|x_j| \leq \beta(|x_0|, j)$$

for all initial states $|x_0| \leq e_1$.

Similarly for an autonomous system where d_k *is a disturbance signal*

$$x_{k+1} = f(x_k, d_k). \tag{2.4}$$

System (2.4) *is said to be locally Input-to-State Stable (ISS) if there exists a positive constant* e_2*, a* $\mathscr{K}\mathscr{L}$*-function* $\beta(\cdot,\cdot)$ *and a* $\mathscr{K}$*-function* $\gamma(\cdot)$ *such that*

$$|x_j| \leq \beta(|x_0|, j) + \gamma(\|d\|_{j-1})$$

for all initial states $|x_0| \leq e_2$.

Moreover, for an autonomous system where d_k *and* w_k *are two disturbances*

$$x_{k+1} = f(x_k, d_k, w_k), \tag{2.5}$$

System (2.5) *is said to be locally ISpS if there exist constants* e_3 *and* e_4*, a* $\mathscr{K}\mathscr{L}$*-function* $\beta(\cdot,\cdot)$ *and a* $\mathscr{K}$*-function* γ *such that*

$$|x_j| \leq \beta(|x_0|, j) + \gamma(\|d\|_{j-1}) + e_4$$

for all initial states $|x_0| \leq e_3$*, and disturbances* $d \in \Omega_d$ *and* $w \in \Omega_w$.

Definition 2 *A function* $V(\cdot)$ *is called a Lyapunov function for system* (2.3)*, if there exist sets* $\mathbb{X}$ *and* $\mathscr{K}_\infty$*-functions* τ_1*,* τ_2*,* τ_3 *such that*

$$\begin{aligned} \tau_1(|x|) &\leq V(x) \leq \tau_2(|x|),\ \forall x \in \mathbb{X} \\ \triangle V(x,d) &= V(f(x,d)) - V(x) \leq -\tau_3(|x|), \\ \forall x &\in \mathbb{X}. \end{aligned} \tag{2.6}$$

A function $V(\cdot)$ is called an ISS-Lyapunov function for system (2.4)*, if there exist sets $\mathbb{X}$, Ω_d and $\mathscr{K}_\infty$-functions τ_4, τ_5, τ_6 and $\mathscr{K}$-function σ_1 such that*

$$\begin{aligned} \tau_4(|x|) &\leq V(x) \leq \tau_5(|x|),\ \forall x \in \mathbb{X} \\ \triangle V(x,d) &= V(f(x,d)) - V(x) \leq -\tau_6(|x|) + \sigma_1(|d|), \\ \forall x &\in \mathbb{X},\ \forall d \in \Omega_d. \end{aligned} \tag{2.7}$$

A function $V(\cdot)$ is called an ISpS-Lyapunov function for system (2.5) *with respect to d, if there exist sets $\mathbb{X}$, Ω_d, Ω_w and $\mathscr{K}_\infty$-functions τ_7, τ_8, τ_9, $\mathscr{K}$-function σ_2 and constants e_5, $e_6 \in \mathbb{R}_{\geq 0}$ such that*

$$\begin{aligned} \tau_7(x) &\leq V(x) \leq \tau_8(x) + e_5,\ \forall x \in \mathbb{X} \\ \triangle V(x,d,w) &= V(f(x,d,w)) - V(x) \leq -\tau_9(|x|) + \sigma_2(|d|) + e_6, \\ \forall x &\in \mathbb{X},\ \forall d \in \Omega_d,\ \forall w \in \Omega_w \end{aligned} \tag{2.8}$$

Lemma 3 *[74, 72] If system* (2.3) *admits a Lyapunov function in $\mathbb{X}$, then it is nominally stable in $\mathbb{X}$. If system* (2.4) *admits an ISS-Lyapunov function in $\mathbb{X}$ with respect to d, then it is ISS in $\mathbb{X}$. If system* (2.5) *admits an ISpS-Lyapunov function in $\mathbb{X}$ with respect to d, then it is ISpS in $\mathbb{X}$.*

Definition 3 *A set $\Gamma \in \mathbb{X}$ is a robust positively invariant (RPI) set for system* (2.4) *if $f(x,d) \in \Gamma$, for all $x \in \Gamma$ and all $d \in \Omega_d$.*

A similar RPI set can be defined for system (2.5).

2.3.2 Nominal Stability

The stability of NMPC for constrained nonlinear systems necessitates the use of Lyapunov stability theory. In this framework, the nominal stability of a closed-loop system is proved

if one can find a Lyapunov function for the system as stated in Definition 2 and Lemma 3. The Lyapunov function has to satisfy three conditions: 1) the Lyapunov function is upper-bounded by a $\mathscr{K}$-function of the plant state; 2) the Lyapunov function is lower-bounded by a $\mathscr{K}$-function of the plant state; 3) the Lyapunov function is decreasing with respect to time. Keerthi and Gilbert [61] first employed the cost function as a Lyapunov function for establishing stability of NMPC. Thereafter, the cost function is almost universally chosen as the Lyapunov function for stability analysis [78]. Strategies to guarantee the nominal stability are summarized in the following:

Infinite-horizon NMPC: The most intuitive way to achieve stability is to use infinite-horizon cost [61]. In the nominal case, feasibility at one sampling time also implies feasibility and optimality at next sampling time. Hence, the control and state trajectories computed in the NMPC problem at any sampling time are in fact the closed-loop trajectories. This indicates the closed-loop stability is satisfied. The detailed proof can be found in [61].

Finite-horizon NMPC with terminal equality constraint: Keerthi and Gilbert [61] further showed that in the nominal case, the infinite-horizon NMPC can be approximated by a finite-horizon formulation with a terminal equality constraint as in the formulation (2.9). Compared to the formulation (2.2), the terminal equality constraint basically ensures that at the end of the finite horizon, the closed-loop system approaches the same steady state as in the infinite-horizon.

$$
\begin{aligned}
& \min && \sum_{i=0}^{N-1} |z_i - x_s|_Q^2 + |v_{i+1} - v_i|_R^2 \\
\text{s.t} \quad & z_{i+1} &=& f(z_i, v_i), \quad i = 0, \ldots, N-1 \\
& z_0 &=& x_k,\ z_N = x_s, \\
& z_i &\in& \mathbb{X},\ v_i \in \mathbb{U},
\end{aligned} \tag{2.9}
$$

where x_s is the set-point, and $z_N = x_s$ is the terminal equality constraint. Since we are considering set-point tracking NMPC with first-principle dynamic model, the plant dynamic $f(\cdot,\cdot)$ is directly used as the model equation and the objective function is chosen to be the quadratic term in the following.

Finite-horizon NMPC with terminal cost: Bitmead et al. [17] proposed to add a terminal cost function which is the algebraic Riccati equation at the end of the finite-horizon as shown in (2.10). Therefore, the cost function over the infinite horizon can be approximated by the finite horizon formulation. Thus the closed-loop stability is retained.

$$
\begin{aligned}
& \min && \sum_{i=0}^{N-1} (|z_i - x_s|_Q^2 + |v_{i+1} - v_i|_R^2) + F(z_N) \\
\text{s.t} \quad & z_{i+1} &=& f(z_i, v_i), \quad i = 0, \ldots, N-1 \\
& z_0 &=& x_k, \\
& z_i &\in& \mathbb{X},\ v_i \in \mathbb{U},
\end{aligned} \tag{2.10}
$$

where $F(z_N)$ is the terminal cost function.

Finite-horizon NMPC with terminal inequality constraint: NMPC formulation (2.11) introduces a terminal constraint set at the end of the horizon to the general formulation (2.2). The finite-horizon NMPC is to steer the plant to the constraint set $\mathbb{X}_N$. Inside $\mathbb{X}_N$, a

local stabilizing controller is used [81, 101]. This idea to guarantee the closed-loop stability is termed the dual mode controller.

$$\begin{aligned} & \min && \sum_{i=0}^{N-1} |z_i - x_s|_Q^2 + |v_{i+1} - v_i|_R^2 \\ \text{s.t} \quad & z_{i+1} &=& f(z_i, v_i), \quad i = 0, \ldots, N-1 \\ & z_0 &=& x_k,\ z_N \in \mathbb{X}_N \\ & z_i &\in& \mathbb{X},\ v_i \in \mathbb{U}. \end{aligned} \tag{2.11}$$

Quasi-infinite horizon NMPC: Chen and Allgöwer [25] proposed the so-called quasi-infinite horizon NMPC (2.12) which incorporates both the terminal cost function and terminal inequality constraint into the finite-horizon formulation. The terminal inequality set is the maximal output admissible set and the terminal cost is the upper bound of the infinite cost. With guaranteed closed-loop stability, most recent NMPC formulations belong to this category.

$$\begin{aligned} & \min && \sum_{i=0}^{N-1} (|z_i - x_s|_Q^2 + |v_{i+1} - v_i|_R^2) + F(z_N) \\ \text{s.t} \quad & z_{i+1} &=& f(z_i, v_i), \quad i = 0, \ldots, N-1 \\ & z_0 &=& x_k,\ z_N \in \mathbb{X}_N \\ & z_i &\in& \mathbb{X},\ v_i \in \mathbb{U}. \end{aligned} \tag{2.12}$$

2.3.3 Robust Stability

To consider plant-model mismatch or disturbance, we use the plant equation (2.13) with an uncertainty parameter.

$$x_{k+1} = f(x_k, u_k, \theta_k), \tag{2.13}$$

where $\theta_k \in \Omega_\theta \subset \mathbb{R}^{n_\theta}$ is the uncertainty parameter, and Ω_θ is a compact set. Note θ_k here is a general form of plant-model mismatch including the additive disturbance which is widely-used in the literature.

In this case, robust stability of the closed-loop system needs to be considered. To some extent, the closed-loop system has inherent robustness, which means that nominal NMPC remains stable even without directly considering the disturbances. However, there are also examples that the nominal NMPC does not have any robust margin at all [39].

The problem to assure recursive feasibility and constraint satisfaction is more involved in the robust stability analysis. There are many different approaches to analyze the robust stability, such as ISS framework (discussed in Definition 2 and Lemma 3), robust stability margin, ultimately bounded evolution and asymptotic gain property. Limon et al [72] have shown that ISS framework can be used as a unifying robust stability framework.

Utilizing invariant set theory coupled with ISS-Lyapunov stability framework, Magni and Scattolini [74] have shown that if further assumptions are satisfied (continuous differentiability for control and cost function), the NMPC control law is inverse optimal. Then by virtue of the inverse optimality, nominal NMPC inherits the same robust stability. This result is also summarized by Limon et al. [72].

The design of NMPC algorithms with robust stability is not mature yet. It was first proposed in the H_∞ context [66, 77] to solve a min-max optimization problem where the cost function is maximized with respect to the admissible disturbance sequence, and minimized with

respect to the control as shown in the formulation (2.14). Moreover tube-based robust NMPC design strategies which calculate the control actions based on different uncertainty regions have been widely studied as well [71, 91, 22, 69]. However, both of these strategies suffer from extensive computational burden.

$$\begin{aligned} \min_{v_i,z_i} \max_{\theta_i} \quad & \sum_{i=0}^{N-1} l(z_i, v_i) \\ \text{s.t} \quad z_{i+1} &= f(z_i, v_i, \theta_i), \quad i = 0, \ldots, N-1 \\ z_0 &= x_k, \\ z_i &\in \mathbb{X},\ v_i \in \mathbb{U},\ \theta_i \in \Omega_\theta. \end{aligned} \tag{2.14}$$

2.4 Stability of Economically-Oriented NMPC

Although it is economically beneficial to use D-RTO or economically-oriented NMPC to directly optimize the economical performance of a process, theoretical studies regarding the stability issues are still lacking. This is in vast contrast to the mature body of stability of the set-point tracking NMPC summarized in Section 2.3. This is mainly because it is difficult to show the cost function satisfies the conditions in Definition 2 as a Lyapunov function.

Recently, some work emerged in the literature to deal with special cases of economically-oriented NMPC. For example, Rawlings et al. [94] proposed an MPC controller with economical objective terms that handles unreachable set-points better than the conventional set-point tracking MPC. Although the stability property of the controller is demonstrated, the analysis is not within the Lyapunov stability framework. Diehl et al. [30] showed stability of a general economically-oriented formulation by establishing a Lyapunov func-

tion. Nevertheless, the analysis is based on the assumption that the system satisfies strong duality, which indicates the optimal operating point is at a steady state. This assumption excludes economically-oriented NMPC scenario for a class of system with cyclic behavior. Moreover, while the strong duality assumption is true for linear systems with convex constraints and strictly convex costs, it is difficult to show that a nonlinear system satisfies this property.

2.5 Concluding Remarks

In this chapter, we present the NMPC problem formulation, notations and basic definitions used throughout this dissertation. Then, we review previous work relevant to this dissertation. The review focuses on the area of real time NMPC strategies and stability analysis of NMPC. It also serves as a centralized literature study for the following chapters, especially Chapters 3, 6 and 7.

Chapter 3

Solution Strategy

In this chapter, we discuss the strategy we adapt to solve large scale optimization problems constrained by differential and algebraic equations (DAEs). It leads to the NMPC formulations discussed in Chapter 2. For applications like nonlinear model predictive control (NMPC) and moving horizon estimation (MHE), solving the DAE-constrained optimization online may introduce large computational delays. To overcome this difficulty, NLP sensitivity that approximates the rigorous solution online is introduced. In addition, sensitivity-based advanced step algorithms for NMPC and MHE are discussed.

3.1 Approaches to DAE-Constrained Optimization

In this chapter, we consider a general DAE-constrained optimization problem (3.1), which includes the continuous-time counterpart of the NMPC problem (2.2).

$$\min_{u(t), z_d(t), z_a(t)} \quad \phi(z_d(t_f)) \tag{3.1a}$$

$$s.t. \ \frac{dz_d(t)}{dt} = f_d(z_d(t), z_a(t), u(t), p) \tag{3.1b}$$

$$0 = f_a(z_d(t), z_a(t), u(t), p) \tag{3.1c}$$

$$z_d(0) = z_0 \tag{3.1d}$$

$$z_d^L \leq z_d(t) \leq z_d^U \tag{3.1e}$$

$$z_a^L \leq z_a(t) \leq z_a^U \tag{3.1f}$$

$$u^L \leq u(t) \leq u^U \tag{3.1g}$$

$$0 \leq t \leq t_f, \tag{3.1h}$$

where $z_d \in \mathbb{R}^{n_d}$ is a vector of differential or state variables, $z_a \in \mathbb{R}^{n_a}$ is a vector of algebraic variables, $u \in \mathbb{R}^{n_u}$ is a vector of control variables, $p \in \mathbb{R}^{n_p}$ is a vector of parameters in the optimization problem, $f_d(\cdot)$ is a vector of differential equations, $f_a(\cdot)$ is a vector of algebraic equations and z_0 is the initial condition for the differential variables. The objective function is chosen to be the *Mayer* form. Nevertheless, any integral or *Bolza* form function can be reformulated to the Mayer form.

There are many strategies to solve the DAE-constrained optimization problem (3.1). Fig. 3.1 shows different approaches with their advantages and disadvantages. The indirect method or variational methods apply *optimize then discretize* strategy and solve the optimization problem (3.1) based on Pontryagins Maximum Principle [23]. Although the indirect methods have solid theoretical foundations, they are generally inefficient for large scale problems or systems with inequality constraints. On the other hand, the direct method

use *discretize then optimize* strategy and directly cast the problem (3.1) as a nonlinear programming (NLP) problem. Therefore, these methods tend to be more general and computationally efficient. Based on different approaches to handle the continuous-time DAE system, the direct approach can be further classified as sequential approach or single shooting, multiple shooting and collocation based method. In the single shooting method, only the control variable is discretized and the optimization is performed with respect to the discretized control variables. Given initial conditions and a set of optimized control variables, the DAE model is integrated using an inner loop DAE solver [106, 107]. Gradients are calculated either from direct sensitivity equations or adjoint sensitivity equations. Although it is easy to implement, the single shooting method can not guarantee to handle open loop unstable system and path constraints are only enforced approximately [6, 15]. Multiple shooting was developed to handle unstable DAE systems and impose inequality constraints. In this approach, the control variables are treated the same way as in the sequential method, but the DAE model is integrated in small elements of the entire time domain [19]. Finally collocation based methods fully discretize the state and control profile [12, 14]. Typically the discretization is performed by using orthogonal collocation on finite elements due to its accuracy and numerical stability properties [59]. It corresponds to a particular Runge-Kutta method. This leads to large scale NLP problems, but it allows the NLP solvers to exploit the sparsity and structure property of DAE system. In addition, this approach requires no DAE integrators, as the DAE system is only solved once at the optimal point [15, 14]. Detailed discussion of the advantages and disadvantage of the above mentioned methods can be found in [15, 14]. In this dissertation, a simultaneous method with Radau collocation points is used. One can find its derivation and stability property in [59, 14].

Without further discussion, DAE-constrained optimization problems and simulation examples throughout this dissertation are discretized using orthogonal collocation with Radau

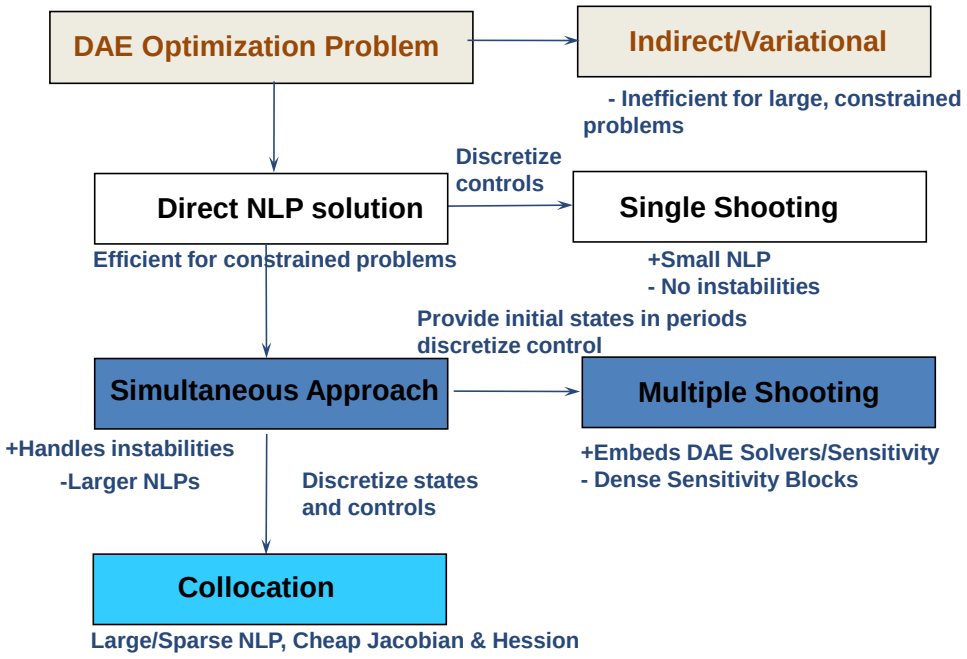

Figure 3.1: Strategies for DAE-constrained optimization problem.

collocation points, unless otherwise noted. This method approximates the control and state variables as piecewise polynomial functions over *finite elements*, $t_0 < t_1 < \cdots < t_{N_e} = t_f$. The element length is $h_i = t_i - t_{i-1}$. Here we represent the state and control profiles by Lagrange interpolation polynomials in each element, as:

$$\left.\begin{array}{c} t = t_{i-1} + h_i \tau \\ z_d(t) \approx \sum_{j=0}^{N_c} \Omega_j(\tau) z_d^{i,j} \end{array}\right\} t \in [t_{i-1}, t_i], \quad \tau \in [0,1] \tag{3.2}$$

where

$$\Omega_j(\tau) = \prod_{k=0, k\neq j}^{N_c} \frac{\tau - \tau_k}{\tau_j - \tau_k}, \tag{3.3}$$

N_c is the number of collocation points. $z_d^{i,j}$ is the state value of collocation point j in finite element i. Note that these polynomials are of order of N_c and satisfy

$$\Omega_j(\tau_i) = \begin{cases} 1, & \tau_i = \tau_j \\ 0, & \tau_i \neq \tau_j. \end{cases} \tag{3.4}$$

With this, the approximated control and algebraic profiles are represented by the Lagrange interpolation over the interval $t \in [t_{i-1}, t_i]$:

$$\begin{aligned} u(t) &= \sum_{j=1}^{N_c} \bar{\Omega}_j(\tau) u^{i,j} \\ z_a(t) &= \sum_{j=1}^{N_c} \bar{\Omega}_j(\tau) z_a^{i,j}, \end{aligned} \tag{3.5}$$

where

$$\bar{\Omega}_j(\tau) = \prod_{k=1, k\neq j}^{N_c} \frac{\tau - \tau_k}{\tau_j - \tau_k}. \tag{3.6}$$

Similarly, $z_a^{i,j}$ and $u^{i,j}$ are algebraic and control variables of collocation point j in finite element i, respectively. The differential and algebraic equations are written as:

$$\begin{aligned} \sum_{k=0}^{N_c} \dot{\Omega}_k(\tau_j) z_d^{i,k} &= h_i f_d(z_d^{i,j}, z_a^{i,j}, u^{i,j}, p) \\ 0 &= f_a(z_d^{i,j}, z_a^{i,j}, u^{i,j}, p), \quad i = 1, \ldots, N_e, \quad j = 1, \ldots, N_c, \end{aligned} \tag{3.7}$$

where $\dot{\Omega}_k(\tau) = d\Omega_k(\tau)/d\tau$.

As a result, after full discretization the DAE-constrained optimization problem (3.1) can be

approximated by the following NLP,

$$\min_{u^{i,j}, z_d^{i,j}, z_a^{i,j}} \quad \phi(z_d(t_f)) \tag{3.8a}$$

$$s.t. \sum_{k=0}^{N_c} \dot{\Omega}_k(\tau_j) z_d^{i,k} = h_i f_d(z_d^{i,j}, z_a^{i,j}, u^{i,j}, p) \tag{3.8b}$$

$$0 = f_a(z_d^{i,j}, z_a^{i,j}, u^{i,j}, p) \tag{3.8c}$$

$$z_d^{1,0} = z_0, \quad z_d(t_f) = \sum_{j=0}^{N_c} \Omega_j(1) z_d^{N_e,j} \tag{3.8d}$$

$$z_d^L \leq z_d^{i,j} \leq z_d^U \tag{3.8e}$$

$$z_a^L \leq z_a^{i,j} \leq z_a^U \tag{3.8f}$$

$$u^L \leq u^{i,j} \leq u^U \tag{3.8g}$$

$$i = 1, \ldots, N_e, \quad j = 1, \ldots, N_c, \tag{3.8h}$$

$$z_d^{k+1,j} = \sum_{j=0}^{N_c} \Omega_j(1) z_d^{k,j}, k = 1, \ldots N_e - 1, \tag{3.8i}$$

where, the last equation ensures the continuity between the neighboring finite elements.

Using the method discussed above, we are able to approximate a continuous-time system by a discrete-time formulation. Hence we directly consider the discrete-time model equation (2.1) and NMPC formulations such as (2.2), (2.9), (2.10), (2.11), (2.12) and (2.14) in this dissertation.

3.2 Ipopt Algorithm and NLP Sensitivity

In this section, the discretized optimization problem (3.8) is simplified as a general parametric NLP problem of the form,

$$\min_{w(p)} \quad f(w(p),p) \tag{3.9a}$$

$$s.t. \quad c(w(p),p)=0, \qquad w(p)\geq 0 \tag{3.9b}$$

with a fixed parameter vector p. Notice the implicit dependence of the problem variables on the particular value of the parameter. In the context of NMPC and MHE, this parameter can be denoted as the initial conditions and updated measurements, respectively.

NLP solvers based on interior-point method are a good choice to solve large scale and sparse NLPs. In particular, the solvers LOQO, Knitro and IPOPT are widely used alternatives. In this work, IPOPT [109] which was developed in our group is chosen as the NLP solver. IPOPT handles the bound constraints implicitly through logarithmic barrier terms added to the objective function,

$$\min_{w(p)} \quad \varphi(w(p),p)=f(w(p),p)-\mu_l\sum_{i=1}^{n}\ln(w^{(i)}(p)) \tag{3.10a}$$

$$s.t. \quad c(w(p),p)=0 \tag{3.10b}$$

where $\mu_l>0$ is a barrier parameter. Symbol $w^{(i)}(p)$ denotes the i^{th} component of vector $w(p)$. The solution of the barrier problem (3.10)) converges to the solution of the original NLP (3.9) as the sequence of barrier parameters μ_l tends to zero.

To solve each barrier problem for μ_l, IPOPT applies Newton's method to the KKT conditions of system (3.10). This results in the following large-scale linear system solved at each

iteration j:

$$\begin{bmatrix} H_j & A_j & -I \\ A_j^T & 0 & 0 \\ V_j & 0 & Z_j \end{bmatrix} \begin{bmatrix} \triangle w \\ \triangle \lambda \\ \triangle \nu \end{bmatrix} = - \begin{bmatrix} \nabla f(w_j(p),p) + A_j \lambda(p)_j - \nu(p)_j \\ c(w_j(p),p) \\ Z_j V_j e - \mu_l e \end{bmatrix} \tag{3.11}$$

where λ and ν are the Lagrange multipliers for the equality constraints and bounds, respectively. In addition, $Z := diag(w(p))$, $V := diag(\nu(p))$, $H := H(w(p),p)$, is the Hessian of the Lagrange function $\mathscr{L} = f(w(p),p) + c(w(p),p)^T \lambda(p) - \nu(p)^T w(p)$, and $A := A(w(p),p)$ is the constraint Jacobian. It is important to emphasize that the most expensive step at each iteration in the algorithm is the factorization of the KKT matrix in the left hand side of equation (3.11). Depending on the size and structure of the problem, this factorization step can take a significant amount of computational time. Here we provide the IPOPT solver with exact Hessian and Jacobian information through the modeling platform AMPL. This accelerates the local convergence of Newton's method and facilitates to solve NLPs with many degrees of freedom efficiently.

The IPOPT sensitivity algorithm [115, 116] is used to further reduce the computational delay associated with solving the large scale NLP problem. Assume that we count with the solution of NLP (3.9) for a given nominal parameter vector $p = p_0$. At this solution, the KKT system (3.11) can be expressed in condensed form as,

$$\mathbf{K}^*(p_0)\Delta s = \varphi(s^*(p_0), p_0) \tag{3.12}$$

where $s^*(p_0)^T = [w^*(p_0)^T, \lambda^*(p_0)^T, \nu^*(p_0)^T]$ is the optimal triplet vector while $\varphi(\cdot,\cdot)$ and $\mathbf{K}^*(\cdot)$ are the KKT conditions and KKT matrix in (3.11) evaluated at this solution, respectively.

Assume that the objective and constraints in NLP (3.9) are at least twice continuously differentiable in p and that a given nominal solution $s^*(p_0)$ satisfies the linear independence

constraint qualification (LICQ) [85, 14], the sufficient second order conditions (SSOC) [85, 14] and strict complementary slackness [85, 14]. If the parameter vector p_0 enters linearly in the objective function and constraints (e.g., as the initial conditions in the dynamic optimization problem), it is possible to show [34, 115] that replacing the nominal parameter p_0 for the perturbed parameter p in (3.12) leads to the first order step $\Delta s = \tilde{s}(p) - s^*(p_0)$. Here, $\tilde{s}(p)$ is an approximation to the true optimal solution $s^*(p)$ satisfying,

$$|\tilde{s}(p) - s^*(p)| \leq L|p - p_0|^2 \tag{3.13}$$

where L is a positive Lipschitz constant. The above result has important practical implications since the factorization of the KKT matrix in (3.12) is already available as a natural outcome of the NLP solver. As a consequence, the second order approximate solution can be obtained through a single backsolve which can be performed at least an order of magnitude faster than the solution of the full NLP problem.

3.3 Advanced Step NMPC

Given the plant dynamics (2.1), we directly consider the NMPC formulation with the first-principle dynamic model as follows.

$$\begin{aligned} & \min && \sum_{i=0}^{N-1} l(z_i, v_i) \\ \text{s.t} \quad & z_{i+1} &=& f(z_i, v_i), \quad i = 0, \ldots, N-1 \\ & z_0 &=& x_k, \\ & z_i &\in& \mathbb{X},\ v_i \in \mathbb{U} \end{aligned} \tag{3.14}$$

where N is the horizon length, x_k is the initial condition which is the plant state at time step k. To differentiate from the actual plant state x and control u, we use z and v as the predicted state and control in the NMPC formulation. $l(\cdot,\cdot)$ is the objective function.

As discussed in Chapter 2, the NMPC controller is implemented in a moving horizon framework [95, 89, 82]. At current time step k, the plant state x_k is used as the initial condition and the optimization problem (3.14) is solved on a horizon N. However, only the first calculated control action is implemented, i.e. $u_k = v_0$. At the next time step, the problem (3.14) is solved with the new plant state as the initial condition. Clearly, NMPC is a time critical application that needs to implement the control action as fast as possible. Performance deterioration of NMPC due to computational delays has been reported [100]. Moreover, it has been analyzed [35] that the computational delay may destroy the stability of the controller. However, as larger and more sophisticated process models are considered, the computational complexity becomes an issue. Motivated by these observations, Zavala and Biegler [115] proposed the so-called advanced step NMPC algorithm (asNMPC). The controller is based on a separation principle between background and inexpensive on-line computational tasks [32]. The controller exploits the predictive capabilities of the rigorous dynamic model to predict the future state of the plant and solve a predicted problem in background (between sampling times). Once the true state is revealed at the next sampling time, the controller responds to the inherent model errors and/or external disturbances through a fast on-line correction of the predicted solution.

The algorithm can be summarized as:

1. **Background calculation:** Having x_k and u_k at time step k, predict the future state of the system z_{k+1} using the dynamic model. Assuming the computations can be completed within one sampling time, solve the NLP (3.9) based on (3.14) with $p_0 = z_{k+1}$.

2. **On-line update:** At time step $k+1$, obtain the true state x_{k+1}. Set $p = x_{k+1}$ and use (3.12) to get the fast updated solution. Extract the control action u_{k+1} from the approximate solution vector and inject to the plant.

3. **Iterate:** Set $k \leftarrow k+1$ and go to background.

The asNMPC controller presents an attractive alternative to approximate the performance of a hypothetical *ideal* NMPC strategy that provides optimal instantaneous feedback at each sampling time (i.e. no computational delay). Using NLP sensitivity theory, it is possible to bound the approximation error of the asNMPC controller in a rigorous manner [34]. In addition, the controller enjoys the same nominal stability properties of the ideal NMPC, and its robust stability margins can be bounded by the uncertainty description implicit in the perturbation $|x_k - z_k|$ [115].

3.4 Advanced Step MHE

State estimation uses limited input and output information to infer the state of the process. It is required for the NMPC controller as the estimated state serves as the initial condition in the NMPC calculation. Moving horizon estimation (MHE) is an optimization-based method with the advantage to handle constraints on the state easily.

To study the state estimation problem, we introduce the nonlinear output mapping into the plant dynamics (2.1) as the following.

$$\begin{aligned} x_{k+1} &= f(x_k, u_k),\ x_k \in \mathbb{X},\ u_k \in \mathbb{U}, \\ y_k &= h(x_k), \end{aligned} \tag{3.15}$$

where $y_k \in \mathbb{R}^{n_y}$ is the output, and $h(\cdot) : \mathbb{R}^{n_x} \to \mathbb{R}^{n_y}$ is a nonlinear output mapping function.

At time step k, with the measured output sequence $y_{k-N_e},\ y_{k-N_e+1},\ \ldots,\ y_k$, the MHE prob-

lem is formulated as

$$\min \sum_{j=0}^{N_e} (\zeta_{k-N_e+j}^T \Pi_y \zeta_{k-N_e+j}) + (\hat{x}_{k-N_e} - \bar{x}_{k-N_e})^T \Pi_0 (\hat{x}_{k-N_e} - \bar{x}_{k-N_e}) \tag{3.16a}$$

$$\text{s.t.} \quad \hat{x}_{k-N_e+j+1} = f(\hat{x}_{k-N_e+j}, u_{k-N_e+j}) \tag{3.16b}$$

$$\hat{y}_{k-N_e+j} = h(\hat{x}_{k-N_e+j}) \tag{3.16c}$$

$$\zeta_{k-N_e+j} = y_{k-N_e+j} - \hat{y}_{k-N_e+j} \tag{3.16d}$$

$$\hat{x}_{k-N_e+j} \in \mathbb{X}, \quad j = 0, \ldots, N_e, \tag{3.16e}$$

where N_e is the estimation horizon length, Π_y, Π_0 are symmetric positive definite tuning matrices, $\hat{x}_k$ and $\hat{y}_k$ are the estimated state and output values. Particularly, Π_0 is also termed as the arrival cost, which has important implications on the stability of the MHE [92]. In addition, $\bar{x}_k$ is the estimated value of the state variable at time step k and $\bar{x}_{k-N_e}$ is the most likely *prior* value of x_{k-N_e}. After the MHE problem is solved at time step k, we choose $\hat{x}_{k-Ne+1}$ as the prior value $\bar{x}_{k-N_e+1}$ for the arrival cost at time step $k+1$.

Similar to the NMPC controller, MHE is the state estimation algorithm based on moving horizon framework. Hence, a crucial limitation of the MHE is that it requires solving computationally expensive optimization problems online. Moreover, the solution time of the MHE affects the stability and performance of NMPC, since MHE provides the state estimates required by the controller. Similar to the asNMPC, Zavala et al. [116] proposed the advanced step MHE (asMHE) on the basis of NLP sensitivity. The algorithm is summarized as:

1. **Background calculation:** Having $\hat{x}_k$ and u_k, compute the disturbance-free extrapolation of the state $\tilde{x}_{k+1}$ and the corresponding output $\tilde{y}_{k+1}$. Solve an extended MHE problem (3.16) with horizon N_e+1 and output sequence y_{k-N_e}, y_{k-N_e+1}, $\ldots$, y_k, $\tilde{y}_{k+1}$. Let $p_0 = \tilde{y}_{k+1}$ (in (3.9)) and hold the KKT matrix at the solution.

2. **On-line update:** Obtain the true measurement y_{k+1}. Set $p = y_{k+1}$ and compute the fast approximation solution using equation (3.12). Extract the estimated state $\hat{x}_{k+1}$.

3. **Iterate:** Set $k \leftarrow k+1$ and go to background.

3.5 Concluding Remarks

In this chapter, we have summarized advantages and disadvantages of different approaches to DAE-constrained optimization. A simultaneous method, orthogonal collocation on finite elements is used in this dissertation. Thus, the DAE-constrained optimization problem is converted into large scale and sparse NLPs. IPOPT algorithm is used to solve the large scale NLPs. Moreover, the concept of NLP-sensitivity is introduced to provide fast approximation of the solution. Finally two moving-horizon-based applications, NMPC and MHE, are described. In addition, sensitivity-based advanced step algorithm is formulated for both NMPC and MHE to reduce the computational delay online.

Chapter 4

Advanced Step NMPC for Air Separation Unit

In this chapter, we utilize the methods discussed in the previous chapter to control a large scale air separation unit (ASU). First, simulation study of the set-point tracking NMPC is shown and better performance against linear MPC is observed. Then, economically-oriented NMPC which takes advantage of the varying electricity price is studied and around 6% cost reduction is achieved. Moreover, multi-scenario formulation is introduced to deal with uncertainties in electricity price information. In these simulations, asNMPC algorithm reduces the online computational delay by two orders of magnitude.

4.1 Introduction

Air separation units (ASUs) are cryogenic distillation systems that produce high purity nitrogen, oxygen and argon. Due to the high demand of these commodity materials, the ASU has become a crucial technology in many processes including next generation power plants. These units involve single or multiple energy-intensive cryogenic columns running at extremely low temperatures (-170 to -195 °C). As a consequence, the required degree of energy integration in these systems is quite high, which makes them difficult to operate. In addition, as the electricity price fluctuates significantly, the operating conditions of the

ASUs need to be switched frequently. As expected, there is significant economic interest in reducing the operating costs of ASUs through advanced process control technology.

So far, the dominating control practice in ASU processes has been to adapt traditional regulatory controllers to maintain good performance. Today's trend has shifted towards multivariable control strategies such as MPC [98, 108]. Despite the success of linear MPC strategies, it is clear that their applicability to dynamic processes operating over wide operating regions would be strongly affected by the limited predictive capabilities of linear input-output *empirical* models. In the last few years, there has been an increasing interest to apply NMPC with rigorous dynamic models in ASU processes. Chen et al. [26] have addressed the on-line computational expense of NMPC through the development of models of reduced complexity based on compartmentalization concepts.

In addition, one difficulty that energy-intensive plants like ASU face during operation is the fluctuating power price at which utility company supplies to the plants. The electricity is not readily stored and must be used or wasted after it is produced. In order to maintain stable operation of the electricity grid, power plants must ramp up and down frequently in order to match generating capacity to current demand. Therefore, the power price is often subject to high fluctuations, which may significantly increase the total operational cast for energy-intensive plants. Ierapetritou [54] proposed a scheduling scheme for ASU plant considering the fluctuating power price. However, the ASU is represented by a simplified empirical model and no dynamics are considered.

To simplify the simulation study, we assume all the states are measurable in this chapter. Therefore no state estimator is needed. We study both set-point tracking and economical NMPC controllers with state-feedback for an ASU process. In particular, the economically-oriented NMPC directly minimizes the operational cost by considering the fluctuated power price. Moreover, both the controllers are designed based on the detailed first-principle

dynamic model of the ASU to cope with a wide operating range. Finally, the asNMPC algorithm is used to reduce the computational delay.

4.2 Air Separation Unit Model

We consider an air separation unit that produces nitrogen with at least 99.9% purity, and oxygen with at least 96% purity. The impurity associated with the oxygen is argon. The specifics of the ASU process under study were reported in [18, 110]. Here, ambient air is compressed in a large multistage compressor with intercooling followed by removal of water, carbon dioxide and hydrocarbons and by cooling in a multistream heat exchanger. As sketched in Figure 4.1, this air feed mixture of oxygen, nitrogen and argon is then split into two substreams. The first stream consists of pure air entering the bottom of the high pressure column (MA) and the second one consists of expanded air entering the 20^{th} tray of the low pressure column (EA). Crude nitrogen gas (GN) from the main heat exchanger is also added to the 25^{th} tray of the high pressure column. The high pressure column (bottom) contains 40 trays and operates at 5-6 bars, while the low pressure column (top) operates at 1-1.5 bars and also contains 40 trays. The reboiler of the low pressure column is integrated with the condenser of the high pressure column. The main products of the high pressure column are pure nitrogen (PNI) ($> 99.99\%$) and crude liquid oxygen ($\sim 50\%$). The crude oxygen stream is fed into the 19^{th} tray of the low pressure column. In addition, an intermediate side stream from the 15^{th} tray of the high pressure column (LN) is fed to the top of the low pressure column. A high purity separation is achieved in the low pressure column, leading to nitrogen gas with $\sim 99\%$ purity and oxygen (POX) with $\sim 97\%$ purity as products.

Mathematical modeling of dynamic distillation columns is a well studied area [13, 18,

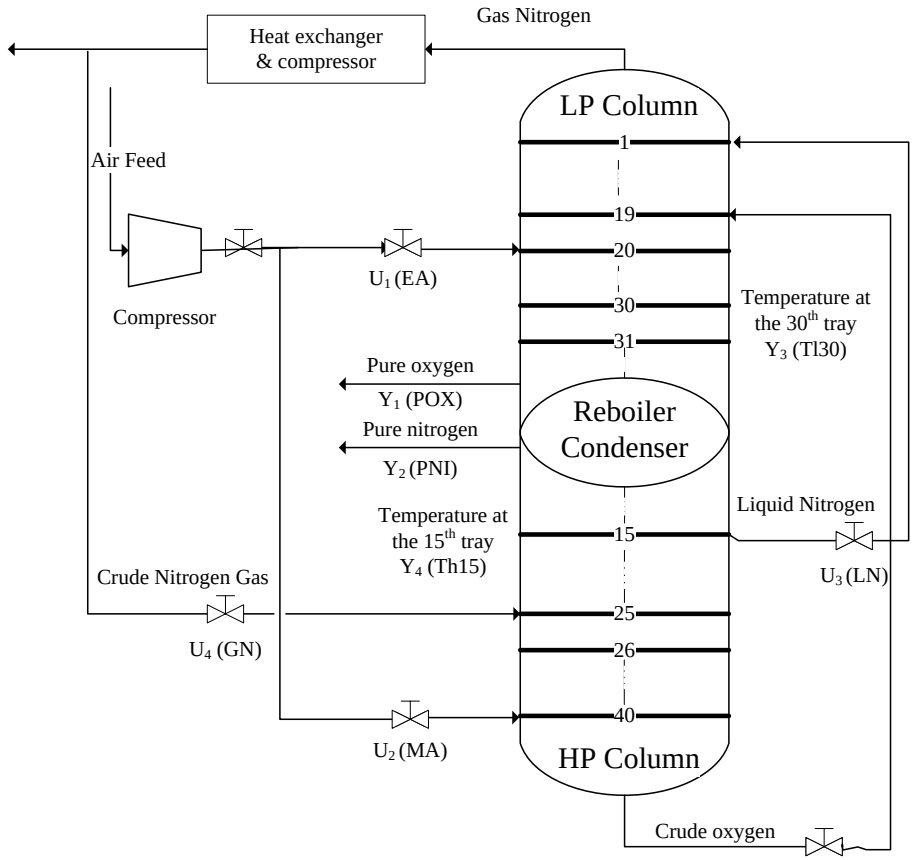

Figure 4.1: Simplified flowsheet of ASU studied.

32, 63, 90, 98]. Here, a detailed ASU model is derived under the following simplifying assumptions:

- Negligible vapor holdups on each tray, as the dynamics of the vapor phase are much faster than that of liquid phase.
- Ideal vapor phases.
- Well-mixed entering streams.
- Constant pressure drop on each tray.
- Equilibrium stage model.

The ASU model is represented by tray-by-tray equations consisting of mass balances (overall and component balances of nitrogen, oxygen and argon), energy balances, phase equilibrium, hydraulic and summation equations.

Overall Mass Balance

$$\frac{dM_i}{dt} = L_{i-1} + V_{i+1} - L_i - V_i + F_i \tag{4.1}$$

where i is the index of each tray, starting from the top of the column. M_i is the liquid mole holdup ($[mol]$) on tray i, L_i and V_i are liquid and vapor molar flow rates, respectively and F_i is the molar feed ($[\frac{mol}{min}]$). If there is no feed to tray i, then $F_i = 0$. In this case, the only nonzero values of F_i are those corresponding to expanded air (EA, U_1), pure air (MA, U_2), liquid nitrogen (LN, U_3), crude gas nitrogen (GN, U_4) and crude oxygen stream as shown in Figure 4.1.

Component Balances

$$\frac{d(M_i x_{i,j})}{dt} = L_{i-1} x_{i-1,j} + V_{i+1} y_{i+1,j} - L_i x_{i,j} - V_i y_{i,j} + F_i x_{i,j}^f \tag{4.2}$$

where $j \in \text{COMP}$ is the index of each component, $x_{i,j}$ and $y_{i,j}$ are component mole fractions in the liquid and vapor phases, $x^f_{i,j}$ are the mole fractions of the feed. Alternatively, we can rewrite equation (4.2) using equation (4.1) as follows:

$$M_i \frac{dx_{i,j}}{dt} = L_{i-1}(x_{i-1,j} - x_{i,j}) + V_{i+1}(y_{i+1,j} - x_{i,j}) - V_i(y_{i,j} - x_{i,j}) + F_i(x^f_{i,j} - x_{i,j}) \quad (4.3)$$

Energy Balance

$$\frac{d(M_i h^L_i)}{dt} = L_{i-1}h^L_{i-1} + V_{i+1}h^V_{i+1} - L_i h^L_i - V_i h^V_i + F_i h^f_i \quad (4.4)$$

where $h^L_i = f^{hl}(T_i, P_i)$ and $h^V_i = f^{hv}(T_i, P_i)$ are liquid and vapor enthalpies in $[\frac{kJ}{mol}]$, and h^f_i is the feed enthalpy. Expressions and data to compute h^V_i and h^L_i can be found in a number of standard references. For this study, we use the information in [96]. Using equation (4.1), the energy balance (4.4) can be rewritten as:

$$M_i \frac{dh^L_i}{dt} = L_{i-1}(h^L_{i-1} - h^L_i) + V_{i+1}(h^V_{i+1} - h^L_i) - V_i(h^V_i - h^L_i) + F_i(h^f_i - h^l_i) \quad (4.5)$$

Summation Equation

$$1 = \sum_{j \in \text{COMP}} y_{i,j} \quad (4.6)$$

Hydraulic Equation

$$L_i = k_d M_i \quad (4.7)$$

where $k_d = 0.5\ min^{-1}$ is a tuning constant determined from empirical data.

Vapor-Liquid Equilibrium

$$y_{i,j} p_i = \gamma_{i,j} x_{i,j} p^{sat}_{i,j} \quad (4.8)$$

where p_i is the total pressure on tray i, and $p^{sat}_{i,j} = f^p(T_i)$ is the saturation pressure of pure component j on tray i. Expressions to compute $p^{sat}_{i,j}$ can be found in a number of standard

references. For this study, we used the information in [96]. Symbol $\gamma_{i,j}$ denotes the liquid activity coefficient describing the non-ideal vapor-liquid equilibrium calculated from,

$$\gamma_{i,\mathrm{N_2}} = \exp[\frac{A_{\mathrm{N_2,O_2}} x_{i,\mathrm{O_2}}^2 + A_{\mathrm{N_2,Ar}} x_{i,\mathrm{Ar}}^2 + (A_{\mathrm{N_2,O_2}} + A_{\mathrm{N_2,Ar}} - A_{\mathrm{O_2,Ar}}) x_{i,\mathrm{O_2}} x_{i,\mathrm{Ar}}}{RT_i}] \tag{4.9a}$$

$$\gamma_{i,\mathrm{O_2}} = \exp[\frac{A_{\mathrm{N_2,O_2}} x_{i,\mathrm{N_2}}^2 + A_{\mathrm{O_2,Ar}} x_{i,\mathrm{Ar}}^2 + (A_{\mathrm{N_2,O_2}} + A_{\mathrm{O_2,Ar}} - A_{\mathrm{N_2,Ar}}) x_{i,\mathrm{N_2}} x_{i,\mathrm{Ar}}}{RT_i}] \tag{4.9b}$$

$$\gamma_{i,\mathrm{Ar}} = \exp[\frac{A_{\mathrm{N_2,Ar}} x_{i,\mathrm{N_2}}^2 + A_{\mathrm{O_2,Ar}} x_{i,\mathrm{O_2}}^2 + (A_{\mathrm{N_2,Ar}} + A_{\mathrm{O_2,Ar}} - A_{\mathrm{N_2,O_2}}) x_{i,\mathrm{N_2}} x_{i,\mathrm{O_2}}}{RT_i}] \tag{4.9c}$$

Here R is the ideal gas constant and the coefficients $A_{j,k}$ account for the liquid phase interactions between components j and k. These can be calculated using the Margules equations as reported in [13].

Equations (4.1), (4.3), (4.5)- (4.9) lead to a Differential Algebraic Equation (DAE) system, with the differential variables M_i, $x_{i,j}$ and h_i^L. Eliminating the dynamics of the vapor phase reduces the stiffness of the model but makes the DAE system index 2. In other words, we found that the algebraic variable V_i cannot be explicitly recovered from the algebraic equations.

Solving the index 2 DAE system is often difficult as consistent initial conditions need to be determined. In order to avoid this, the system was reduced to index 1 by differentiating the summation equation (4.6) with respect to time:

$$0 = \sum_{j \in \mathrm{COMP}} \frac{dy_{i,j}}{dt} = \sum_{j \in \mathrm{COMP}} \left[\frac{dK_{i,j}}{dt} x_{i,j} + K_{i,j} \frac{dx_{i,j}}{dt} \right] \tag{4.10}$$

where we define $K_{i,j} = \gamma_{i,j} p_{i,j}^{sat} / p_i$ to simplify the notation. As a result, $K_{i,j}$ is a function of temperature T_i and component concentration in each tray $x_{i,j}$. Applying the chain rule to (4.10), we obtain:

$$0 = \sum_{j \in \mathrm{COMP}} x_{i,j} \left[\frac{\partial K_{i,j}}{\partial T_i} \frac{dT_i}{dt} + \sum_{k \in \mathrm{COMP}} \frac{\partial K_{i,j}}{\partial x_{i,k}} \frac{dx_{i,j}}{dt} \right] + \sum_{j \in \mathrm{COMP}} K_{i,j} \frac{dx_{i,j}}{dt} \tag{4.11}$$

By combining equations (4.11) and (4.3) and introducing the dummy variables $\bar{x}_{i,j}$ and $\bar{T}_i$, we obtain:

$$\bar{x}_{i,j} := \frac{dx_{i,j}}{dt} = \frac{L_{i-1}(x_{i-1,j} - x_{i,j}) + V_{i+1}(y_{i+1,j} - x_{i,j}) - V_i(y_{i,j} - x_{i,j}) + F_i(x^f_{i,j} - x_{i,j})}{M_i} \tag{4.12}$$

$$\bar{T}_i := \frac{dT_i}{dt} = -\frac{\sum_{j\in\text{COMP}} \left[x_{i,j} \sum_{k\in\text{COMP}} (\frac{\partial K_{i,j}}{\partial x_{i,k}} \bar{x}_{i,k}) + K_{i,j}\bar{x}_{i,k} \right]}{\sum_{j\in\text{COMP}} x_{i,j} \partial K_{i,j}/\partial T_i} \tag{4.13}$$

Note that by changing the left hand side of the the energy balance (4.5) we can rewrite this as an algebraic equation in terms of the dummy variables:

$$M_i(\frac{\partial h^L_i}{\partial T_i}\bar{T}_i + \sum_{j\in\text{COMP}} \frac{\partial h^L_i}{\partial x_{i,j}}\bar{x}_{i,j}) = L_{i-1}(h^L_{i-1} - h^L_i) + V_{i+1}(h^V_{i+1} - h^L_i) - V_i(h^V_i - h^L_i) + F_i(h^f_i - h^l_i) \tag{4.14}$$

The reformulated index 1 DAE system now consists of equations (4.1), (4.3), (4.6)-(4.12), (4.13) - (4.14) for each tray and component. The ASU model contains 320 differential equations and 1200 algebraic equations with M_i and $x_{i,j}$ as differential variables.

4.3 Set-Point Tracking NMPC

In this section, we evaluate the performance of the set-point tracking asNMPC controller for the ASU with changing production demands. To design the controller, we choose the molar flow rate of pure oxygen (POX-Y_1) and the molar flow rate of pure nitrogen (PNI-Y_2) as output variables. The objective is to force the outputs to follow their set-points while satisfying purity requirements.

Current ASU technology allows product composition to be measured directly. Moreover, nonlinear transformation of these measurements are commonly used for linear MPC con-

trollers. We prefer to use the tray temperatures because they are a cheap, continuous indirect composition measurement common to distillation control, and we can also choose more sensitive intermediate tray temperatures that can add more robustness to the controller. In this study, temperatures at several sensitive trays are chosen as output variables. In particular, we choose the temperature at 30^{th} tray in the low pressure column (Tl30-Y_3), and temperature at the 15^{th} tray in the high pressure column (Th15-Y_4). Four stream flow rates are considered as manipulated variables. This includes the expanded air feed (EA-U_1), main air feed (MA-U_2), reflux liquid nitrogen (LN-U_3) and crude gas nitrogen (GN-U_4). All set-points (Y_{set} and U_{ref}) and reference values for the manipulated variables were determined through steady-state simulations with AspenPlus.

In this section, the NMPC (3.14) is formulated as the set-point tracking formulation. As a result, the quadratic form

$$Min_{U_i} \quad \sum_{k}^{k+N} \left((Y_i - Y_{set})^T \mathscr{Y} ((Y_i - Y_{set}) + (U_i - U_{ref})^T \mathscr{U} (U_i - U_{ref})\right) \tag{4.15}$$

is used as the objective function. Here Y_i is a vector of controlled variables, U_i is a vector of manipulated variables and Y_{set} and U_{ref} are the set-points and reference values for the output and manipulated variables, respectively. The symbols $\mathscr{Y}$ and $\mathscr{U}$ denote diagonal weighting matrices. The diagonal element in $\mathscr{U}$ corresponding to each manipulated variable is set to 1×10^{-5} except the one corresponding to EA-U_1, which is set to 1×10^{-4}. The diagonal elements in $\mathscr{Y}$ corresponding to Tl30 and Th15 are set to 3×10^{-2} while the elements corresponding to POX and PNI are 1×10^{-4}. N is the prediction horizon length with a total length of 100 minutes distributed over 20 finite elements. The control horizon is chosen to be the same as the prediction horizon and the sampling time is set to 5 minutes. After full discretization of the dynamic optimization problem using Radau collocation points on finite elements as discussed in Chapter 3, the resulting NLP contains $117,140$ variables and $116,900$ constraints. However, the NLP is very sparse with up to 5

nonzero entries per row in the Jacobian, and 4 nonzero entries per row in the Hessian.

In this section, we consider two case studies to demonstrate the performance of the proposed asNMPC controller. The first case considers *ramp* changes of the production rate set-point. Here, we contrast the performance of asNMPC controller against that of a MPC controller that uses a fixed linearized dynamic process model. The linear model is identified using matlab system identification tool box from a set of step response data. With this, we demonstrate that, despite the error introduced by NLP sensitivity approximations, the asNMPC controller can still handle the nonlinear process dynamics over a wide range of operating conditions. The second case considers *step* changes of the production rate set-point in the presence of random disturbances. Here, we compare the performance of asNMPC with that of an hypothetical or ideal NMPC controller (without computational delay).

4.3.1 Ramping change of Set-Point

In this scenario, the ASU starts from a nominal steady-state computed from simulation. The oxygen and nitrogen production rate set-points (and associated reference values for the manipulated variables) are reduced by 30% through a ramp change from $t = 30$ to $t = 60$ minutes. After this, they undergo a ramp increase from $t = 1000$ to $t = 1030$ back to their original values. For this simulation, we assume that the model is perfect and no unmeasured disturbances are present. A total of 400 moving horizon optimization problems was solved. We set the initial barrier parameter in equation (3.10) to $\mu = 10^{-7}$ in order to promote fast convergence of the solver. The solver took 5 to 8 iterations and 120 to 220 CPU seconds to converge with a tight tolerance of 1×10^{-6}. All simulations were performed on an Intel DuoCore 2.4GHz personal computer. Based on these computational times, it is clear that a conventional implementation of NMPC would introduce a feedback delay of almost 4

minutes. The asNMPC controller brings the online computational time down to around 1 CPU second, corresponding to the time required to perform a single backsolve with the fixed KKT matrix. This online computational time is over 100 times less than the full solution of the NLP.

The closed-loop profiles for the first case study are shown in Fig. 4.2 and 4.3. Note that the asNMPC controller is able to track the production rate ramps well while maintaining the tray temperatures close to their set-points (compare the dashed and dot-dashed lines). To illustrate the benefits of the NMPC controller and its nonlinear dynamic model, we considered the same controller but with a linear dynamic model. Here the linear process model is derived by identifying the data generated by dynamic simulation of the rigorous nonlinear model using MATLAB. The linear Multiple Input Multiple Output (MIMO) model is then obtained by combining all the Multiple Input Single Output (MISO) ARX models between inputs and outputs. Each ARX model is chosen with a structure that achieves the smallest Akaike Information Criteria (AIC) [21]. In order to assess the impact of the nonlinear model within the NMPC controller, the prediction horizon and sampling times are also set to 100 minutes and 5 minutes, respectively.

From Fig. 4.2 and 4.3 note that the asNMPC controller keeps the controlled variables close to their set-points. On the other hand, the controller with the linear model presents large deviations while asNMPC recovers quickly. This is mainly due to the fact that the asNMPC controller can still handle the nonlinear process dynamics due to the background update of the KKT matrix at each time step.

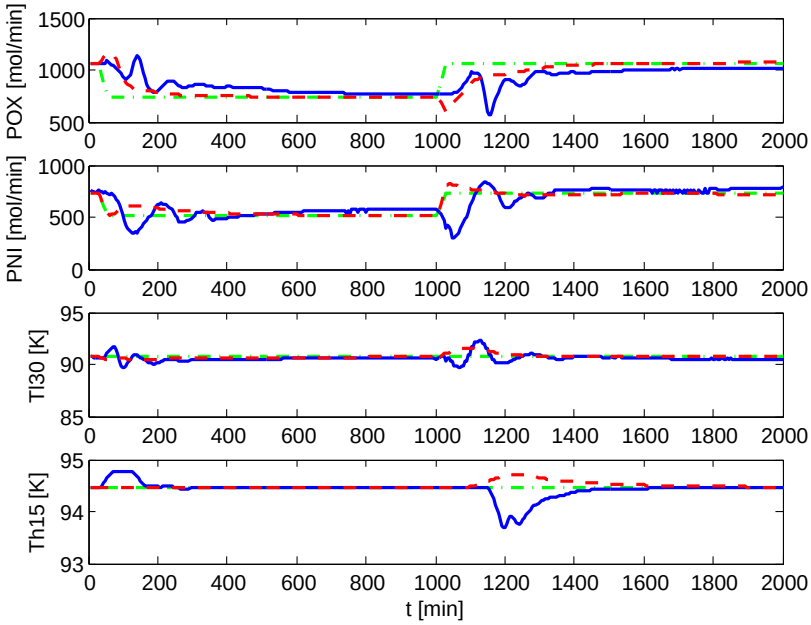

Figure 4.2: Controlled variables for case one. The dot-dashed line is the set-point, the solid line is the linear controller profile and the dashed line is the asNMPC profile.

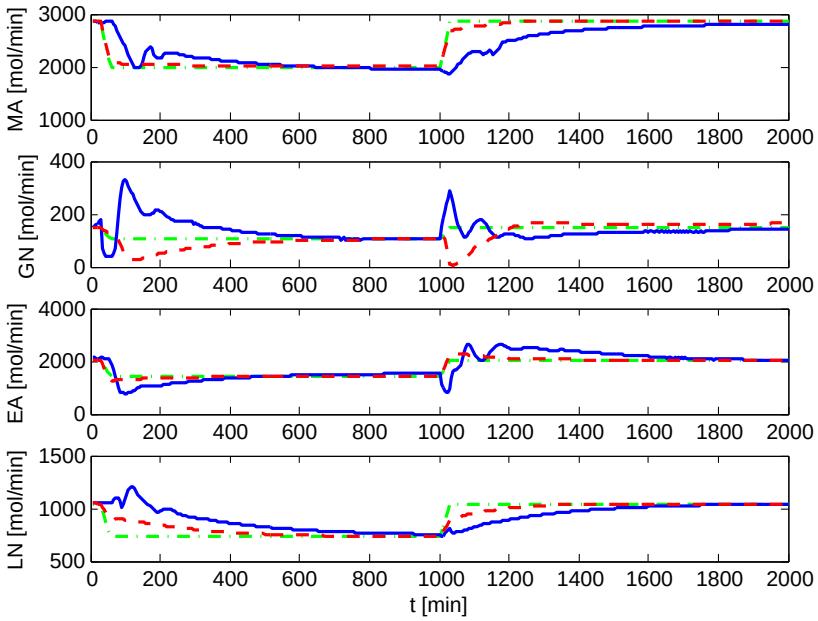

Figure 4.3: Manipulated variables for case one. The dot-dashed line is the reference value, the solid line is the linear controller profile and the dashed line is the asNMPC profile.

4.3.2 Step Change of Set-Point

The first case demonstrates that asNMPC with a rigorous nonlinear model is expected to have better performance over a wide range than a controller based on a fixed linear model. In the second case study, the set-points of the controlled variables undergo a more aggressive step change. The profiles are presented in Fig. 4.4 and 4.5. At $t = 30$, the set-points and reference values are instantaneously reduced by 30%, and later increased back to their original values at $t = 1000$. In addition, a 5% random disturbance is added to the molar holdups to test the robustness of the controllers. A total of 400 moving horizon problems was solved. For the same barrier parameter μ and tolerance levels, IPOPT takes up to 10 iterations and 240 CPU seconds to converge the NLPs. The time required for the on-line calculation of the asNMPC controller was still around 1 second. In addition, it is worth mentioning that our linear controller with the same tuning parameters tends to be unstable for this case.

In this case study, we also compare the performance of the asNMPC controller with that of the hypothetical ideal NMPC controller. As shown in Fig. 4.4 and 4.5, the asNMPC controller is able to reject the random disturbances during both transients. Moreover, note from Fig. 4.6 that the product purities are satisfied during the entire time frame even though they are controlled indirectly through the tray temperatures. Compared to the product purities, the temperature profiles seem to show larger deviations due to the more aggressive step change. Finally, it is clear that the asNMPC controller yields very good sensitivity approximations despite relatively large disturbances.

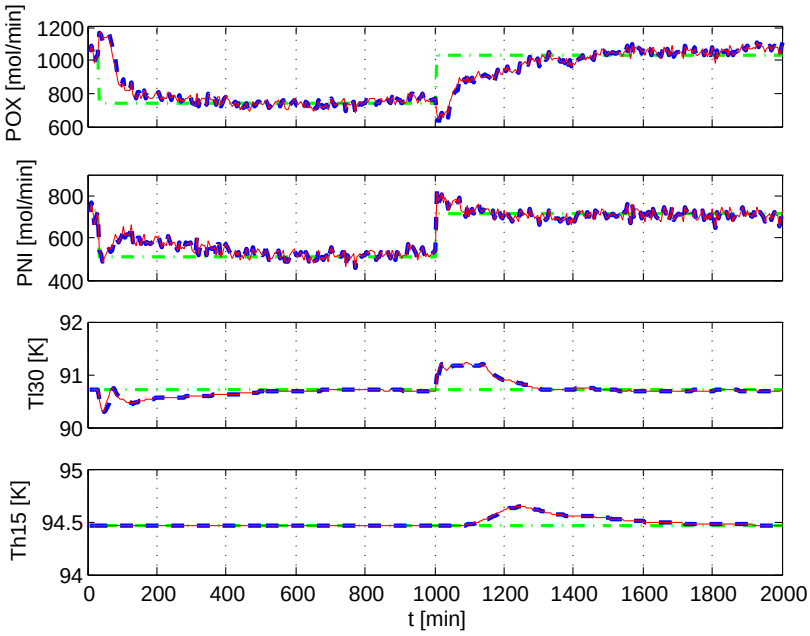

Figure 4.4: Controlled variables for case two. The dot-dashed line is the set-point, the thin solid line is the ideal NMPC profile and the dashed line is the asNMPC profile.

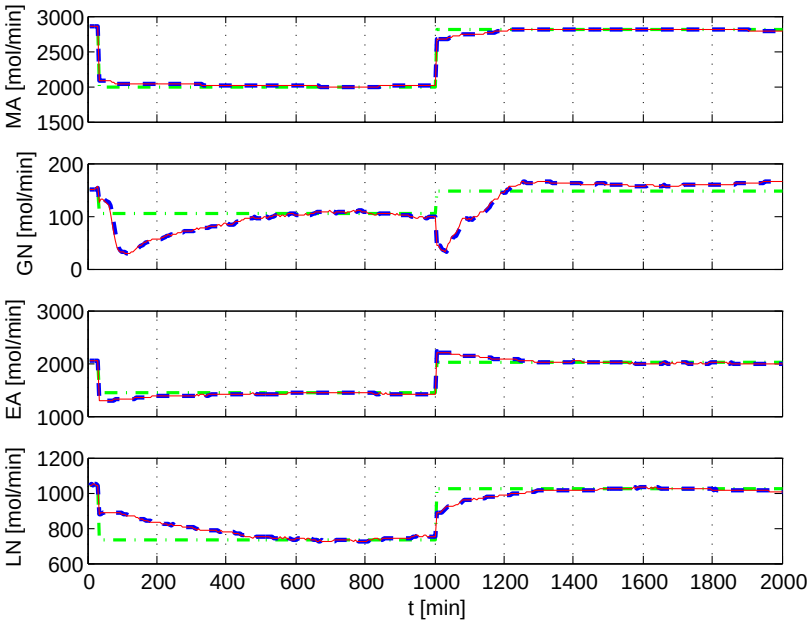

Figure 4.5: Manipulated variables for case two. The dot-dashed line is the reference value, the thin solid line is the ideal NMPC profile and the dashed line is the asNMPC profile.

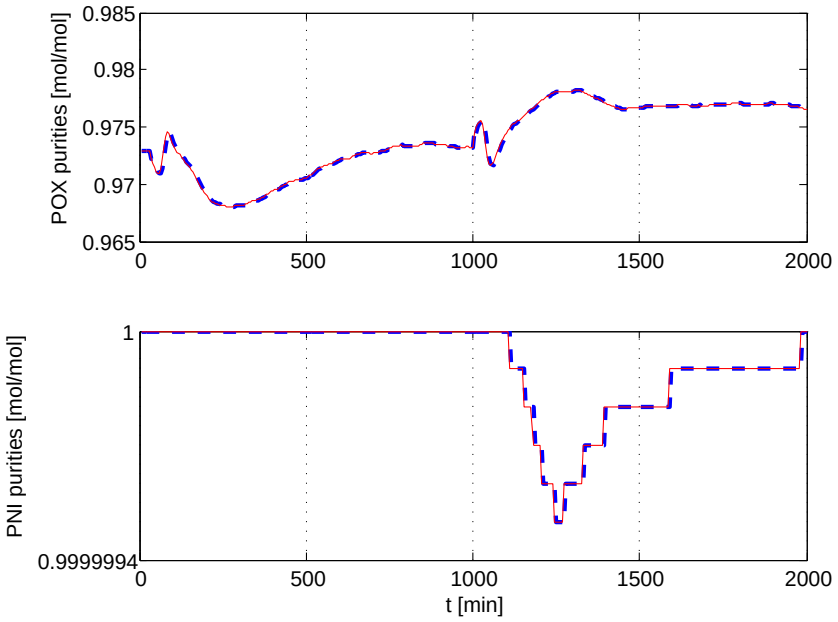

Figure 4.6: Product purities of case two. The thin solid line is the ideal NMPC profile and the dashed line is the asNMPC profile.

4.4 Economically-Oriented NMPC

The air separation unit is an energy intensive application because the ambient air needs to be cooled to extremely low temperature (-170°C to -195 °C). Since the raw material, ambient air is free, the major operational cost is the energy consumed to cool the air. On the other hand, the energy price is often subject to high fluctuations throughout the time of a day. This creates an opportunity to minimize the average utility cost by changing the operating conditions of the ASU. In this case, it is difficult to apply the two-layered optimization structure because the electricity price may change at a high frequency (every hour). Thus, in this section, we use the economically-oriented NMPC that directly minimizes the operational cost to take the advantage of the varying electricity price.

4.4.1 Electricity Pricing Scheme

The price of electricity depends on many different factors such as time of day, location and so on. It is mainly because, the electricity is not readily stored and has to be used or wasted after its production. As a result, utility companies resort to complex pricing schemes to allocate resources, which have been reported by Baumrucker and Biegler [9] and Ierapetritou et al. [54]. They include *fixed rate structure* and *time of day* pricing schemes [9] which are mainly for individual households. In this section, we consider more complicated *day ahead pricing* and *real-time pricing* schemes which are mainly for industrial sectors.

- *Day ahead pricing* is a strategy that changes the electricity price every hour. Utility companies estimate the production cost and the energy demand for the next day to come up with the energy price they charge. It is usually published 24 hours in advance. It is similar to the commodities futures contract price.

- *Real time pricing* also changes the electricity price hourly, but the price is determined by the real time market. This is similar to the spot market price.

Fig. 4.7 shows the day ahead price and real time price of the day 3/23/2010 from Ameren, a utility company serving St. Louis area. The price information is found on the website (https://www2.ameren.com/RetailEnergy/realtimeprices.aspx). We see that the day ahead prices change smoothly, while the real time prices vary drastically and even a negative price occurs for a two-hour period.

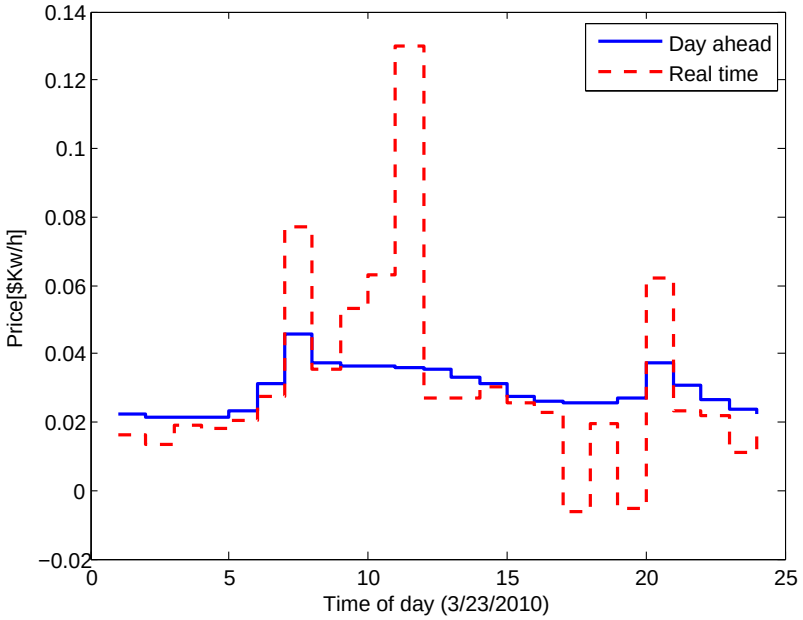

Figure 4.7: Day ahead price and real time price from Ameren.

4.4.2 Economical NMPC with Day Ahead Pricing for ASU

In this section, the NMPC (3.14) is formulated to minimize the operational cost of the ASU. Thus,

$$Min_{U_i} \quad \sum_{k}^{k+N} (U(1)_i + U(2)_i) \times \text{ele}_i + \text{reg}_i. \tag{4.16}$$

is used as the objective function. Here $U(1)$ and $U(2)$ correspond to the two air feed flowrate EA and MA in Fig. 4.1, respectively. Since majority of energy is used to compress the air, we consider the operational cost is proportional to the two inlet air flows multiplied by the varying electricity price. ele_i is the electricity price at time step i. $\text{reg}_i. = (Y_i - Y_{set})^T \mathscr{Y} ((Y_i - Y_{set}) + (U_i - U_{ref})^T \mathscr{U} (U_i - U_{ref})$ is a regularization term which is the same as used in the set-point tracking formulation (4.15) in the previous section. This regularization term is used to improve the problem formulation. Without it, the optimization problem is likely to be ill-conditioned and can not guarantee a unique solution. In order to adjust to the hourly varying electricity price, the horizon length N is changed to 120 minutes distributed over 20 finite elements. Consequently, the sampling time is 6 minutes. After full discretization, the resulting NLP contains $117,140$ variables and $116,900$ constraints.

In this scenario, we assume that the day ahead pricing scheme is used. Fig. 4.8 shows a 48-hour period electricity price from Ameren (3/23/2010-3/24/2010), which is used in the economical NMPC formulation. It is observed that the price in the day ahead pricing scheme has a very similar shape with a 24-hour period.

For this simulation, the nominal ASU model is used and there is no disturbance. A total of 480 moving horizon problems are solved and the closed-loop plant responses are presented in Fig. 4.9 and 4.10. The change of inlet air flowrate MA and EA follows the inverse trend of the electricity price change. They are decreasing when the electricity price is

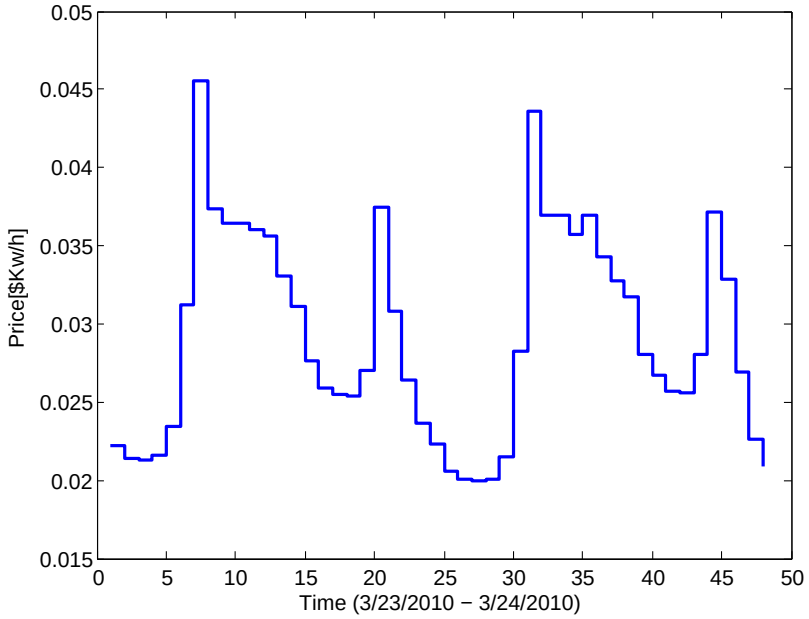

Figure 4.8: Day ahead price for 2 days from Ameren.

high and increasing when the electricity price is low. More specifically, the economically-oriented NMPC with the objective function (4.16) renders an operational cost ($(\mathrm{EA} + \mathrm{MA}) \times$ ele price) of \$12,511 over this 48-hour period, while the operational cost of the set-point tracking NMPC (4.15) with a fixed set-point yields \$13,042. Hence it generates 4.25% cost reduction by using the economically-oriented NMPC.

To solve the ideal NMPC problems, the solver IPOPT took between 8 to 18 iterations and 180 to 380 CPU seconds to converge. On the other hand, the asNMPC algorithm reduces the computational delay to less than 1 CPU second. Therefore, the computational delay is reduced by more than 300 times. Nevertheless, the asNMPC controller yields exactly the same result with the ideal NMPC controller because there is no plant-model mismatch in this scenario and the sensitivity error is 0. This simulation is performed on an Intel Core i7 2.8GHz personal computer. The reason for the computational time varying dramatically is that the optimal solution may have huge changes based on the change of the electricity

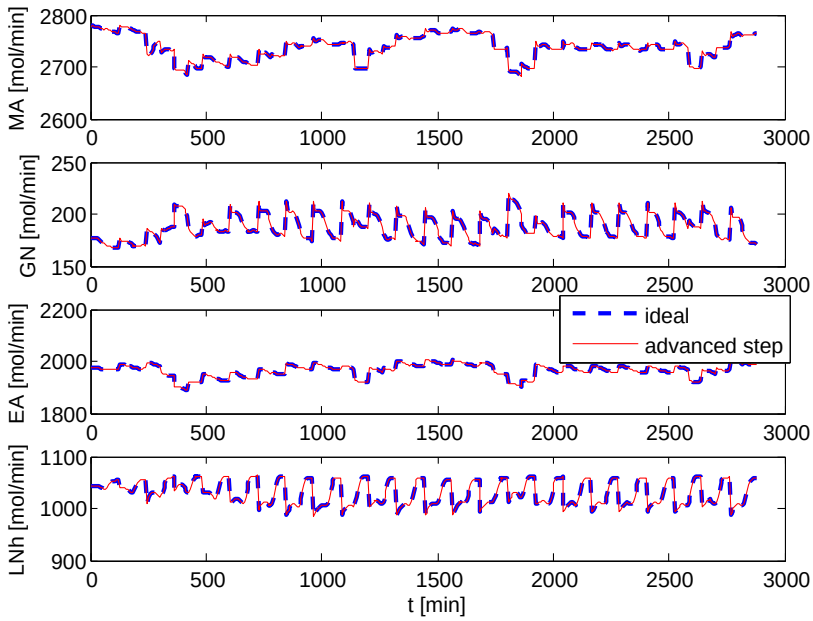

Figure 4.9: Manipulated variables in the day ahead pricing scheme.

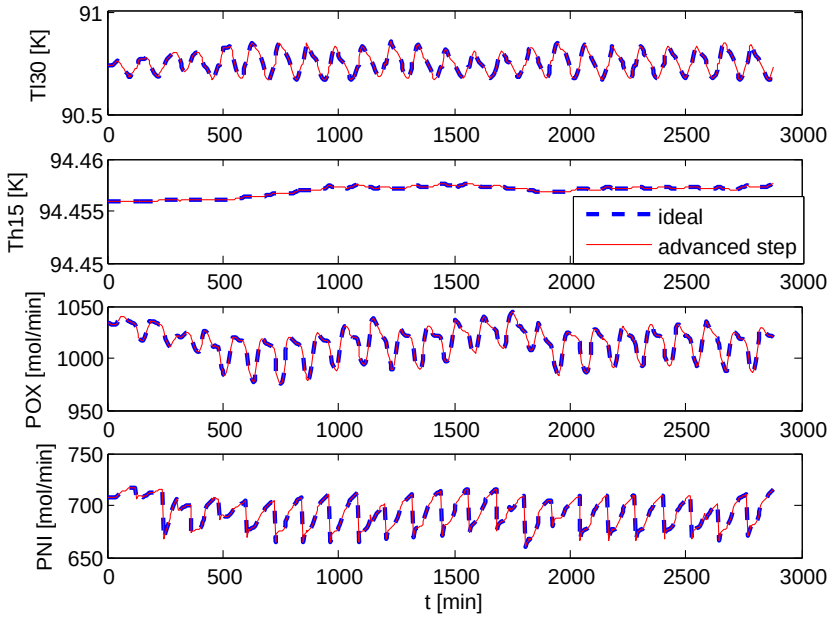

Figure 4.10: Output variables in the day ahead pricing scheme.

price. Unlike the set-point tracking NMPC, IPOPT needs to take longer time to find the optimal solution at each time step.

4.4.3 Economical NMPC with Real Time Pricing for ASU

In this scenario, we assume that the real time pricing scheme is used. In this scheme, the price information is only available at the end of every hour. However, the NMPC formulation (4.16) needs the future price for prediction. As a result, we develop a forecasting model to predict the future price based on the past real time price information. From Fig. 4.11 note that although the real time price fluctuates drastically, it still follows the similar trend with 24-hour period. Hence, we utilize an Autoregressive Integrated Moving Average (ARIMA) model [21], which is a commonly-used model for time series analysis to forecast the future real time price.

To develop the ARIMA model in this study, we use an add-on Microsoft Excel tool XLSTAT which can be found on the website www.xlstat.com. It is indicated that the ARIMA(2,1,1) model has the best balance of model complexity and predicability. Fig. 4.11 shows the prediction result based on historical data on a 96-hour period. Moreover, a new real time price information is available for us at every hour, so we use the moving horizon framework to update the ARIMA(2,1,1) model at every hour to make use the newly available information. After solving the moving horizon problem to update ARIMA model 24 times, we obtain the predicted real time price over 24-hour period as shown in Fig. 4.12. Based on the predicted price, a Monte Carlo simulation with 25 samples is performed to simulate the true real time price, which is shown as the red-dashed line in Fig. 4.12. We assume the result from the Monte Carlo simulation can approximate the true real time price. Therefore it is used to evaluate the proposed economical NMPC formulation.

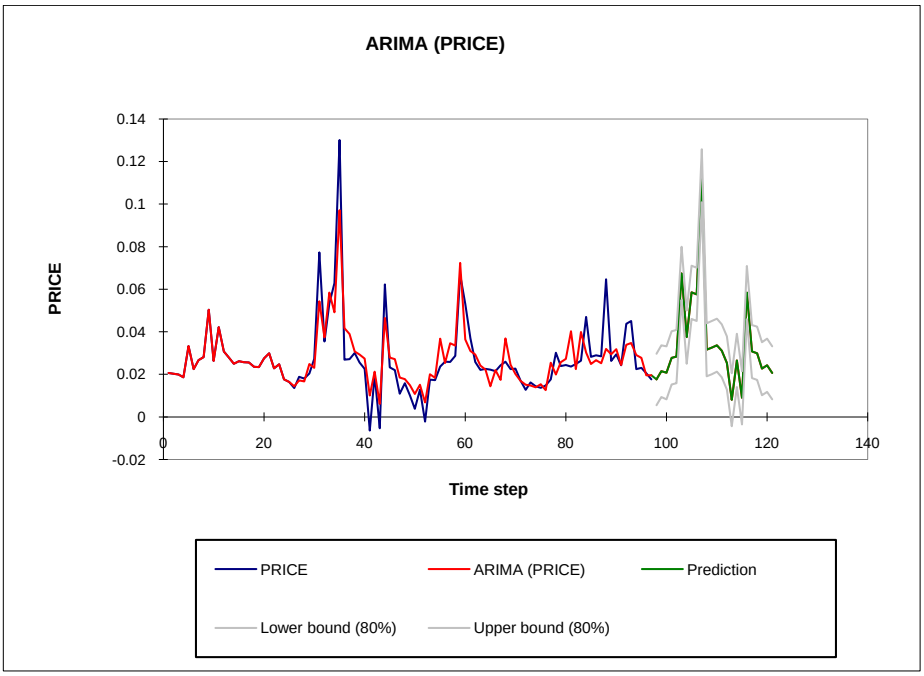

Figure 4.11: Predicted real time price based on 96-hour historical data.

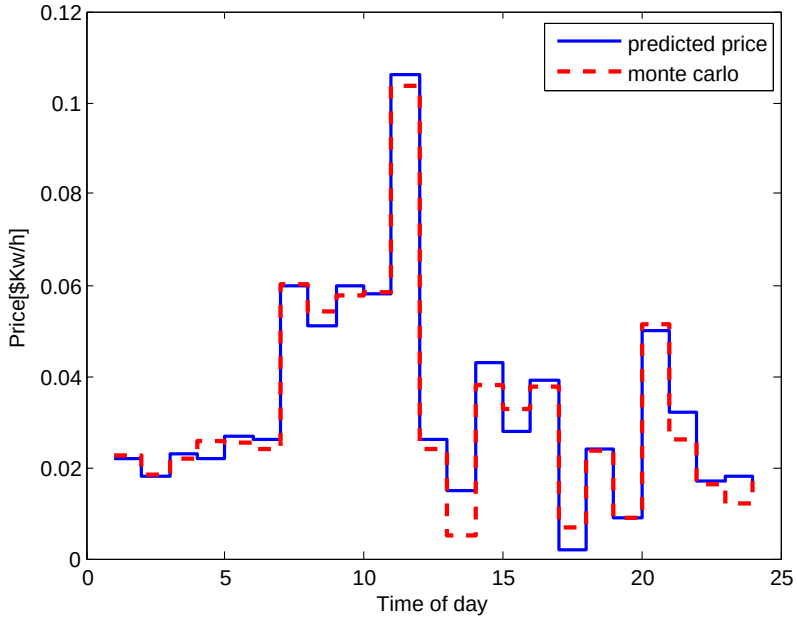

Figure 4.12: Predicted real time price for 24 hours using the updated ARIMA models within moving horizon framework.

The economical NMPC is set to be the same as in the day ahead scenario in section 4.4.2, with the only difference that the ele_i is the predicted price from ARIMA model. A total of 240 moving horizon problems are solved and the closed-loop plant responses are presented in Fig. 4.13 and 4.14. In this case, operational cost ($(EA + MA) \times$ ele price) of the economical NMPC is \$5,939 over the 24-hour period, while the operational cost of the set-point tracking NMPC (4.15) with a fixed set-point yield \$6,306.6. Hence it generates 6.19% cost reduction by using the economically-oriented NMPC in the real time pricing scheme. In addition, it is observed that the asNMPC controller has the same performance with the ideal NMPC.

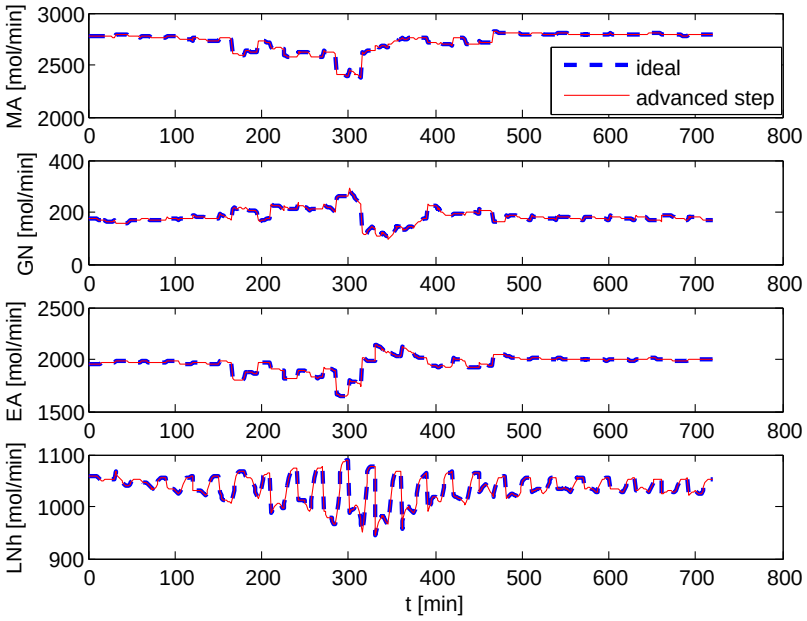

Figure 4.13: Manipulated variables in the real time pricing scheme.

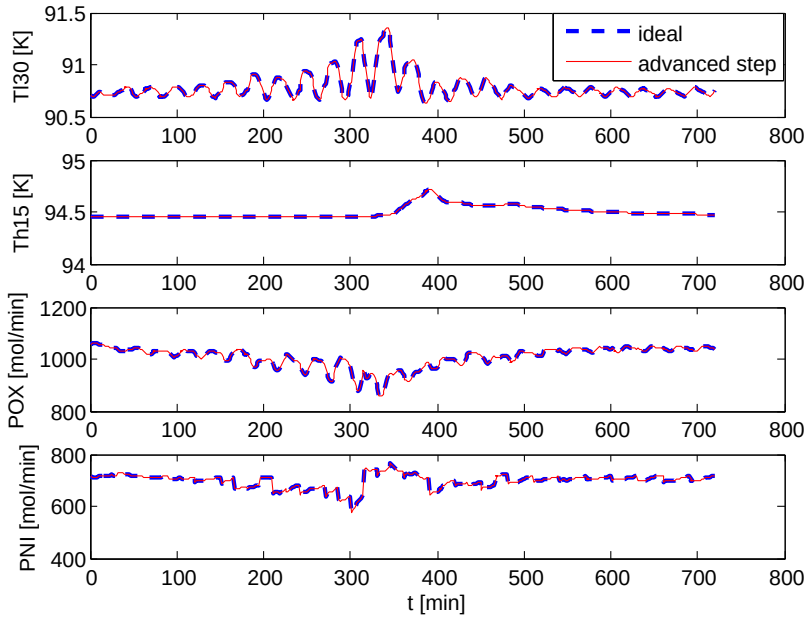

Figure 4.14: Output variables in the real time pricing scheme.

4.4.4 Multi-Scenario formulation to Deal with Uncertainty

Note from Fig. 4.11 that there is a confidence interval associated with the predicted real time price. The predicted real time price with 80% confidence region on the 24-hour period is shown in Fig. 4.15.

To deal with the uncertainty in the predicted price and achieve better performance, we propose a multi-scenario formulation [46].

$$\begin{aligned} & \min && \sum_{s=1}^{Se} w_s \left[\sum_{i=0}^{N-1} (U(1)_{i,s} + U(2)_{i,s}) \times \mathrm{ele}_{i,s} + \mathrm{reg}_{i,s} \right] \\ \text{s.t} \quad & z_{i+1,s} && = f(z_{i,s}, v_{i,s}), \quad i = 0, \ldots, N-1, \; s = 1, \ldots, Se \\ & z_{0,s} && = x_k, \quad 0 = v_{0,s} - v_{0,1} \\ & z_{i,s} && \in \mathbb{X}, \; v_{i,s} \in \mathbb{U}, \end{aligned} \tag{4.17}$$

where Se is the number of scenarios and w_s is the statistic weight associated with each

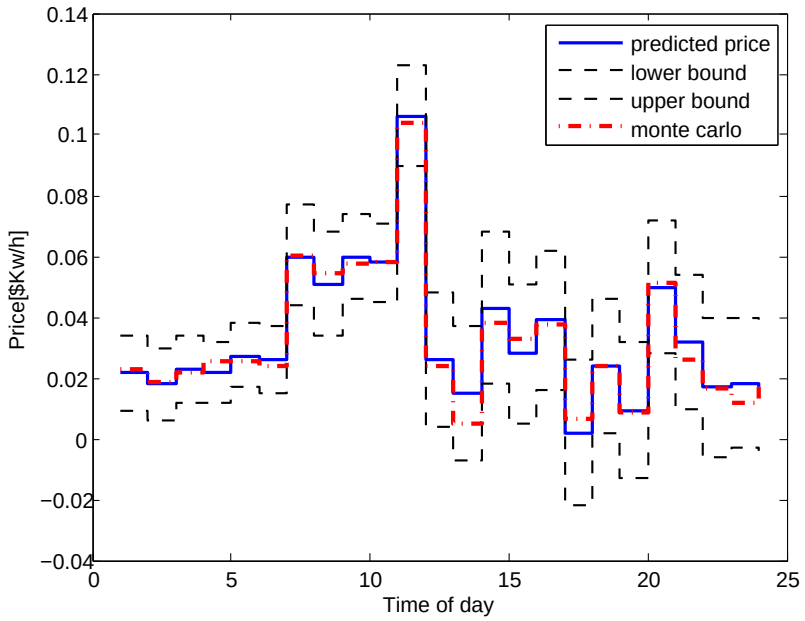

Figure 4.15: Predicted real time price with 80% confidence region for 24 hours

scenario. The uncertain electricity prices in the objective function are spread into different scenarios. In each scenario, the control action is determined to minimize the cost function. In order to ensure that the calculated control action is feasible for all the scenarios, the constraint $0 = v_{0,s} - v_{0,1}$ forces that the first control action to be the same in all scenarios which is implemented into the plant.

In this simulation, three different pricing scenarios are used, including the predicted price with weight $w_1 = 0.6$, the upper and lower bound of the predicted price with weights $w_2 = w_3 = 0.2$. The regularization term in each scenario is chosen to be the same as that used in the day ahead pricing scenario. A total of 240 moving horizon problems are solved and the closed-loop plant responses are presented in Fig. 4.16 and 4.17. The operational cost over the 24-hour period is \$5,912 for this multi-scenario formulation, an additional \$27 cost reduction compare to the single scenario formulation in the section 4.4.3, which has only the expected values. Note that this is a preliminary simulation result, more analysis

regarding the statistical performance is left for our future work.

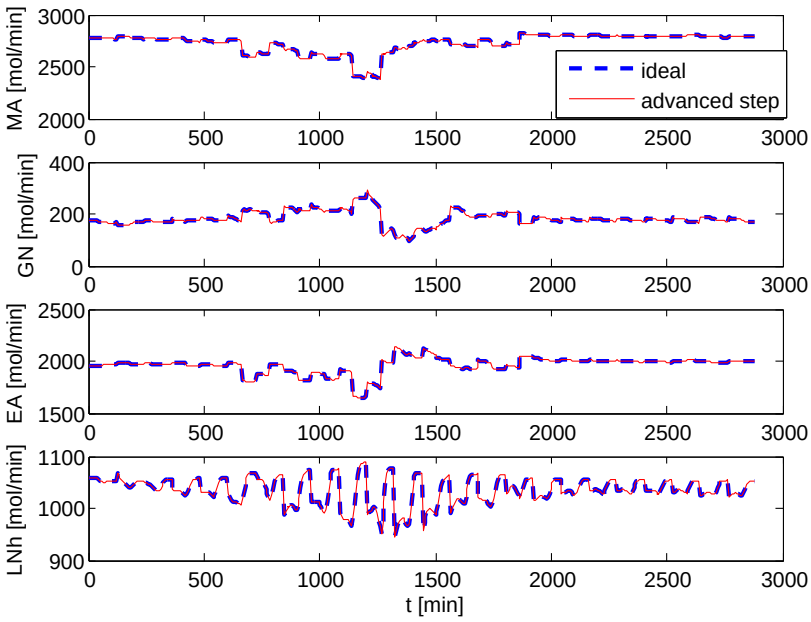

Figure 4.16: Manipulated variables with the multi-scenario formulation.

After full discretization, the multi-scenario optimization problem with three scenarios leads to a NLP contains 351,396 variables and 350,700 constraints. For each NLP problem, IPOPT took 15-30 CPU minutes for the background calculation, while sensitivity update took around 1.5 CPU seconds. Hence the online computation time is reduced by at least 1000 times with virtually no loss in performance. This simulation is performed on an Intel Core i7 2.8GHz personal computer.

4.5 Concluding Remarks

In this chapter, we have developed a first-principle dynamic model for a two-column cryogenic ASU. Simulation studies show that set-point tracking NMPC based on this model can

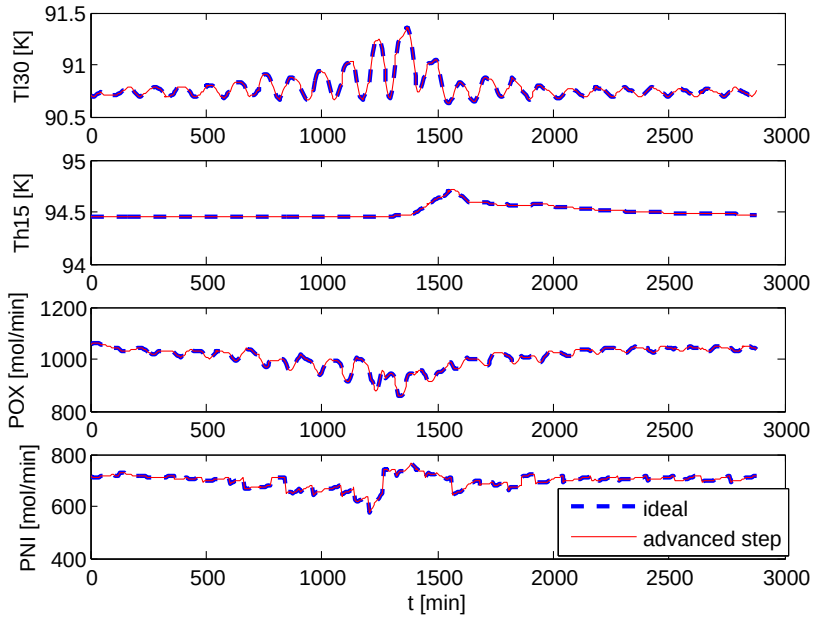

Figure 4.17: Output variables with the multi-scenario formulation.

operate the ASU for a wide range of production rate, which may be problematic for linear MPC with empirical models. Moreover, an economically-oriented NMPC that directly minimizes the operational cost is also proposed to take the advantage of the fluctuating electricity price. ARIMA models based on moving horizon framework are proposed to forecast the future real time price. Moreover, multi-scenario formulation is developed to deal with the uncertainty in the forecasted price. It is observed that the economically-oriented NMPC is able to reduce the operational cost by more than 6% compare to the set-point tracking NMPC. In addition, the asNMPC controller is utilized to reduce the online computational delay by at least 200 times with no performance loss.

Chapter 5

Offset-Free Output-Feedback NMPC

In Chapter 4, we demonstrate that both the set-point tracking and economical NMPC with state-feedback can be implemented for large scale processes. They exhibit better performance compared to linear MPC based on the assumption that all the states are available for measurement and there is no plant-model mismatch. In this chapter, we study a more realistic control scenario where only part of the state is measurable and critical control performance needs to be retained in the presence of plant-model mismatch. In this case, an output-feedback NMPC with state estimators is necessary.

5.1 Introduction

Offset-free behavior, i.e. maintaining the controlled outputs at their desired steady state set-points, is an important requirement in control applications. In order to achieve offset-free behavior for linear systems, Muske and Badgwell [84] presented a general disturbance model that accommodates unmeasured disturbances by state augmentation. Pannocchia and Bemporad [87] proposed an integrated design strategy for disturbance model and dynamic observer. Moreover, Pannocchia and Kerrigan [88] proposed a target setting strategy based on state augmentation to guarantee offset-free behavior for linear systems. For nonlinear systems, Meadows and Rawlings [79] summarized a conventional offset-free (N)MPC method which adds an output disturbance into the objective function for the en-

tire predictive horizon. The output disturbance is generated by comparing the measured plant output to the model prediction at the current time step. Srinivasrao et. al [103, 104] proposed an offset-free NMPC formulation that integrates both the state and output disturbances from the extended Kalman filter (EKF). It has the advantage of being able to be applied to open-loop unstable systems.

However, design of EKF for complex nonlinear system can be a challenging problem, especially when inequality constraints are enforced on state variables. One strategy for constrained state estimation is MHE as discussed in Chapter 3. In this chapter, we propose a general offset-free NMPC framework using MHE as the state estimator. In addition to the formulation with state and output disturbances, MHE can estimate the plant state and uncertainty parameter simultaneously, if the uncertainty structure is known. Therefore, the plant-model mismatch is adaptively removed. Moreover, the analysis in this chapter can be extended to general nonlinear recursive observers, such as EKF. We focus on the MHE formulation in this chapter and defer the discussion of offset-free formulation with NMPC and EKF to Chapter 6.

To introduce plant-model mismatch, we combine the plant model with nonlinear output mapping (3.15) in Chapter 3 and the uncertainty plant model (2.13) in Chapter 2.

$$\begin{aligned} x_{k+1} &= f(x_k, u_k, \theta_k), \\ y_k &= h(x_k), \end{aligned} \tag{5.1}$$

where $\theta_k \in \Omega_\theta \subset \mathbb{R}^{n_\theta}$ is the uncertainty parameter, and Ω_θ is a compact set. Here if $\theta_k = 0$, equation (5.1) represents the nominal plant (3.15). Without losing generality, we assume that the given plant (5.1) has an equilibrium point at the origin, that is $f(0,0,0) = 0$. Moreover, no trajectory of this system exhibits finite escape time.

Depending on the prior knowledge of the plant-model mismatch, two variations of the

offset-free NMPC with MHE are proposed in this section. In general, the uncertainty structure of a process is unknown; this could be due to sensor failures and process disturbances. In this case, we introduce state and output disturbances in both the NMPC and MHE problems to compensate for plant-model mismatch and achieve offset-free control behavior. On the contrary, some uncertainty structure of a process can be determined beforehand, e.g. a certain parameter drifts away from its nominal value along a chemical reaction. Then we propose an MHE formulation to estimate the uncertainty parameter and plant state simultaneously. This formulation yields offset-free control behavior as well, due to the removal of the plant-model mismatch.

5.2 Offset-Free Formulation with State and Output Disturbance

In the first scenario, we assume that the uncertainty structure is unknown. Hence, the nominal zero value of the uncertainty parameter is used in the predictive model. To compensate for the plant-model mismatch, state and output disturbances are introduced into the general MHE (3.16) and NMPC (3.14) for a nominal system.

At time step k, the MHE proble (3.16) is modified as

$$\min \sum_{j=0}^{N_e} (\zeta_{k-N_e+j}^T \Pi_y \zeta_{k-N_e+j} + \xi_{k-N_e+j}^T \Pi_x \xi_{k-N_e+j}) + (\hat{x}_{k-N_e} - \bar{x}_{k-N_e})^T \Pi_0 (\hat{x}_{k-N_e} - \bar{x}_{k-N_e}) \tag{5.2a}$$

$$\text{s.t.} \quad \hat{x}_{k-N_e+j+1} = f(\hat{x}_{k-N_e+j}, u_{k-N_e+j}, 0) + \xi_{k-N_e+j} \tag{5.2b}$$

$$\hat{y}_{k-N_e+j} = h(\hat{x}_{k-N_e+j}) \tag{5.2c}$$

$$\zeta_{k-N_e+j} = y_{k-N_e+j} - \hat{y}_{k-N_e+j} \tag{5.2d}$$

$$\hat{x}_{k-N_e+j} \in \mathbb{X},\ \zeta_{k-N_e+j} \in \Omega_\zeta,\ \xi_{k-N_e+j} \in \Omega_\xi \tag{5.2e}$$

$$j = 0, \ldots, N_e, \tag{5.2f}$$

where Π_x is a symmetric positive definite tuning matric, and ξ_k, ζ_k are the state and output disturbances which are assumed to be bounded in compact sets Ω_ζ and Ω_ξ, respectively.

Note that though we consider a noise free plant (5.1) for notational simplicity, the proposed MHE and NMPC can easily incorporate the state and output noises, due to the introduction of the state and output disturbances. In addition, state noise can be considered as a special form of the uncertainty parameter θ.

After the MHE problem (5.2) is solved, it yields the optimal estimated state ($\hat{x}_k$), as well as the state and output disturbances (ξ_k, ζ_k) at the current time step k. Therefore, set-point tracking output-feedback NMPC with state and output disturbances is formulated as:

$$\min \sum_{j=0}^{N_p} (l_{k+j} - y_r)^T \Gamma_y (l_{k+j} - y_r) + \sum_{i=0}^{N_c-1} \triangle v_{k+i}^T \Gamma_u \triangle v_{k+i} \tag{5.3a}$$

$$\text{s.t} \quad z_{k+j+1} = f(z_{k+j}, v_{k+j}, 0) + \xi_k, \quad j = 0, \ldots, N_p - 1 \tag{5.3b}$$

$$z_k = \hat{x}_k, \; z_{k+j} \in \mathbb{X} \tag{5.3c}$$

$$l_{k+j} = h(z_{k+j}) + \zeta_k, \; \triangle v_{k+i} = v_{k+i+1} - v_{k+i} \tag{5.3d}$$

$$v_{k+j} = v_{k+t_i} \text{ for } t_i \leq j < t_{i+1}, \; v_{k+i} \in \mathbb{U}, \tag{5.3e}$$

$$t_0 = 0 \leq t_1 \leq t_2 \leq, \ldots, \leq N_p - 1 \tag{5.3f}$$

where N_p, N_c are the prediction and control horizon length respectively; y_r is the set point for the output; z_k, l_k, v_k are the predicted state, output and control movement, respectively. NMPC is initialized with the estimated state $\hat{x}_k$. In typical NMPC applications, fewer degrees of freedom are available for the control movement. The last two constraints indicate that the control action is the input blocking form, ensuring that the available degrees of freedom spread over the entire prediction horizon.

Note that unlike NMPC formulation (3.14), the predictive model (5.3b) is perturbed by the state and output disturbances (ζ_k and ξ_k) to compensate for the unknown uncertainty parameter θ_k. It is worth mentioning that ζ_k and ξ_k, which are calculated at the end of the estimation horizon in MHE, are fixed parameters in the NMPC problem.

We now show that the proposed method yields zero steady state offset. The analysis is similar to that in [79]. However, it does not depend on a target setting optimization problem.

Theorem 1 *If*

1. *the set point y_r is reachable for the perturbed predictive model $z_{k+j+1} = f(z_{k+j}, v_{k+j}, 0) + \xi_k$ and $l_{k+j} = h(z_{k+j}) + \zeta_k$,*

2. *the NMPC controller* (5.3) *is asymptotically stabilizing for the perturbed predictive model,*

3. *the closed-loop system goes to a steady state,*

4. *the perturbed predictive model is observable at the steady state,*

then the system controlled by the MHE (5.2) *and the NMPC* (5.3) *has zero steady state offset.*

Proof: In the following analysis, the superscript *ss* denotes the steady state value. Since y_r is reachable for the perturbed predictive model and the NMPC control law is asymptotically stable, the stage cost in NMPC (5.3) is zero at steady state, i.e.

$$l^{ss} = y_r. \tag{5.4}$$

Moreover, at the steady state, the predictive state remains constant, $z^{ss} = \hat{x}^{ss}$. The control action is also a constant, i.e. $u^{ss} = v^{ss}$. The state and output disturbances (ξ^{ss} and ζ^{ss}) can be estimated from the assumption that the perturbed predictive model is observable. Thus the following equations hold true,

$$\hat{x}^{ss} = f(\hat{x}^{ss}, u^{ss}, 0) + \xi^{ss}, \tag{5.5a}$$

$$l^{ss} = h(\hat{x}^{ss}) + \zeta^{ss}. \tag{5.5b}$$

In addition, at the steady state the MHE evolves according to

$$\hat{x}^{ss} = f(\hat{x}^{ss}, u^{ss}, 0) + \xi^{ss}, \tag{5.6a}$$

$$\hat{y}^{ss} = h(\hat{x}^{ss}), \tag{5.6b}$$

$$\zeta^{ss} = y^{ss} - \hat{y}^{ss}. \tag{5.6c}$$

Since the predictive model in the MHE (5.6a) is exactly the same as that in the NMPC (5.5a), by combining equations (5.5b), (5.6b) and (5.6c), we see

$$l^{ss} = y^{ss}. \tag{5.7}$$

Then by virtue of equations (5.4) and (5.7), the following equation can be derived

$$y^{ss} = y_r. \tag{5.8}$$

This indicates that the plant output equals the set point at the steady state. ■

Remark 1 *If the set point y_r is not feasible, then the proposed approach minimizes the steady state output difference, i.e.* $(y^{ss} - y_r)^T \Gamma_y (y^{ss} - y_r)$.

Remark 2 *Note that in this analysis, the observer is in a general formulation* (5.6)*. Thus, the Theorem also applies to the NMPC* (5.3) *incorporated with nonlinear recursive observers, such as EKF and extended Luenberger Observer. In Chapter 6, we will discuss the offset-free formulation of NMPC with EKF and the theoretical result obtained in Theorem 1 still applies.*

5.3 Offset-free Formulation with State and Parameter Estimation

In the second scenario, we assume that the uncertainty parameter structure is known. Then instead of compensating for the uncertainty by state and output disturbances, MHE can estimate both the state and uncertainty simultaneously. Thus, the model for the MHE and the NMPC is modified adaptively online.

At time step k, with the measured output sequence y_{k-N_e}, y_{k-N_e+1}, $\ldots$, y_k, the MHE is formulated as:

$$\min \sum_{j=0}^{N_e} (\zeta_{k-N_e+j}^T \Pi_y \zeta_{k-N_e+j}) + \hat{\theta}_k^T \Pi_\theta \hat{\theta}_k + (\hat{x}_{k-N_e} - \bar{x}_{k-N_e})^T \Pi_0 (\hat{x}_{k-N_e} - \bar{x}_{k-N_e}) \tag{5.9a}$$

$$\text{s.t.} \quad \hat{x}_{k-N_e+j+1} = f(\hat{x}_{k-N_e+j}, u_{k-N_e+j}, \hat{\theta}_k) \tag{5.9b}$$

$$\hat{y}_{k-N_e+j} = h(\hat{x}_{k-N_e+j}) \tag{5.9c}$$

$$\zeta_{k-N_e+j} = y_{k-N_e+j} - \hat{y}_{k-N_e+j} \tag{5.9d}$$

$$\hat{x}_{k-N_e+j} \in \mathbb{X}, \zeta_{k-N_e+j} \in \Omega_\zeta, \hat{\theta}_k \in \Omega_\theta \tag{5.9e}$$

$$j = 0, \ldots, N_e, \tag{5.9f}$$

where $\hat{\theta}_k$ is the estimated uncertainty parameter which is bounded in a compact set Ω_θ. Similar to the MHE formulation (5.2b), ζ_{k-N_e+j} is the output disturbance, bounded in the compact set Ω_ζ. However, there is no state disturbance in this formulation. MHE (5.9) yields the optimal uncertainty parameter $\hat{\theta}_k$ that minimizes the difference between the estimated output $\hat{y}$, and the measured output y over the entire estimation horizon. As a result, the estimated state $\hat{x}$ is also smoothed over the entire estimation horizon.

With the optimal estimated state $\hat{x}_k$, output disturbance ζ_k and the optimal uncertainty parameter $\hat{\theta}_k$ at the current time step k, the output-feedback NMPC with parameter estimation

is formulated as the following:

$$\min \sum_{j=0}^{N_p} (l_{k+j} - y_r)^T \Gamma_y (l_{k+j} - y_r) + \sum_{j=0}^{N_c-1} \triangle v_{k+j}^T \Gamma_u \triangle v_{k+j} \tag{5.10a}$$

$$\text{s.t} \quad z_{k+j+1} = f(z_{k+j}, v_{k+j}, \hat{\theta}_k), \;\; j = 0, \ldots, N_p - 1 \tag{5.10b}$$

$$z_k = \hat{x}_k, \; z_{k+j} \in \mathbb{X} \tag{5.10c}$$

$$l_{k+j} = h(z_{k+j}) + \zeta_k, \; \triangle v_{k+j} = v_{k+j+1} - v_{k+j} \tag{5.10d}$$

$$v_{k+j} = v_{k+t_i} \text{ for } t_i \leq j < t_{i+1}, \; v_{k+j} \in \mathbb{U}, \tag{5.10e}$$

$$t_0 = 0 \leq t_1 \leq t_2 \leq, \ldots, \leq N_p - 1. \tag{5.10f}$$

Similar to the NMPC formulation with state and output disturbances (5.3b), this NMPC problem is initialized with the estimated state variable $\hat{x}_k$ and the planned control movement is chosen as the input-blocking form. However, this NMPC formulation does not perturb the predictive model with the state disturbance. Instead, it adaptively updates the uncertainty parameter with the optimal value from the MHE.

Similar to the analysis in Theorem 1, we can show that the NMPC and MHE with parameter estimation (MHE (5.9) and NMPC (5.10)) is able to provide offset-free control behavior. The proof follows in the same way as that in Theorem 1, and is omitted here.

5.4 Simulation Examples

In this section, the proposed methods are demonstrated on simulation examples. In addition, the advanced step algorithm in Chapter 3 is also utilized to reduce the online computational time.

5.4.1 CSTR Simulation

In this subsection, a simulated NMPC scenario with a nonlinear continuous stirred tank reactor (CSTR) is considered, which is adopted from the CSTR model in [41]. The CSTR is represented by the following differential equations:

$$\frac{dz_c}{dt} = (z_c - 1)/u_2 + k_0 z_c \exp(-E_a/z_T) \tag{5.11a}$$

$$\frac{dz_T}{dt} = (z_T^f - z_T)/u_2 + k_0 z_c \exp(-E_a/z_T) - \nu u_1 (z_T - z_T^{cw}). \tag{5.11b}$$

This system involves two states $z = [z_c, z_T]$ corresponding to dimensionless concentration and temperature, and two manipulated inputs, corresponding to the cooling water flow rate u_1 and the inverse of dilution rate u_2. The model parameters are $z_T^{cw} = 0.38$, $z_T^f = 0.395$, $E_a = 5$, $\nu = 1.95 \times 10^{-4}$ and k_0 is an uncertainty parameter in the plant with nominal value $k_0 = 300$. The system is operated at steady state $z_{ss} = [0.12466, 0.74068]$ corresponding to $u_{ss} = [378, 20]$. In this simulation, it is assumed that both the states are measured, i.e. the output mapping function in (5.1) is chosen to be $h(\cdot) = \text{diag}[1,1] \times [z_c, z_T]^T$.

This model is regulated by the proposed two variations of offset-free output-feedback NMPC with MHE. The horizon of the MHE, N_e is chosen as 6 time units with sampling time equals to 1 time unit. Let $Q = \text{diag}[1,1]$ and $R = \text{diag}[1,1]$, and define $A_{ss} = \frac{\partial f}{\partial z}|_{z_{ss},u_{ss}}$, $B_{ss} = \frac{\partial f}{\partial u}|_{z_{ss},u_{ss}}$, $C_{ss} = \frac{\partial h}{\partial z}|_{z_{ss}}$ and $V_{ss} = R + C_{ss} Q C_{ss}^T$. The weighting matrices are chosen to be inverse of the covariance information which is calculated similar to the extended Kalman filter, i.e., $\Pi_0^{-1} = A_{ss} Q A_{ss}^T + B_{ss} Q B_{ss}^T - A_{ss} Q C_{ss}^T V_{ss}^{-1} C_{ss} Q A_{ss}^T$, $\Pi_x^{-1} = Q$, $\Pi_y^{-1} = R$ and $\Pi_\theta = 0$. The NMPC is tuned with prediction horizon N_p chosen to be 10 time units, control horizon N_c chosen to be 5 time units and equally distributed over the entire prediction horizon. The tuning matrices are $\Gamma_y = \text{diag}[1 \times 10^6,\ 1 \times 10^6]$, $\Gamma_u = 0$.

In the first simulation, the plant is controlled by the formulation with state and output disturbances (MHE (5.2) and NMPC (5.3)). The plant starts from the nominal steady state

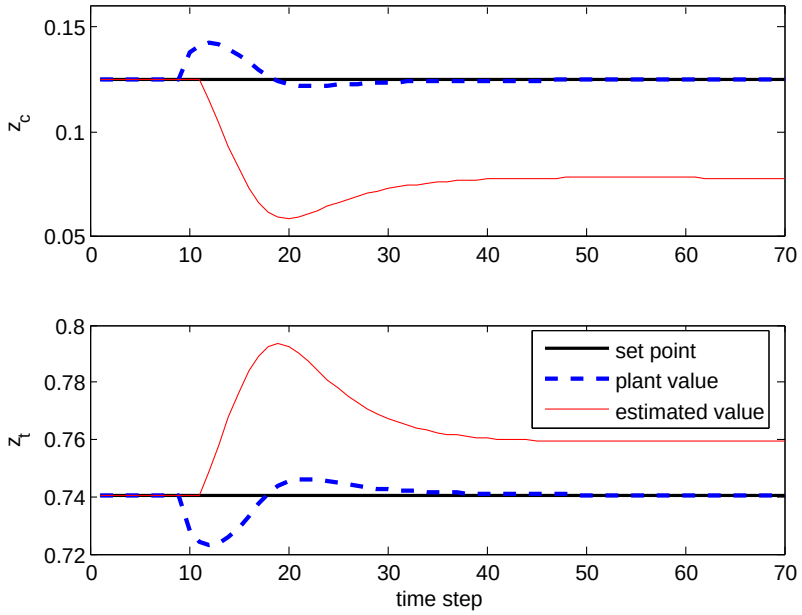

Figure 5.1: State profile in scenario 1 in the CSTR simulation.

value. At time step 10, the uncertainty parameter k_0 is reduced to 70% of its nominal value as shown at the bottom of Fig. 5.3. The resulting closed-loop responses are shown in Fig. 5.1 and 5.2. It is observed that although both states are measured, the state estimates are biased after the plant-model mismatch is introduced. However, these differences are utilized in the NMPC formulation to remove the steady state offset of the plant outputs. As shown in Fig. 5.1, the proposed method is able to regulate the plant outputs at the desired set points.

The second simulation scenario is the same as the first one, except that the plant is regulated by the formulation with state and parameter estimation (MHE (5.9) and NMPC (5.10)). As shown at the bottom of Fig. 5.5, the estimated uncertainty gradually converges to the plant value after the plant-model mismatch is introduced at time step 10. Thus, after time step 25, the uncertainty parameter in the model equals that in the plant, removing the plant-model mismatch. Fig. 5.4 shows that the proposed method quickly rejects the disturbance and

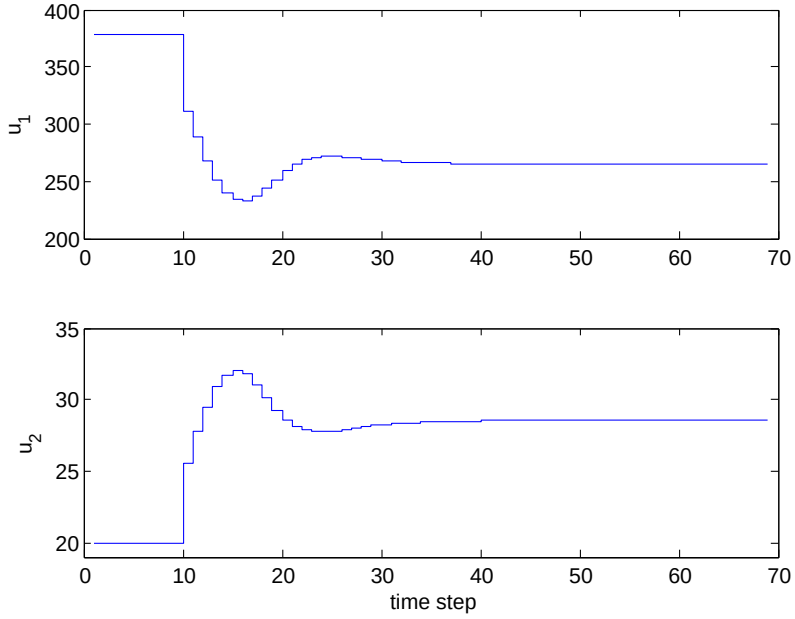

Figure 5.2: Control profile in scenario 1 in the CSTR simulation.

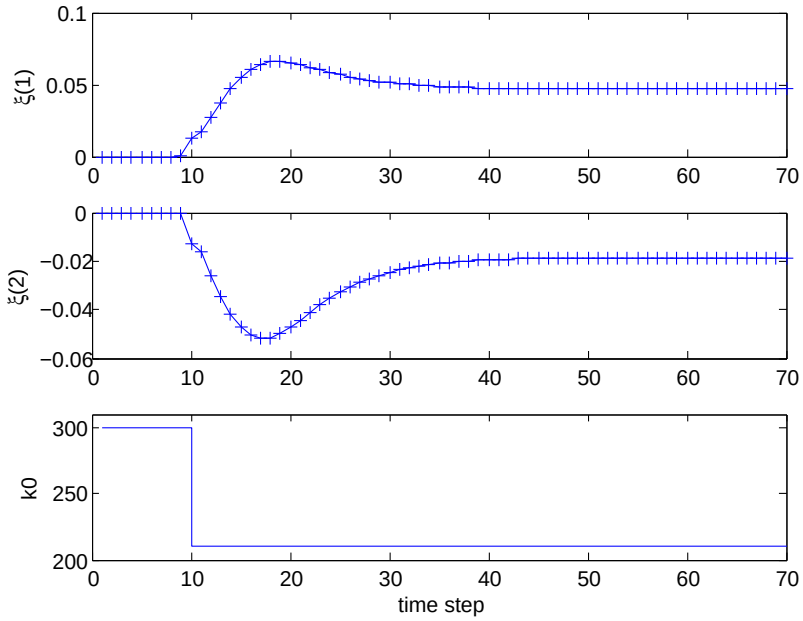

Figure 5.3: Error profile in scenario 1 in the CSTR simulation.

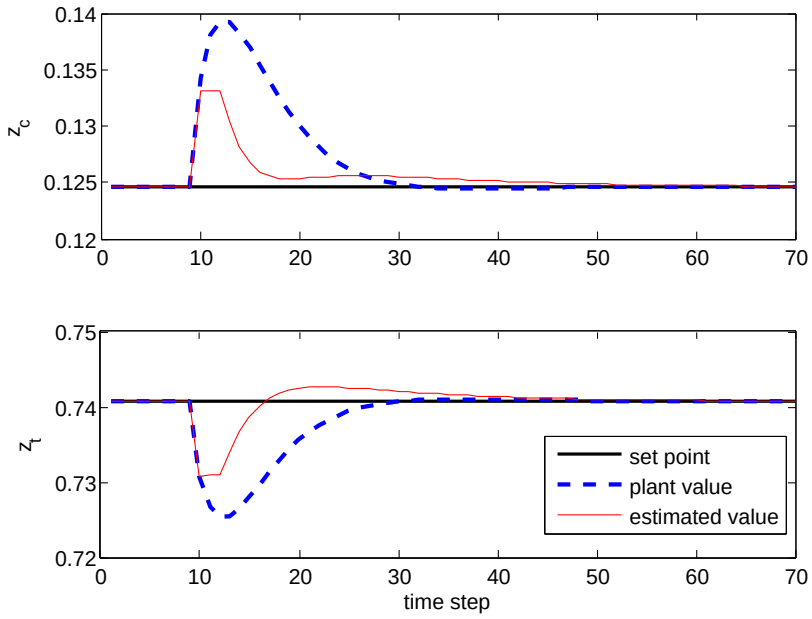

Figure 5.4: State profile in scenario 2 in the CSTR simulation.

yields offset-free control behavior. In addition, the estimated states converge to the measured plant states without any error after the plant-model mismatch is eliminated. It is interesting to compare Fig. 5.1 and 5.4 to see that the formulation with parameter estimation (equations (5.9) and (5.10)) rejects the plant-model mismatch faster than the formulation with state and output disturbances (equations (5.2) and (5.3)).

5.4.2 As-MHE-NMPC for the ASU

In the previous section, the CSTR is controlled by the hypothetical *ideal*-MHE-NMPC, which is based on the assumption that the MHE and NMPC problems can be solved instantaneously, i.e. no computational delay. However, in practice, we need to consider the computational delay resulting from solving the optimization problems associated with MHE and NMPC, especially for the large scale ASU process. Furthermore, the MHE and

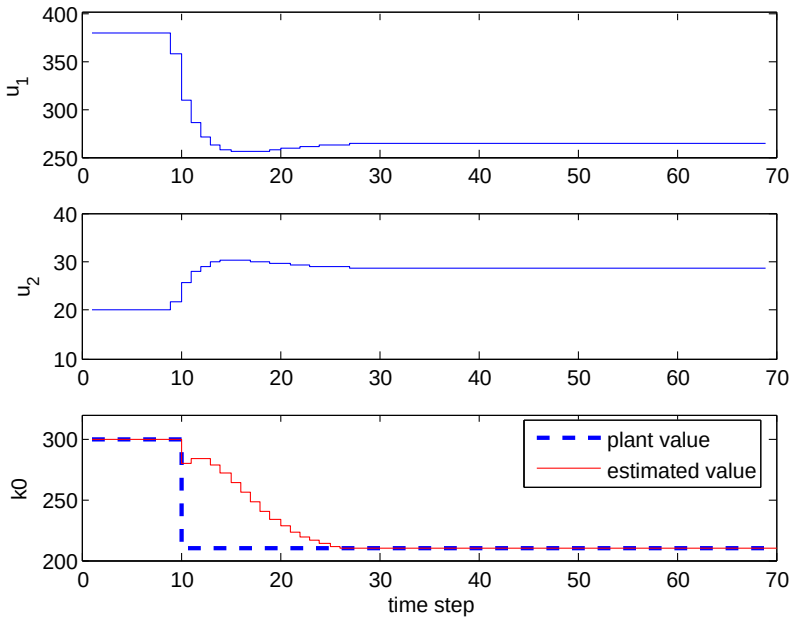

Figure 5.5: Control and uncertainty profile in scenario 2 in the CSTR simulation.

NMPC problems need to be solved sequentially, because the NMPC uses the estimated plant state as the initial condition which is the result of the MHE problem. Therefore, the computational delay is the result of solving two optimization problems online.

In this section, we incorporate the asNMPC and asMHE which are described in Chapter 3 into the proposed offset-free framework to reduce the online computational delay. The algorithm is summarized as the following:

In background, between time step k and $k+1$:

- **asMHE:** having $\hat{x}_k$ and u_k, compute the disturbance-free extrapolation of the state $\tilde{x}_{k+1}$ and the corresponding output $\tilde{y}_{k+1}$. Solve an extended MHE problem (5.2) or (5.9) with horizon N_e+1 and output sequence y_{k-N_e}, y_{k-N_e+1}, $\ldots, y_k$, $\tilde{y}_{k+1}$. Let $p_0 = \tilde{y}_{k+1}$ and hold the KKT matrix at the solution.

- **asNMPC:** having $\hat{x}_k$ and u_k, predict the future state of the system z_{k+1} using the predictive model (5.3b) or (5.10b). Solve the NMPC (5.3) or (5.10) with $p_0 = z_{k+1}$. Hold the KKT matrix at the solution.

Online update, at time step $k+1$:

- **asMHE:** obtain the true measurement y_{k+1}. Set $p = y_{k+1}$ and compute the fast approximation solution using equation (3.12). Extract the estimated state $\hat{x}_{k+1}$.
- **asNMPC:** obtain the state estimate $\hat{x}_{k+1}$. Set $p = \hat{x}_{k+1}$ and use equation (3.12) to get the fast updated solution. Extract the control action u_{k+1} from the approximate solution vector and inject to the plant.

Remark 3 *The background solution of NMPC does not need to wait for the result of the MHE. Therefore, the background solution can be further parallelized on different computing units. The sampling time can be chosen as the longer of the two background solution times, instead of the summation of the two background solution times.*

It is observed that the online computational delay of this as-MHE-NMPC scheme is only two single backsolves associated to the online update of the MHE and NMPC, which is significantly faster compared to solving the MHE and NMPC problems online.

In the following, we apply the as-MHE-NMPC scheme to the ASU model presented in Section 4.2. The hydraulic parameter k_d in equation (4.7) is considered as the uncertainty parameter and is perturbed by 20%. The controller setup is exactly the same as the set-point tracking NMPC controller in Section 4.3. The objective is to regulate the ASU outputs shown in Fig. 4.1 at their set-points in the presence of the plant-model mismatch, and the control objective function is chosen to be equation (4.15).

Since there are many uncertainties in the ASU process, e.g. thermodynamic properties, tray efficiencies, etc., it is not trivial to determine the uncertainty structure of the ASU model in practice. Therefore, we choose to use the formulation with state and output disturbances (MHE (5.2) and NMPC (5.3)).

The simulation starts from the nominal steady state with $k_d = 0.5$. At 25 minutes, the k_d in the plant is increased to 0.6, while $k_d = 0.5$ in the model, introducing a plant-model mismatch. The closed-loop plant output is presented in Fig. 5.6, and the control action is shown in Fig. 5.7. It is observed that both as-MHE-NMPC and *ideal*-MHE-NMPC in the proposed offset-free framework reject the disturbance and regulate the plant outputs at their set points without any steady-state offset. Moreover, the as-MHE-NMPC yields comparable performance as the *ideal*-MHE-NMPC. Finally, the purities in the product streams POX and PNI are not directly measured. Nevertheless, it is interesting to note in Fig. 5.8 that the oxygen and nitrogen purity in the product streams satisfy the requirement (oxygen purity $\geq 96\%$).

In addition, from the output of IPOPT, we see that the solutions of both MHE and NMPC problems satisfy LICQ and SSOC at each time step, meaning that this system is locally observable and controllable at each time step. We believe this is partially due to the fact that the ASU is open-loop stable and the MHE and NMPC problems at each time step are well initialized from their previous solutions.

After full discretization using Radau collocation as discussed in Chapter 3, the resulting Nonlinear Programming (NLP) problem corresponding to the NMPC problem has 116,900 constraints and 117,140 variables; while the NLP corresponding to the MHE problem (5 finite elements and 3 collocations) contains 29,285 constraints and 30,885 variables. Both the NLPs are solved using AMPL and IPOPT on an Intel DuoCore 2.4 GHz personal computer. The ideal-MHE problems take up to 15 iterations and 90 CPU seconds to solve,

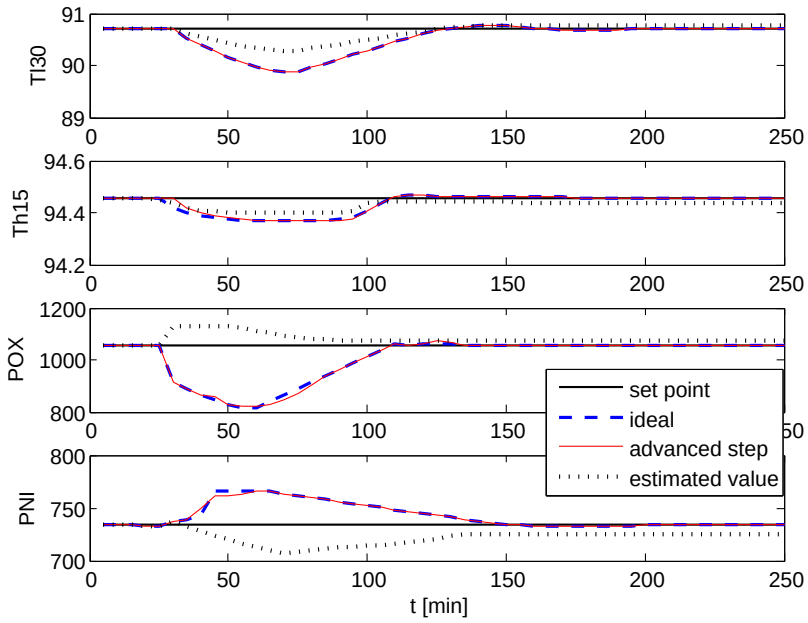

Figure 5.6: Output profile of the ASU with state and output disturbance as-MHE-NMPC.

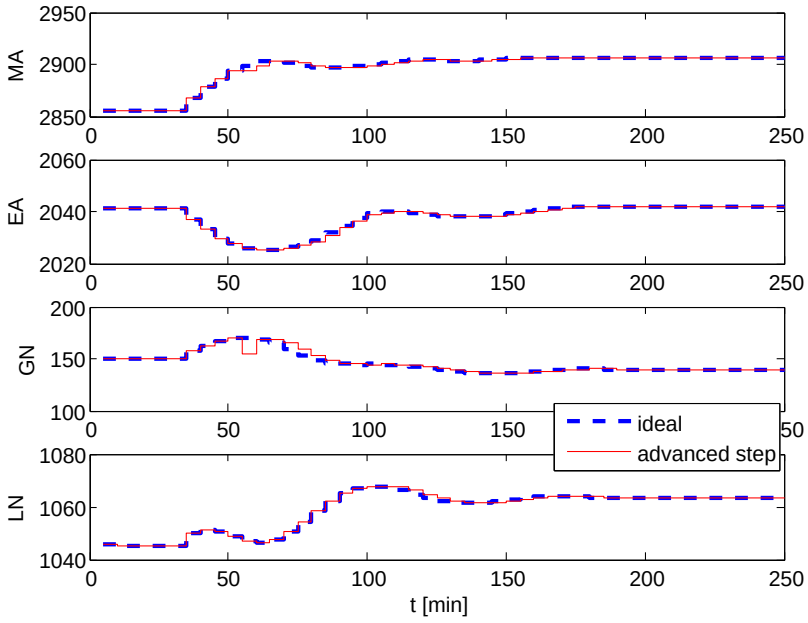

Figure 5.7: Control profile of the ASU with state and output disturbance as-MHE-NMPC.

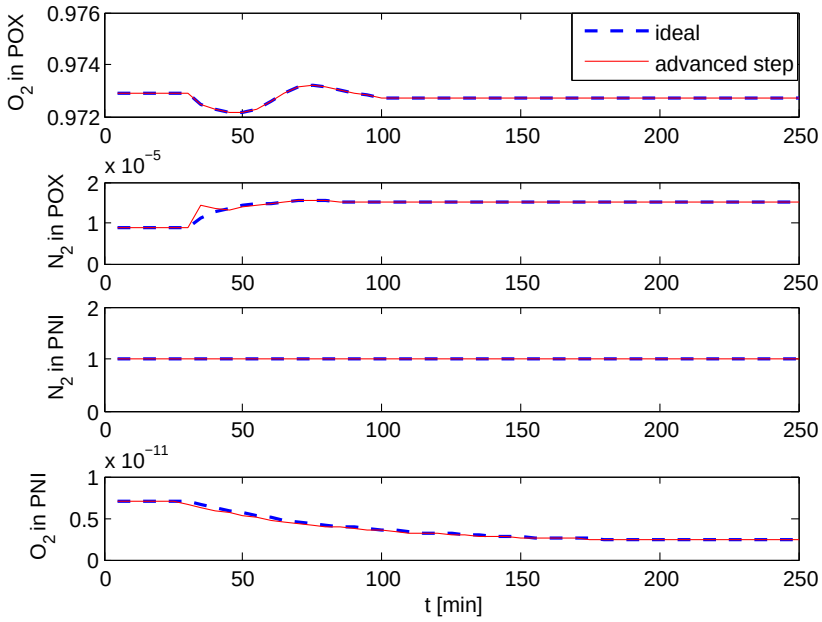

Figure 5.8: Product purity profile of the ASU with state and output disturbance as-MHE-NMPC.

while ideal-NMPC problems take up to 6 IPOPT iterations and 200 CPU seconds to solve. On the other hand, the online computational time is less than 1 CPU second for asMHE and around 1 CPU second for asNMPC, even though as-MHE-NMPC has similar performance as ideal-MHE-NMPC. It indicates that by using as-MHE-NMPC, the online computational delay is reduced by 150 times, from around 5 minutes to less than 2 seconds.

5.5 Concluding Remarks

This chapter addresses the practical issue of achieving offset-free behavior in NMPC applications when plant-model mismatch is present and state estimator is integrated to reconstruct plant state from output. Using MHE as the general state estimator, we propose an offset-free NMPC framework based on state and output disturbances. It can be shown that the proposed method guarantees offset-free behavior if the set-point is feasible for the observable perturbed predictive model and the control law asymptotically converges to the steady state. The analysis can be extended to the general nonlinear recursive observers like extended Kalman filter, which will be discussed in Chapter 6. Moreover, another variation of offset-free NMPC framework is proposed based on integrated state and parameter estimation. Here, MHE is tuned to estimate the plant state and uncertainty parameter simultaneously, in order to remove the plant-model mismatch online. Provided that the uncertainty structure is known, we observe that this framework has better performance than the formulation based on state and output disturbances. In addition, as-NMPC and as-MHE is incorporated into the proposed offset-free frameworks, to reduce online computational delay associated with solving the MHE and NMPC problems. We see that the framework with parameter estimation can improve the robust stability of the as-MHE-NMPC. Finally, the proposed as-MHE-NMPC based on state and output disturbances is successfully imple-

mented on a large scale air separation unit. The online computational delay is reduced by at least 150 times by using as-MHE-NMPC.

Chapter 6

Robust Stability of NMPC with EKF

In Chapter 5, we studied the practical issue of achieving offset-free behavior using output-feedback NMPC with MHE. In this chapter, we are interested in the robust stability property of set-point tracking NMPC with an observer. EKF is chosen as the nonlinear observer due to its popularity in industry. First, the convergence property of the estimated state from EKF in the presence of non-vanishing perturbations is established. A local form of separation principle is shown that the EKF error is not influenced by the NMPC. Then, we further analyze the impact of the estimation error on the robust stability of the output-feedback NMPC. Moreover, a simulation study is shown with the output-feedback NMPC plus EKF which inherits the offset-free theoretical result in Theorem 1.

6.1 Introduction

Based on the assumption that all the states in plants are measurable, stability analyses of the closed-loop system with state-feedback nonlinear MPC have been extensively studied for both nominal and robust systems. Thorough reviews can be found in [78, 74, 95]. In addition, Limon et al. [72] presented the theory of Input-to-State Stability (ISS) as a unifying framework for robust NMPC. In practice, however, the system state is seldom fully available. Although output-feedback (N)MPC, in which nominal (N)MPC is integrated with a separately designed observer is extensively used in industry, relatively little contribution

has been made in the literature in terms of its stability analysis. This is mainly because there is no valid separation principle for a general constraint nonlinear system.

Recently, stability properties of output-feedback NMPC with focus of particular systems are studied. Findeisen et al. [36] obtained practical stability of systems by synthesizing a sufficiently fast high-gain observer with a robust NMPC controller. In addition, Kothare and Morari [62] demonstrated that MPC with contractive constraints is asymptotically stable provided with asymptotically convergent estimates. These results focus on continuous time systems with vanishing perturbations. For discrete time systems, Magni and Scattolini [65] studied the stability under vanishing perturbations by requiring Lipschitz continuity for both the observer and controller. Messina et al. [80] presented stability results of output-feedback controllers. In addition, Roset et al. [99] showed the robust stability property of NMPC to both state and measurement errors. However, these two studies treat the plant-model mismatch as additive noise.

Here we analyze the robust stability of output-feedback NMPC with state-correction under general non-vanishing plant-model mismatches with a class of widely-used state estimators. The stability of MHE has been studied by Alessandri et al [3] and Zavala [114] by assuming the control action is known. However, it is not clear how the result changes in the closed-loop case, when the control action is calculated by using the MHE result as the initial condition. In this chapter, we use a class of nonlinear observers based on recursive calculations such as EKF and ELO. The open-loop stability of this class of observers has been addressed by utilizing a generalized Lyapunov framework in [52]. Here, we use the EKF as a representation due to its advantage to control the estimation error by tuning parameters. Nevertheless, the stability result in this chapter still holds if ELO is used as the observer.

Although EKF is arguably the most popular state estimation tool in industry since 1970,

few properties regarding the stability and convergence property of the EKF have been established until recently. Given observability, recent research [97, 20] shows the nominal stability property of the estimator. In particular, Reif and Unbehauen [97] presented convergence analysis for the estimation error sequence and obtained the desired convergence rate.

In this chapter, we first establish the robust stability of an EKF by extending the analysis in [97] to systems with non-vanishing plant-model mismatch. With the help of a *local form of separation principle* and utilizing the unifying ISS framework [72], we demonstrate that the robust stability of the output-feedback NMPC deteriorates to Input-to-State practical Stability (ISpS) [72] due to the estimation error of the EKF. Moreover, simulation studies of using offset-free output-feedback NMPC with EKF, which inherits the theoretical result in Theorem 1, are shown.

This chapter studies a general nonlinear plant with linear-output mapping as shown by equation (6.1), which is a special case of the general nonlinear plant in equation (5.1).

$$x_{k+1} = f(x_k, u_k, \theta_k) \tag{6.1a}$$

$$y_k = Cx_k, \tag{6.1b}$$

where C is a constant matrix. Although applications with nonlinear-output mapping exist in many engineering fields such as robotics, electric and mechanical systems, majority of the chemical engineering applications exhibit the linear-output mapping.

Notations and definitions used in this chapter are introduced in Section 2.3.1.

6.2 Robust Stability of EKF

In this study, we use the same EKF formulation as in [97, 47].

$$x_{k+1}^{-} = f(\hat{x}_k, u_k, 0) \tag{6.2a}$$

$$\hat{x}_k = x_k^{-} + K_k(y_k - Cx_k^{-}) \tag{6.2b}$$

where x_k^{-} and $\hat{x}_k$ are called the *a priori* and *a posteriori* estimate, respectively. Note the uncertainty parameter is 0 in the model, introducing a non-vanishing plant-model mismatch. K_k here is the Kalman gain calculated by:

$$\begin{aligned} K_k &= P_k^{-} C^T (C P_k^{-} C^T + R)^{-1} \\ P_{k+1}^{-} &= \alpha^2 A_k P_k^{+} A_k^T + Q \quad P_k^{+} = (I - K_k C) P_k^{-} \end{aligned} \tag{6.3}$$

where $A_k = \frac{\partial f}{\partial x}(\hat{x}_k, u_k, 0)$ is the linearization of the model, Q and R are symmetric positive definite matrices, $\alpha \geq 1$ is a real number, which is the exponential data weight and can control the convergence rate of the EKF. The Kalman gain equation can be rewritten as $K_k = P_k^{+} C^T R^{-1}$ [97].

Let $\varphi(\cdot,\cdot,\cdot,\cdot)$ be the higher order term, then the residual of the EKF can be defined by the following equation:

$$\begin{aligned} x_{k+1} - x_{k+1}^{-} &= f(x_k, u_k, \theta) - f(\hat{x}_k, u_k, 0) \\ &= A_k[x_k - \hat{x}_k] + G_k \theta_k + \varphi(x_k, \hat{x}_k, u_k, \theta_k) \end{aligned} \tag{6.4}$$

where $G_k \triangleq \frac{\partial f}{\partial \theta}(\hat{x}_k, u_k, 0)$. Now introduce prior and posterior error, ζ_k and ξ_k as

$$\zeta_k = x_k - x_k^{-} \tag{6.5a}$$

$$\xi_k = x_k - \hat{x}_k \tag{6.5b}$$

From equation (6.2b) we have

$$\xi_k = (I - K_k C)\, \zeta_k. \tag{6.6}$$

Subtracting equation (6.2a) from (6.1a) and using equations (6.1b), (6.2b) and (6.4) yields

$$\zeta_{k+1} = A_k(I - K_k C)\zeta_k + r_k = A_k \xi_k + r_k \tag{6.7a}$$

$$r_k = \varphi(x_k, \hat{x}_k, u_k, \theta_k) + G_k \theta_k \tag{6.7b}$$

From equations (6.4), (6.6) and (6.7),

$$\xi_k = [(I - K_k C)A_{k-1}]\,\xi_{k-1} + [(I - K_k C)r_{k-1}] \tag{6.8}$$

Lemma 4 *Assume*

i) there are constants $\overline{a}, \overline{k}$, *and* $\overline{g} \geq 0$ *such that:*

$$|A| \leq \overline{a},\ |G| \leq \overline{g},\ |K| \leq \overline{k}, \tag{6.9}$$

ii) there are constants $\varepsilon,\ \kappa_\varphi,\ \kappa_\theta \geq 0$ *such that:*

$$|\varphi(x, \hat{x}, u, \theta)| \leq \kappa_\varphi |x - \hat{x}|^2 + \kappa_\theta |\theta|^2 + \kappa_{\varphi\theta} |\theta||x - \hat{x}| \tag{6.10}$$

for $|\xi| = |x - \hat{x}| \leq \varepsilon$,

iii) $\hat{x}$ *satisfies* $\hat{x} = x^- + KC(x - x^-)$.

Let r be defined by $r = \varphi(x, \hat{x}, u, \theta) + G\theta$, *then there exists a* $\mathscr{K}$*-function* $\delta_r(\cdot)$ *such that* $|r| \leq \kappa_\varphi \xi^2 + \delta_r(|\theta|)$ *for* $|\xi| \leq \varepsilon$.

Proof: Using triangle inequality as well as equations (6.9) (6.10), we have $|r| \leq |\varphi(x, \hat{x}, u, \theta)| + \overline{g}|\theta|$. Then we define a $\mathscr{K}$-function $\delta_r(|\theta|) \triangleq (\overline{g} + \kappa_{\varphi\theta}\varepsilon)|\theta| + \kappa_\theta |\theta|^2$. Thus considering equation (6.10) and $\xi = x - \hat{x}$, the Lemma follows. ■

Defining $\Pi_k^- = (P_k^-)^{-1}$, $\Pi_k^+ = (P_k^+)^{-1}$, we use Lemma 6 in [97] to obtain:

$$\begin{aligned} \Pi_{k+1}^- \leq\ & \alpha^{-2} A_k^{-T} (I - K_k C)^{-T} \left[\Pi_k^- - \Pi_k^- (\Pi_k^+ + \alpha^2 A_k^T Q^{-1} A_k)^{-1} \Pi_k^-\right] \\ & \times (I - K_k C)^{-1} A_k^{-1} \end{aligned} \tag{6.11}$$

Theorem 2 *Let the assumptions in Lemma 4 hold for the EKF* (6.2)*,* (6.3)*, and assume that A_k is nonsingular at each time step. Besides there exist constants $\underline{p}$ and $\overline{p} \geq 0$ such that*

$$\underline{p}I \leq P_k^- \leq \overline{p}I,\ \underline{p}I \leq P_k^+ \leq \overline{p}I. \tag{6.12}$$

Then $V(\xi_k) \triangleq \xi_k^T (I-K_kC)^{-T} \Pi_k^- (I-K_kC)^{-1} \xi_k$ is an ISS Lypunov function. Moreover there exist constants $\eta,\ \widetilde{\varepsilon},\ \varepsilon_{\xi_0} > 0$, $\beta > 1$ and a $\mathscr{K}$-function $\delta(\|\theta\|_{k-1})$ such that the posterior error sequence behaves according to $|\xi_k| \leq \eta |\xi_0| \beta^{-k} + \delta(\|\theta\|_{k-1})$ when $|\xi_0| \leq \varepsilon_{\xi_0}$.

Proof: The basic idea of the proof is to first establish a Lyapunov function for the prior error, from which the ISS Lyapunov function for the posterior error can be derived.

We start by considering a Lyapunov function defined with prior error, i.e. $\widetilde{V}(\zeta_k) \triangleq \zeta_k^T \Pi_k^- \zeta_k$. Using (6.7) and (6.11)

$$\begin{aligned}
\widetilde{V}(\zeta_{k+1}) &\triangleq \zeta_{k+1}^T \Pi_{k+1}^- \zeta_{k+1} \\
&\leq \alpha^{-2} \zeta_k^T \left[\Pi_k^- - \Pi_k^- (\Pi_k^+ + \alpha^2 A_k^T Q^{-1} A_k)^{-1} \Pi_k^- \right] \zeta_k \\
&+ \left[2 r_k^T \Pi_{k+1}^- A_k (I - K_k C) \zeta_k \right] + \left[r_k^T \Pi_{k+1}^- r_k \right] \\
&\leq \alpha^{-2} \zeta_k \Pi_k^- \zeta_k - \frac{1}{\alpha^2 \overline{p}^2 (\overline{p} + \alpha^2 \overline{a}^2 / \underline{q})} |\zeta_k|^2 \\
&+ 2 r_k^T \Pi_{k+1}^- A_k (I - K_k C) \zeta_k + r_k^T \Pi_{k+1}^- r_k
\end{aligned} \tag{6.13}$$

where $\underline{q} > 0$ is the smallest eigenvalue of the positive definite matrix Q.

From (6.12), we see P_k^- and P_k^+ are nonsingular and because of equation (6.3), the matrix $(I-K_kC)^{-1} = P_k^- \Pi_k^+$ exists. Then from equations (6.6) and (6.3), it follows that

$$\zeta_k = (I-K_kC)^{-1} \xi_k \quad \Pi_k^+ = \Pi_k^- (I-K_kC)^{-1} \tag{6.14}$$

Furthermore using equations (6.14), we have

$$\zeta_k^T \Pi_k^- \zeta_k = \xi_k^T (I-K_kC)^{-T} \Pi_k^- (I-K_kC)^{-1} \xi_k \tag{6.15}$$

Now we define the Lyapunov function regarding to ξ_k

$$\begin{aligned} V(\xi_k) &\triangleq \xi_k^T \left[(I - K_k C)^{-T} \Pi_k^- (I - K_k C)^{-1} \right] \xi_k \\ &= \xi_k^T \left[(\Pi_k^+)^T (P_k^-)^T \Pi_k^+ \right] \xi_k. \end{aligned} \tag{6.16}$$

Using equation (6.6) and $|(I - K_k C)^{-1}| = |P_k^- \Pi_k^+| \leq \frac{\overline{p}}{\underline{p}}$, the inequality (6.13) can be written in terms of $V(\xi_{k+1})$ as

$$\begin{aligned} V(\xi_{k+1}) \leq\ & \alpha^{-2} V(\xi_k) - \frac{1}{\alpha^2 \overline{p}^2 (\overline{p} + \alpha^2 \overline{a}^2 / \underline{q})(\overline{p}/\underline{p})^2} |\xi_k|^2 \\ & + 2 r_k^T \Pi_{k+1}^- A_k \xi_k + r_k^T \Pi_{k+1}^- r_k \end{aligned} \tag{6.17}$$

Denoting the smallest eigenvalue of R by $\underline{r}$, we obtain

$$|K_k| \leq \left| P_k^+ \right| |C| \left| R^{-1} \right| \leq \overline{k} \tag{6.18}$$

where $\overline{k} = \overline{p}|C|/\underline{r}$.

Then applying Lemma 4, $2 r_k^T \Pi_{k+1}^- A_k \xi_k$ can be expressed as

$$\begin{aligned} 2 r_k^T \Pi_{k+1}^- A_k \xi_k &\leq 2|r_k| \frac{\overline{a}}{\underline{p}} |\xi_k| \leq 2 \left[\kappa_\varphi |\xi_k|^2 + \delta_r(|\theta_k|) \right] \frac{\overline{a}}{\underline{p}} |\xi_k| \\ &\leq 2 \kappa_\varphi |\xi_k|^2 \frac{\overline{a}}{\underline{p}} |\xi_k| + \frac{2\overline{a}}{\underline{p}} \varepsilon \left[\delta_r(|\theta_k|) \right] \end{aligned} \tag{6.19}$$

Similarly, from Lemma 4, $r_k^T \Pi_{k+1}^- r_k$ can be expressed as

$$\begin{aligned} & r_k^T \Pi_{k+1}^- r_k \leq \frac{1}{\underline{p}} |r_k|^2 \leq \frac{1}{\underline{p}} \left[\kappa_\varphi |\xi_k|^2 + \delta_r(|\theta_k|) \right]^2 \\ & \leq \frac{1}{\underline{p}} (\kappa_\varphi |\xi_k|^2 \kappa_\varphi \varepsilon |\xi_k|) + \frac{1}{\underline{p}} \left[2 \left[\kappa_\varphi \varepsilon^2 \right] \delta_r(|\theta_k|) + \left[\delta_r(|\theta_k|) \right]^2 \right] \end{aligned} \tag{6.20}$$

Combining (6.19) and (6.20) with equation (6.17), we have

$$\begin{aligned} V(\xi_{k+1}) &\leq \alpha^{-2}V(\xi_k) - \Big[\frac{1}{\alpha^2\overline{p}^2(\overline{p}+\alpha^2\overline{a}^2/\underline{q})\left(\overline{p}/\underline{p}\right)^2} \\ &\quad -\widetilde{\kappa}|\xi_k|\Big]|\xi_k|^2 + \delta_V(|\theta_k|) \qquad (6.21) \\ \widetilde{\kappa} &= \frac{\kappa_\varphi}{\underline{p}}(2\overline{a}+\kappa_\varphi\varepsilon) \\ \delta_V(|\theta_k|) &= \frac{1}{\underline{p}}\Big[2\left(\kappa_\varphi\varepsilon^2+\overline{a}\varepsilon\right)\delta_r(|\theta_k|)+(\delta_r(|\theta_k|))^2\Big] \qquad (6.22) \end{aligned}$$

where $\delta_V(|\theta_k|)$ is a $\mathscr{K}$-function. Thus, we have

$$\begin{aligned} &V(\xi_{k+1})-V(\xi_k) \leq (\alpha^{-2}-1)V(\xi_k) \\ &-\left[\frac{1}{\alpha^2\overline{p}^2(\overline{p}+\alpha^2\overline{a}^2/\underline{q})\left(\overline{p}/\underline{p}\right)^2}-\widetilde{\kappa}|\xi_k|\right]|\xi_k|^2+\delta_V(|\theta_k|) \\ &\leq (\alpha^{-2}-1)V(\xi_k) - \frac{1}{2\alpha^2\overline{p}^2(\overline{p}+\alpha^2\overline{a}^2/\underline{q})\left(\overline{p}/\underline{p}\right)^2}|\xi_k|^2 \\ &-\left[\frac{1}{2\alpha^2\overline{p}^2(\overline{p}+\alpha^2\overline{a}^2/\underline{q})\left(\overline{p}/\underline{p}\right)^2}-\widetilde{\kappa}|\xi_k|\right]|\xi_k|^2+\delta_V(|\theta_k|). \qquad (6.23) \end{aligned}$$

Choosing $\widetilde{\varepsilon}$ as

$$\widetilde{\varepsilon} = \min\left(\varepsilon, \frac{1}{2\alpha^2\overline{p}^2\widetilde{\kappa}(\overline{p}+\alpha^2\overline{a}^2/\underline{q})\left(\overline{p}/\underline{p}\right)^2}\right) \qquad (6.24)$$

such that

$$\left[\frac{1}{2\alpha^2\overline{p}^2(\overline{p}+\alpha^2\overline{a}^2/\underline{q})\left(\overline{p}/\underline{p}\right)^2}-\widetilde{\kappa}|\xi_k|\right] \geq 0$$

holds true when $|\xi_k| \leq \widetilde{\varepsilon}$, leads to

$$\begin{aligned} V(\xi_{k+1})-V(\xi_k) \leq &-\frac{1}{2\alpha^2\overline{p}^2(\overline{p}+\alpha^2\overline{a}^2/\underline{q})\left(\overline{p}/\underline{p}\right)^2}|\xi_k|^2 \\ &+(\alpha^{-2}-1)V(\xi_k)+\delta_V(|\theta_k|). \qquad (6.25) \end{aligned}$$

Thus, $V(\xi_k)$ is a locally ISS-Lyapunov function when $|\xi_k| \leq \widetilde{\varepsilon}$. It follows from the definition of $V(\xi_k)$ that

$$\begin{aligned} \frac{1}{\overline{\sigma}}|\xi_k|^2 &\leq V(\xi_k) \leq \frac{1}{\underline{\sigma}}|\xi_k|^2 \\ \overline{\sigma} &= \frac{(\overline{p})^2}{\underline{p}} \quad \text{and} \quad \underline{\sigma} = \frac{\left(\underline{p}\right)^2}{\overline{p}} \end{aligned} \tag{6.26}$$

Using (6.25) together with (6.26), we have

$$V(\xi_{k+1}) \leq \omega V(\xi_k) + \delta_V(|\theta_k|) \tag{6.27}$$

$$\text{where } \omega \triangleq \alpha^{-2}\left(1 - \frac{\left(\underline{p}\right)^4}{2\overline{p}^5(\overline{p} + \alpha^2\overline{a}^2/\underline{q})}\right) \tag{6.28}$$

Without loss of generality, we assume that $\overline{p} > 1$, which implies $0 < 1 - \frac{\left(\underline{p}\right)^4}{2\overline{p}^5(\overline{p}+\alpha^2\overline{a}^2/\underline{q})} < 1$. If we choose $\alpha \geq 1$, then $\omega < 1$.

Equations (6.27) together with (6.26) imply that

$$\frac{1}{\overline{\sigma}}|\xi_{k+1}|^2 \leq \omega\frac{1}{\underline{\sigma}}|\xi_k|^2 + \delta_V(|\theta_k|) \tag{6.29}$$

and furthermore

$$|\xi_{k+1}| \leq \omega^{\frac{1}{2}}\left(\frac{\overline{p}}{\underline{p}}\right)^{\frac{3}{2}}|\xi_k| + (\overline{\sigma}\delta_V(|\theta_k|))^{\frac{1}{2}}. \tag{6.30}$$

It is clear that if we choose α such that $\omega^{\frac{1}{2}}\left(\frac{\overline{p}}{\underline{p}}\right)^{\frac{3}{2}} < 1$ and $\{\theta_j\}_{j\geq k} = 0$, then the error $\{\xi_j\}$ asymptotically converges to 0.

In addition, equation (6.27) also leads to

$$\begin{aligned} V(\xi_k) &\leq \omega^k V(\xi_0) + (\omega^{k-1} + \omega^{k-2} + \ldots + 1)\delta_V(\|\theta\|_{k-1}) \\ &\leq \omega^k V(\xi_0) + \frac{1}{1-\omega}\delta_V(\|\theta\|_{k-1}). \end{aligned} \tag{6.31}$$

Using inequality (6.26) again, we get

$$|\xi_k|^2 \leq \omega^k \left(\frac{\overline{\sigma}}{\underline{\sigma}}\right) |\xi_0|^2 + \frac{\overline{\sigma}}{1-\omega}\delta_V\left(\|\theta\|_{k-1}\right). \tag{6.32}$$

From the inequality $a^2+b^2 \leq (a+b)^2, \forall a,b \geq 0$, it leads to

$$|\xi_k|^2 \leq \left[\omega^{\frac{k}{2}}\sqrt{\frac{\overline{\sigma}}{\underline{\sigma}}}|\xi_0| + \left(\frac{\overline{\sigma}}{1-\omega}\delta_V\left(\|\theta\|_{k-1}\right)\right)^{1/2}\right]^2 \tag{6.33}$$

which can be further simplified as

$$|\xi_k| \leq \omega^{\frac{k}{2}}\left(\frac{\overline{p}}{\underline{p}}\right)^{3/2}|\xi_0| + \left(\frac{\overline{\sigma}}{1-\omega}\right)^{1/2}\left[\delta_V\left(\|\theta\|_{k-1}\right)\right]^{1/2}. \tag{6.34}$$

Then we define $\eta = \left(\frac{\overline{p}}{\underline{p}}\right)^{3/2} > 0$, $\beta = 1/\sqrt{\omega} > 1$, and a $\mathscr{K}$-function

$$\delta\left(\|\theta\|_{k-1}\right) = \sqrt{\frac{(\overline{p})^2}{\underline{p}(1-\omega)}}\left[\delta_V\left(\|\theta\|_{k-1}\right)\right]^{1/2},$$

and observe that the posteriori error sequence $\{\xi_k\}$ behaves according to

$$|\xi_k| \leq \eta|\xi_0|\beta^{-k} + \delta\left(\|\theta\|_{k-1}\right)$$

and is ISS stable. ■

Remark 4

a) Equation (6.28) *in the proof indicates that the convergence rate can be controlled by choosing parameter* α.

b) Equation (6.12) *implies that the system is observable.*

c) For the nominal case, i.e. $\{\theta_k\} = 0, \forall k \geq 0$, *the theorem reduces to an exponential observer as obtained in [97]. In addition, in the case when plant-model mismatch vanishes after a certain time step* $\bar{t}$, *i.e.* $\{\theta_k\} \neq 0, k \leq \bar{t}$ *and* $\{\theta_k\} = 0, k > \bar{t}$, *the proof (equation* (6.30)*) implies the observer error asymptotically converges to 0 after* $\bar{t}$.

The above theorem states the robust stability for EKF in the open-loop case, when the control action u is assumed given. In the following, we show that the stability result still applies to the closed-loop case, when the control action u is a general function of estimated state and output, $u_k = h_k(\hat{x}_k, y_k)$. Note that this formulation admits the fact that the control law of NMPC with state constraints is generally not continuous.

Corollary 1 *In the closed-loop case, assume that the feedback control law u_k exists and is bounded, and let u_k be defined as $u_k = h_k(\hat{x}_k, y_k)$. Then Theorem 2 still applies to the EKF* (6.2).

Proof: Let $\varphi_1(\cdot,\cdot,\cdot)$ and $\varphi_2(\cdot,\cdot,\cdot)$ be the higher order terms, the residual definition (6.4) of the EKF is modified as:

$$x_{k+1} - x_{k+1}^{-} = f(x_k, h_k(\hat{x}_k, y_k), \theta_k) - f(\hat{x}_k, h_k(\hat{x}_k, y_k), 0) \tag{6.35}$$

Now expand each term in the neighborhood of $\hat{x}_k$,

$$\begin{aligned} f(x_k, h_k(\hat{x}_k, y_k), \theta_k) &= f(\hat{x}_k, h_k(\hat{x}_k, C\hat{x}_k), 0) + A_k(x_k - \hat{x}_k) \\ &+ \frac{\partial f}{\partial u}[h_k(\hat{x}_k, y_k) - h_k(\hat{x}_k, C\hat{x}_k)] + G_k\theta_k + \varphi_1(x_k, \hat{x}_k, \theta_k) \end{aligned} \tag{6.36}$$

$$\begin{aligned} f(\hat{x}_k, h(\hat{x}_k, y_k), 0) &= f(\hat{x}_k, h(\hat{x}_k, C\hat{x}_k), 0) + A_k(\hat{x}_k - \hat{x}_k) \\ &+ \frac{\partial f}{\partial u}[h_k(\hat{x}_k, y_k) - h_k(\hat{x}_k, C\hat{x}_k)] + \varphi_2(x_k, \hat{x}_k, \theta_k). \end{aligned} \tag{6.37}$$

Since the control law is not generally differentiable, the difference term $[h_k(\hat{x}_k, y_k) - h_k(\hat{x}_k, C\hat{x}_k)]$ is used. After subtracting (6.37) from (6.36), and defining $\varphi(x_k, \hat{x}_k, u_k, \theta_k) \triangleq \varphi_1(x_k, \hat{x}_k, \theta_k) - \varphi_2(x_k, \hat{x}_k, \theta_k)$, equation (6.35) equals to (6.4). The analysis from then on stays the same. Hence Theorem 2 is still true for the EKF in the closed-loop case. ■

Corollary 1 can be viewed as a *local form of separation principle* for the NMPC and EKF. It indicates that the EKF error is not influenced by the control input in this setting. In the following, we analyze the impact of the EKF error on the NMPC stability property.

6.3 Robust Stability of Output-Feedback NMPC

The previous analysis shows that the estimated state from the EKF converges to a bounded region around the true state, introducing an estimation error. In this section, we analyze the impact of this estimation error on the robust stability of output-feedback NMPC controller. We first recall the stability result of state-feedback NMPC.

6.3.1 Stability of State-Feedback NMPC

Given x_k, the current state value at time step k, the state-feedback NMPC formulation can be described in the following discretized form:

$$V_N(x_k) := \min \sum_{j=0}^{N-1} l(z_j, v_j) + F(z_N) \tag{6.38a}$$

$$\text{s.t} \qquad z_{j+1} = f(z_j, v_j, 0), \quad j = 0, \ldots, N-1 \tag{6.38b}$$

$$z_0 = x_k,\ z_N \in \mathbb{X}_f,\ v_j \in \mathbb{U} \tag{6.38c}$$

where N is the finite time horizon, z_j is the predicted state variables, and v_j is the calculated control action based on the plant state x_k. The calculated state-feedback control law from (6.38) can be written as $u_k = v_0 = h_k(x_k)$, and the plant state at the next time step $k+1$ can be expressed as $x_{k+1} = f(x_k, h_k(x_k), \theta_k)$.

Assumption 1 *[72, 95] There exists a $\mathcal{K}_\infty$-function $\varsigma_l(\cdot)$ such that $l(x,u) \geq \varsigma_l(|x|)$ for all $x \in \mathbb{R}^{n_x}$ and $u \in \mathbb{U}$. $\mathbb{X}_f$ is an admissible control invariant set for the nominal system, i.e. for all $x \in \mathbb{X}_f$, there exists $u \in \mathbb{U}$ such that $f(x,u,0) \in \mathbb{X}_f$. $F(\cdot)$ is a control Lyapunov function (CLF) for the nominal system such that for all $x \in \mathbb{X}_f$ there exist $\mathcal{K}_\infty$-functions $\alpha_F(\cdot)$ and $\beta_F(\cdot)$ satisfying $\alpha_F(|x|) \leq F(x) \leq \beta_F(|x|)$ and $F(f(x,u,0)) - F(x) + l(x,u) \leq 0$, where u is the first element of the control sequence calculated from* (6.38).

It is shown in section 2.5 of [95] that the assumption is not restrictive in general NMPC applications. In fact, if the NMPC has a quadratic objective function, then the $\mathscr{K}_\infty$-functions in the assumption are also in quadratic form. Moreover, Chen and Allgöwer [25] proposed an approach to calculate the terminal cost to ensure the nominal stability for state-feedback NMPC. With Assumption 1, it is well known that the cost function $V_N(x)$ is a Lyapunov function for the nominal system. The NMPC controller (6.38) asymptotically stabilizes the nominal system.

For uncertain systems, using Assumption 1, Limon et al. [72] (Theorem 4) further established the ISS property of the objective function $V_N(x)$ within an robust positive invariant (RPI) set (Section 2.3.1). As illustrated in Fig. 6.1, if the initial state x_0 lies in the RPI set $\mathbb{X}_0$, the state-feedback NMPC (6.38) stabilizes the uncertain system in a neighborhood of the origin, $\mathbb{X}_N(\theta)$. This neighborhood is a $\mathscr{K}$-function of the uncertainty parameter θ. As pointed out in [72], the uncertainty set Ω_θ must be sufficiently small to ensure the existence of the RPI set $\mathbb{X}_0$.

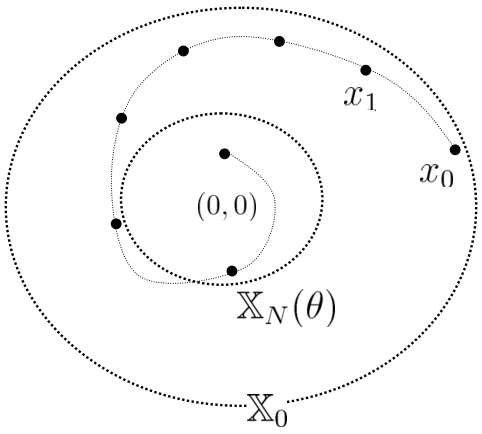

Figure 6.1: Robust stability of state-feedback NMPC.

6.3.2 Stability of Output-Feedback NMPC

For output-feedback NMPC, an state estimator such as EKF, is used to construct the initial state for the NMPC. In this section, we analyze the effect that the EKF error deteriorates the robust stability of the NMPC controller.

For the purpose of generality, we consider a state observer with a general form $\hat{x}_{k+1} = g(\hat{x}_k, y_k, h_k(\hat{x}_k, y_k)), \quad k \geq 0$, where $\hat{x}_k$ is the estimated state from the outputs y_k at time step k. Hence, the initial condition in the NMPC formulation (6.38) is modified as $z_0 = \hat{x}_k$, instead of $z_0 = x_k$ in (6.38c). The calculated output-feedback control law is $u_k = h_k(\hat{x}_k, y_k)$, and the plant state at $k+1$ can be modified as:

$$x_{k+1} = f(x_k, u_k, \theta_k) = f(x_k, h_k(\hat{x}_k, y_k), \theta_k) \tag{6.39}$$

In order to establish the robust stability of the output-feedback NMPC formulation, we make use of the following assumption.

Assumption 2 *The initial observer error is bounded by a positive constant ε_{ξ_0}, i.e. $|\hat{x}_0 - x_0| \leq \varepsilon_{\xi_0}$.*

By virtue of Theorem 2 and Assumption 2, the EKF error behaves according to $|\xi_k| \leq \eta|\xi_0|\beta^{-k} + \delta(\|\theta\|_{k-1})$. Hence there exists a constant $\widetilde{\varepsilon} \in \mathbb{R}_{\geq 0}$ that $\widetilde{\varepsilon} \geq \eta|\xi_0|\beta^{-k}$, and

$$|\xi_k| \leq \widetilde{\varepsilon} + \delta(\|\theta\|_{k-1}). \tag{6.40}$$

Then the robust stability of the output-feedback NMPC based on the nominal model is established by the following theorem.

Theorem 3 *Let function $f(x,u,\theta)$ be uniformly continuous in θ for all $x \in \mathbb{R}^{n_x}$, $u \in \mathbb{U}$, $\theta \in \Omega_\theta$ and the state-feedback NMPC* (6.38) *satisfies Assumption 1. Let $\mathbb{X}_0$ be the RPI*

set for system (6.1a)*, and Assumption 2 is satisfied. If* $f(x,u,\theta)$ *and* $l(x,u)$ *are uniformly continuous in x, and* $F(x)$ *is uniformly continuous in x for all* $u \in \mathbb{U}$ *and* $\theta \in \Omega_\theta$*, then there exists a compact set* $\widetilde{\mathbb{X}}_0 \subseteq \mathbb{X}_0$*, which is defined as* $\widetilde{\mathbb{X}}_0 \triangleq \{x | x + \varepsilon_{\xi_0} \in \mathbb{X}_0\}$*, such that the cost function* $V_N(x)$ *is an ISpS-Lyapunov function for system* (6.1a) *for all* $x \in \widetilde{\mathbb{X}}_0$*.*

Proof: The idea of the proof is to establish the ISpS property of the cost function $V_N(x)$ within $\widetilde{\mathbb{X}}_0$.

Since $x \in \widetilde{\mathbb{X}}_0$, from the definition of the RPI set $\mathbb{X}_0$, it is easy to see that $f(x,u,\theta) \in \mathbb{X}_0$ and $f(\hat{x},u,\theta) \in \mathbb{X}_0$.

Then the difference of the two neighboring optimal cost function can be decomposed as,

$$\begin{aligned} V_N(f(x,u,\theta)) - V_N(x) = {} & V_N(f(\hat{x},u,0)) - V_N(\hat{x}) + V_N(\hat{x}) \\ & - V_N(x) + V_N(f(x,u,\theta)) - V_N(f(\hat{x},u,0)) \end{aligned} \tag{6.41}$$

Assumption 1 ensures the nominal system without estimation error is asymptotically stable, and there exists a $\mathscr{K}$-function γ,

$$V_N(f(\hat{x},u,0)) - V_N(\hat{x}) \leq -\gamma(|\hat{x}|). \tag{6.42}$$

Moreover, it has been shown in [72, 95] that under the conditions stated in Theorem 3, there exists a $\mathscr{K}$-function $\upsilon_V(\cdot)$, such that

$$V_N(\hat{x}) - V_N(x) \leq \upsilon_V(|\hat{x} - x|). \tag{6.43}$$

In addition, from the uniform continuity of $f(x,u,\theta)$, there exist $\mathscr{K}$-functions υ_f and υ_θ such that

$$\begin{aligned} V_N(f(x,u,\theta)) - V_N(f(\hat{x},u,0)) &\leq \upsilon_V(|f(x,u,\theta) - f(\hat{x},u,0)|) \\ &\leq \upsilon_V \circ (\upsilon_f(|\hat{x} - x|) + \upsilon_\theta(|\theta|)) \end{aligned} \tag{6.44}$$

As a result, utilizing the identities (6.42), (6.43) and (6.44), inequality (6.41) leads to

$$\begin{aligned} V_N(f(x,u,\theta)) - V_N(x) \leq & -\gamma(|\hat{x}|) + \upsilon_V(|\hat{x}-x|) \\ & + \upsilon_V \circ (\upsilon_f(|\hat{x}-x|) + \upsilon_\theta(|\theta|)) \end{aligned} \tag{6.45}$$

The estimation state and estimation error have to be bounded. From Assumption 2, the following identity can be derived for the initial estimation state.

$$|\hat{x}-x| \leq \varepsilon_{\xi_0} \implies |x| - \varepsilon_{\xi_0} \leq |\hat{x}| \leq |x| + \varepsilon_{\xi_0}. \tag{6.46}$$

Hence, for a $\mathscr{K}$-function $\gamma(\cdot)$, we can find other $\mathscr{K}$-functions $\gamma_L(\cdot)$, $\gamma_U(\cdot)$ and positive constant c_1, c_2, such that

$$\gamma_L(|x|) - c_1 \leq \gamma(|x| - \varepsilon_{\xi_0}) \leq \gamma(|\hat{x}|) \leq \gamma(|x| + \varepsilon_{\xi_0}) \leq \gamma_U(|x|) + c_2. \tag{6.47}$$

Similarly for the later stage of the EKF, we see from equation (6.40) that $|\hat{x}-x| \leq \widetilde{\varepsilon} + \delta(\|\theta\|)$. There exist other $\mathscr{K}$-functions $\hat{\gamma}_L(\cdot)$, $\hat{\gamma}_U(\cdot)$, $\delta_L(\cdot)$, $\delta_U(\cdot)$ and positive constants c_3, c_4, such that

$$\hat{\gamma}_L(|x|) - \delta_L(\|\theta\|) - c_3 \leq \gamma(|\hat{x}|) \leq \hat{\gamma}_U(|x|) + \delta_U(\|\theta\|) + c_4. \tag{6.48}$$

As a result, for the initial estimation state, equation (6.47) indicates $-\gamma(|\hat{x}_0|) \leq -\gamma_L(|x_0|) + c_1$. In addition, we can find a constant $c_5 > 0$ such that $\upsilon_V(\varepsilon_{\xi_0}) + \upsilon_V \circ \upsilon_f(\varepsilon_{\xi_0}) + c_1 \leq c_5$, and a $\mathscr{K}$-function υ_2 that $\upsilon_2(|\theta_0|) \triangleq \upsilon_V \circ \upsilon_\theta(|\theta_0|)$. Consequently equation (6.45) leads to:

$$\begin{aligned} V_N(f(x_0,u_0,\theta_0)) - V_N(x_0) &\leq -\gamma(|\hat{x}_0|) + \upsilon_V(|\hat{x}_0 - x_0|) \\ &\quad + \upsilon_V \circ (\upsilon_f(|\hat{x}_0 - x_0|) + \upsilon_\theta(|\theta_0|)) \\ &\leq -\gamma_L(|x_0|) + \upsilon_2(|\theta_0|) + c_5 \end{aligned} \tag{6.49}$$

For the later stage of the EKF, equation (6.48) indicates $-\gamma(|\hat{x}_k|) \leq -\hat{\gamma}_L(|x_k|) + \delta_L(\|\theta\|_{k-1}) + c_3$. Then we pick a constant $c_6 > 0$ and a $\mathscr{K}$-function υ_3 such that $\delta_L(\|\theta\|_{k-1}) + c_3 +$

$\upsilon_V(|\hat{x}_k - x_k|) + \upsilon_V \circ \upsilon_f(|\hat{x}_k - x_k|) + \upsilon_V \circ \upsilon_\theta(|\theta_k|) \leq \upsilon_3(\|\theta\|_k) + c_6$. Consequently equation (6.45) leads to

$$\begin{aligned} V_N(f(x_k, u_k, \theta_k)) - V_N(x_k) &\leq -\hat{\gamma}_L(|x_k|) + \delta_L(\|\theta\|_{k-1}) + c_3 \\ &+ \upsilon_V(|\hat{x}_k - x_k|) + \upsilon_V \circ \upsilon_f(|\hat{x}_k - x_k|) + \upsilon_V \circ \upsilon_\theta(|\theta_k|) \\ &\leq -\hat{\gamma}_L(|x_k|) + \upsilon_3(\|\theta\|_k) + c_6 \end{aligned} \tag{6.50}$$

As the closed-loop system is ISpS stable for both the initial and later stages of the output-feedback NMPC integrated with the EKF, the theorem is proved. ■

Remark 5

a) As illustrated in Fig. 6.2, due to the estimation error, the system controlled by the output-feedback NMPC has to start in a smaller set $\widetilde{\mathbb{X}}_0$, in order to converge to $\mathbb{X}_N(\theta)$. Moreover, the center of $\mathbb{X}_N(\theta)$ may shift away from the origin, as the ISS stability of the state-feedback NMPC deteriorates to ISpS stability of the output-feedback NMPC. This is due to the initial estimation error. If $\xi_0 = 0$, then $|\hat{x}_k - x_k|$ is only a function of θ, and the ISS stability is restored for the output-feedback NMPC.

b) The bound of the initial error ε_{ξ_0} must be sufficiently small to ensure the existence of the set $\widetilde{\mathbb{X}}_0$.

c) From equation (6.50)*, we see that all the past uncertainty signals affect the difference between the two neighboring cost functions of the output-feedback NMPC, while only the current uncertainty signal appears in the difference term of state-feedback NMPC* (6.38).

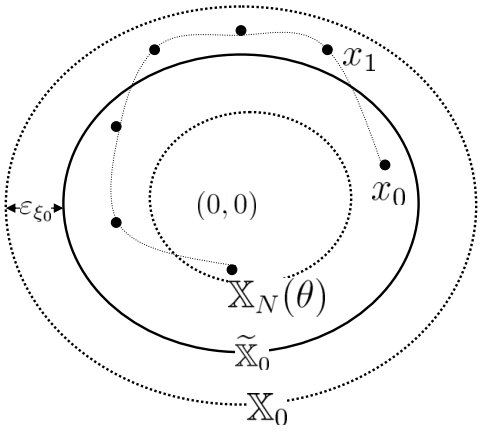

Figure 6.2: Robust stability of output-feedback NMPC.

6.4 Simulation Examples

In this section, we present two variations of offset-free output-feedback NMPC with EKF that inherit the theoretical result in Theorem 1. In addition, a simulated nonlinear CSTR with output-multiplicity is studied to demonstrate the two strategies.

Summarized in [79, 95], a conventional method for general nonlinear systems is to generate a disturbance term by comparing the predicted output and the actual output, which is then added to the objective function for the entire horizon. This method is formulated as equation (6.51). Here ρ is the disturbance term, which can be viewed as an integrator. In this section, we refer to this approach as output-feedback NMPC with *output-correction*

(OFOC).

$$\begin{aligned}
\min_{u} \sum_{j=1}^{N_p} [E_j^T W_E E_j] + \sum_{i=0}^{N_c-1} \Delta v_i^T W_{\Delta u} \Delta v_i + E_N^T W_\infty E_N \\
\text{s.t.} \quad z_{j+1} = f(z_j, v_j, 0),\ z_0 = \hat{x}_k \\
y_j = C z_j + \rho_j,\ \rho_{j+1} = \rho_j,\ \rho_0 = y_k - C\hat{x}_k \\
j = 0, \ldots, N_p - 1,\ i = 0, \ldots, N_c - 1 \\
v_j = v_{t_i} \text{ for } t_i \leq j \leq t_{i+1},\ v_i \in \mathbb{U}, \\
t_0 = 0 \leq t_1 \leq t_2 \leq, \ldots, \leq N_p - 1.
\end{aligned} \tag{6.51}$$

where $E_j \triangleq (y_j - y_r)$, y_r is the set-point for the output, $\Delta v_i = v_i - v_{i-1}$, W_E, W_∞ and $W_{\Delta u}$ are positive semidefinite weighting matrices, N_p represents the prediction horizon and N_c represents the control horizon. Similar to the NMPC formulation (5.3), we use input blocking formulation as shown by the last two constraints. They ensure that the available degrees of freedom are spread across the entire prediction horizon, since fewer degrees of freedom are available for the control movement in typical NMPC applications.

Despite the simplicity of the OFOC NMPC, the open-loop observer or online model simulations have to be used while carrying out predictions. Hence, this strategy is unable to regulate unstable systems [79]. To address this problem, Srinivasrao et al. [103] proposed an output-feedback NMPC with *state-correction* (OFSC) for empirical models, in which the observer is in the filter form. As a result, the OFSC strategy is able to regulate certain unstable systems. In this work, we extend this idea to systems with first-principle models.

The OFSC NMPC is formulated as:

$$
\begin{aligned}
\min_{u} \; & \sum_{j=1}^{N_p-1} [E_j^T W_E E_j] + \sum_{i=0}^{N_c-1} \Delta v_i^T W_{\Delta u} \Delta v_i + E_N^T W_\infty E_N \\
\text{s.t. } & z_{j+1} = f(z_j, v_j, 0) + K_k \psi_j, \\
& \psi_{j+1} = \psi_j, \; \varpi_{j+1} = \varpi_j \\
& y_j = C z_j + \varpi_j \\
& z_0 = \hat{x}_k, \; \psi_0 = y_k - C x_k^-, \; \varpi_0 = y_k - C\hat{x}_k \\
& j = 0, \ldots, N_p - 1, \; i = 0, \ldots, N_c - 1 \\
& v_j = v_{t_i} \text{ for } t_i \leq j \leq t_{i+1}, \; v_i \in \mathbb{U}, \\
& t_0 = 0 \leq t_1 \leq t_2 \leq, \ldots, \leq N_p - 1
\end{aligned} \tag{6.52}
$$

where K is the Kalman gain, and ψ and ϖ are the state and output disturbances, respectively. It may be noted that another advantage of this formulation is that it does not require adding artificial integrator states in the state estimation, as is common practice for linear and nonlinear systems [68].

It is not hard to see that both the OFOC and OFSC formulations satisfy the conditions in Theorem 1, since a general observer formulation including the EKF formulation in OFOC and OFSC strategies is used in Theorem 1. Therefore, both the strategies based on NMPC and EKF yield offset-free behavior, by virtue of Theorem 1.

The simulation studies in this section are performed on the same CSTR system (5.11) with exactly the modeling parameters in Section 5.4. In the first case, the control objective is to regulate the CSTR at a stable steady state $z_{ss} = [0.10144, 0.76708]$. The parameter k_0 in the plant is changed from its nominal value by introducing a square pulse of amplitude equal to $\pm 20\%$ at sampling instants 5, 40 and 80 as shown at the bottom of Fig. 6.5. For comparison, the CSTR is controlled by both OFOC and OFSC strategies. The EKF in both pre-

dictor and filter form is tuned with $Q = \left[\frac{\partial f}{\partial u}|_{z_{ss},u_{ss}}\right] \bar{Q} \left[\frac{\partial f}{\partial u}|_{z_{ss},u_{ss}}\right]^T$ and $\bar{Q} = \text{diag}[6.25, 0.04]$, $R = \text{diag}[1 \times 10^{-6}, 1 \times 10^{-6}]$; α in equation (6.3) is chosen equal to 1.5. The NMPC is formulated using $W_E = W_\infty = \text{diag}[1 \times 10^6,\ 1 \times 10^5]$, prediction horizon $N_p = 16$, control horizon is $N_c = 8$ and sampling time is 1. $W_{\Delta u}$ is chosen as a null matrix.

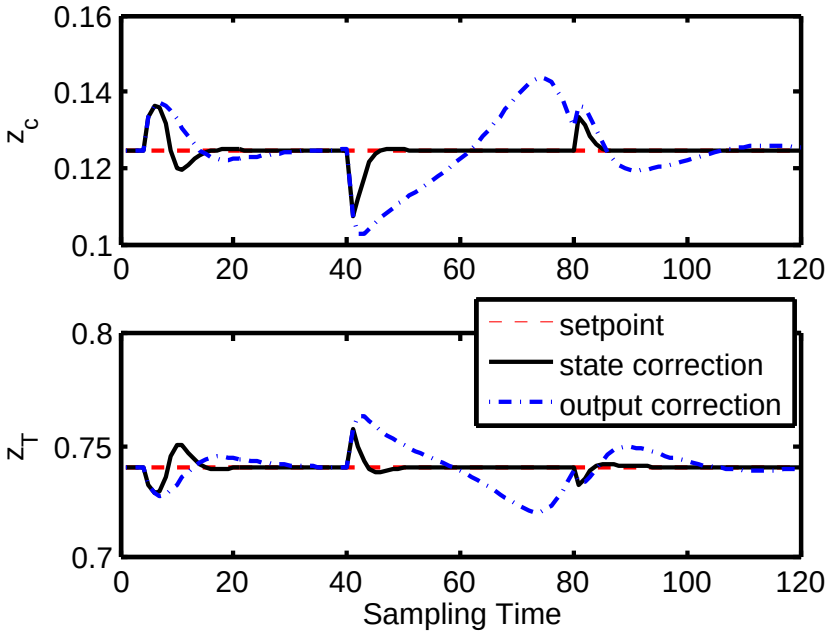

Figure 6.3: Output profile of the CSTR at the stable steady state

The resulting closed-loop responses are shown in Fig. 6.3 and 6.4, and the corresponding variation of the state estimation errors is shown in Fig. 6.5. We see that the EKF in both the predictor and filter form yields biased state estimates due to the presence of the plant-model mismatch. Fig. 6.3 shows that both the OFOC (6.51) and OFSC (6.52) strategies are able to reject the first disturbance introduced at time step 5, and regulate the output at the setpoint without any offset. The OFSC strategy (6.52) settles the system faster. After the second disturbance is introduced at time step 40, the OFSC strategy (6.52) quickly rejects the disturbance and controls the system at the set point. However, the OFOC strategy

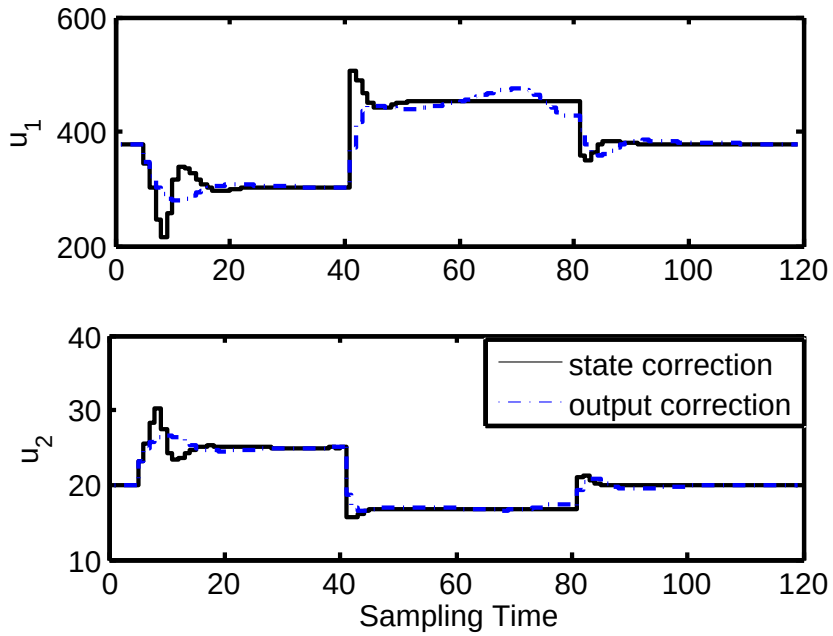

Figure 6.4: Input profile of the CSTR at the stable steady state

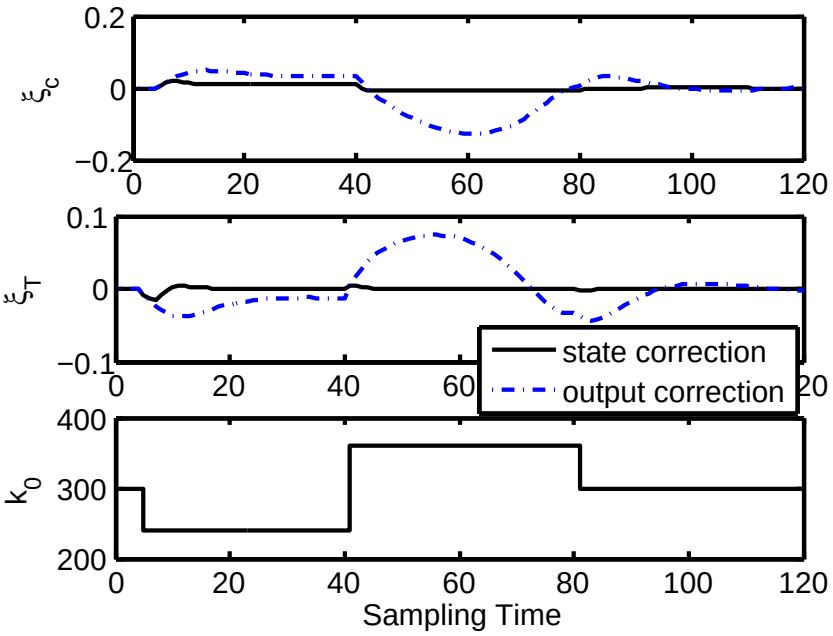

Figure 6.5: Error profile of the CSTR at the stable steady state

(6.51) needs significantly longer time to achieve the desired setpoint. Moreover, after the plant parameter k_0 is reset to its nominal value at time step 80, both the OFOC and OFSC strategies reduce to nominal NMPC since the estimated state exactly equals the actual plant state.

In the second case, the control objective is to regulate the CSTR at the unstable steady state $z_{ss} = [0.6416, 0.5387]$. The OFOC strategy (6.51) fails since the EKF in the predictor form can not work at the unstable steady state and conditions 2 and 3 in Theorem 1 are violated. The parameter k_0 in the plant is changed from its nominal value by introducing a square pulse of amplitude equal to $\pm 30\%$ at sampling instants 5 and 20 as shown at the bottom of Fig. 6.8. The OFSC strategy (6.52) is tuned to be the same as in the first case. Fig. 6.6 and 6.7 show the closed-loop plant response. We see that the OFSC strategy rejects this relatively large disturbance and regulates the plant at the unstable steady state without any offset.

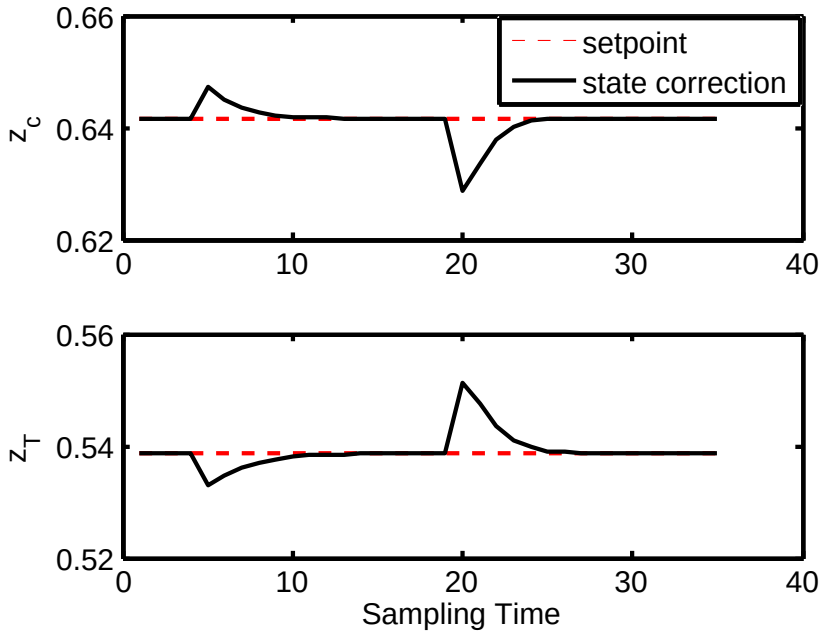

Figure 6.6: Output profile of the CSTR at the unstable steady state

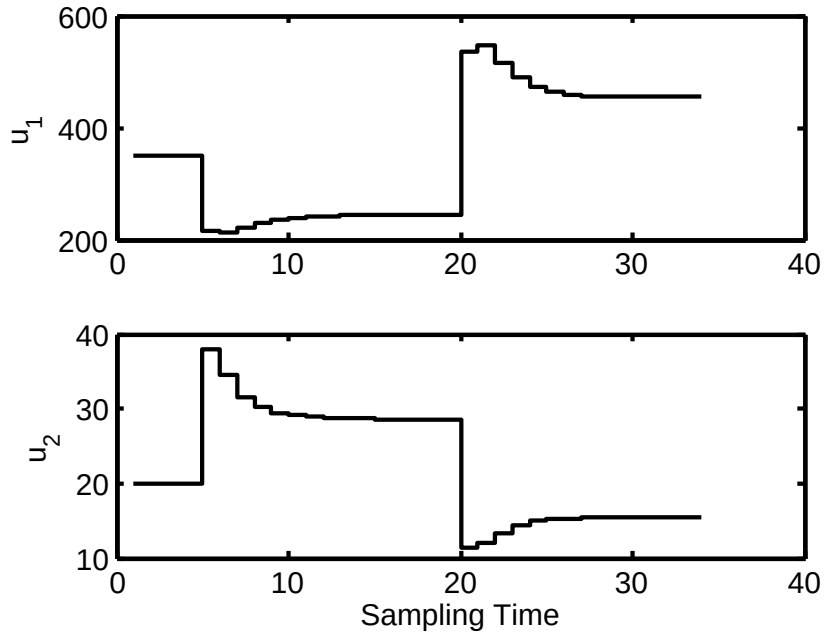

Figure 6.7: Input profile of the CSTR at the unstable steady state

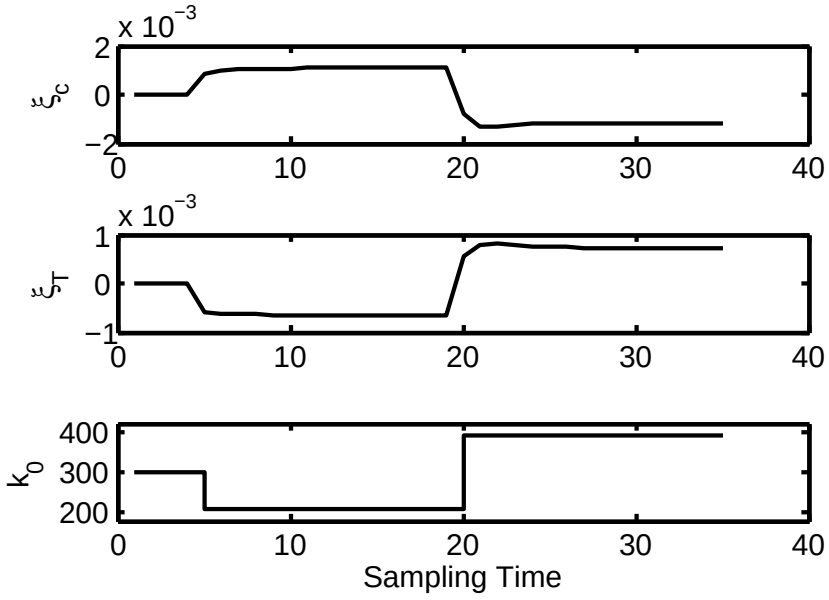

Figure 6.8: Error profile of the CSTR at the unstable steady state

6.5 Concluding Remarks

This chapter addresses the robust stability issue of output-feedback NMPC for general nonlinear systems with bounded but non-vanishing perturbations. We choose EKF as the observer, due to its wide application in control practice and its ability to control the error convergence rate. Given observability, we show that the estimated state exponentially converges to a bounded region around the true state in the presence of non-vanishing plant-model mismatches, and the convergence rate can be controlled by tuning a parameter. More importantly, we prove that this analysis holds true even for the closed-loop cases when EKF is integrated with NMPC, i.e. the control action is a function of estimated state and output.

With this result, we further analyze the impact of the estimation error on the robust stability of NMPC. Compared to state-feedback NMPC, the robust stability region of the output-feedback NMPC shrinks, due to the presence of estimation error. Moreover, we show that with the similar assumptions as state-feedback NMPC, the ISpS stability of output-feedback NMPC can be established. In addition, the ISS stability is restored if there is no initial estimation error.

Two variations of output-feedback NMPC that inherit the offset-free theoretical result in Theorem 1 are presented. Both of them are implemented on a simulated CSTR example studied in Chapter 5. It is observed that the output-feedback NMPC with state-correction (OFSC) is able to regulate the system at the unstable steady state, and shows superior performance against output-feedback NMPC with output-correction (OFOC).

Chapter 7

Nominal Stability of Economically-Oriented NMPC

In Chapter 5 and Chapter 6, we mainly focus on properties of set-point tracking NMPC. Nevertheless, the simulation result in Chapter 4 indicates that it is economically beneficial to use economically-oriented NMPC to directly minimize the operational cost of the energy intensive ASU and to take advantage of the periodically varying electricity price. In this chapter, we are interested in the nominal stability of the economically-oriented NMPC. For simplicity, we assume all the states are measured. Therefore, state-feedback NMPC is considered in this Chapter. However, the commonly-used Lyapunov framework to analyze the stability can not be applied directly to the economically-oriented NMPC. Therefore, we introduce transformed systems by subtracting the optimal cyclic steady state from the original system, for which the Lyapunov function can easily be established. We show that the asymptotical stability of the transformed system is equivalent to that of the original system. Hence it is inferred that the original systems are nominally stable at the cyclic optimal solution. Moreover, two economically-oriented NMPC formulations are proposed to ensure the system converge to the cyclic steady state.

7.1 Introduction

It has been pointed out by many researchers [33, 1, 105] that the conventional two-layer structured method is based on the assumption that model disturbance and transients are handled entirely by the controller, which may not be true for some applications. Moreover, the model inconsistency in the two layers and the presence of the transient constraints may lead to an unreachable set-point [94]. In addition, since the NMPC layer does not consider economic performance, it may be suboptimal to minimize the transition time and simply track the set-point as fast as possible [93].

Moreover, it is important to deal with systems that may not go to steady state. For instance, several applications in the process industry exhibit cyclic steady state behavior due to their operational nature, such as pressure swing adsorption (PSA) [2] and simulated moving bed (SMB) separation [60]. To deal with these periodic systems, Lee et al. [67] proposed a tracking-MPC method by using the concept of repetitive control, but without considering economic performance. Furthermore, periodically varying power prices suggest that it is difficult to achieve optimal economical performance by running the plant at a steady state. On the contrary, a periodic operation which takes advantage of the varying electricity price is preferred. For the above applications, it is difficult to implement the traditional two-layer structured method since there is no optimal steady state.

As a result, interest has significantly increased in economically-oriented NMPC which directly optimizes the plant's economic performance subject to dynamic constraints. Recently, many NMPC practitioners have reported good practical performance by using heuristic economically-oriented NMPC formulations [117, 93, 33, 7, 8]. However, there is little stability theory supporting the economically-oriented NMPC, in contrast to the mature theoretical basis of set-point tracking NMPC, where one can find good reviews [95, 78, 72] of

Lyapunov-based stability theory for both nominal and robust cases. This is partially due to the objective function of economically-oriented NMPC, which is unbounded on the infinite horizon. A more problematic issue is that the cost function of the economically-oriented NMPC is not decreasing when the plant exhibits cyclic behavior. Hence the common approach summarized in Chapter 2, which proves stability by establishing the cost function as the Lyapunov function does not apply to the economically-oriented NMPC.

This chapter studies the nominal stability of economically-oriented state-feedback NMPC for cyclic systems. As a result, assuming all the states are measurable, we use the general discrete time nonlinear plant (2.1) without uncertainty parameters. Given the cyclic steady state period, we first define the optimal cyclic steady state. To establish the Lyapunov function, a transformed system is introduced by subtracting the optimal cyclic steady state from the original system. We show that the original system is asymptotically stable at the optimal cyclic steady state if the transformed system is asymptotically stable at the origin. A Lyapunov function with respect to the transformed system can be established since it is strictly decreasing. As a result, the transformed system is asymptotically stable at the origin. Equivalently the original system is asymptotically stable at the optimal cyclic steady state.

7.2 Systems with Cyclic Behavior

For the nonlinear plant model (2.1), we consider a general economic cost function $l(x_k, u_k)$, which is not necessarily a quadratic tracking term. We assume $l(x_k, u_k)$ remains bounded for $x_k \in \mathbb{X}$ and $u_k \in \mathbb{U}$. The objective is to find a stabilized feedback control law $u_k = u(x_k)$ so that the system is feasible and the average cost function

$$\lim_{N\to\infty} \frac{1}{N} \sum_{i=0}^{N} l(x_i, u_i)$$

or its close approximation is minimized.

We also assume that K is the period of the cyclic steady state, since in practice the periods of many cyclic processes are known. For example, the periods of PSA and SMB are specified in the system design phase, and the period of the varying power price is generally published by utility companies. Hence, let us define the optimal cyclic steady state $[(x_0^*,u_0^*),(x_1^*,u_1^*),\ldots,(x_{K-1}^*,u_{K-1}^*)]$ with a period K as

$$\begin{aligned} x_{k+1}^* &= f(x_k^*,u_k^*),\ x_k^*\in\mathbb{X},\ u_k^*\in\mathbb{U},\ k=0,\ldots,K-1 \\ & (x_K^*,u_K^*)=(x_0^*,u_0^*),\ \text{and} \\ & \sum_{i=0}^{K-1} l(x_k^*,u_k^*) < \sum_{i=0}^{K-1} l(x_k,u_k),\ (x_k,u_k)\neq(x_k^*,u_k^*),\forall x_k\in\mathbb{X},u_k\in\mathbb{U}. \end{aligned} \tag{7.1}$$

As shown in Fig. 7.1, we assume the optimal cyclic steady state is unique and evolves according to the system dynamic function $f(\cdot,\cdot)$. Moreover, the optimal cyclic steady state has a period K, that is $(x_k^*,u_k^*)=(x_{k+cK}^*,u_{k+cK}^*)$, where c is any positive integer. In the following, we propose two economically-oriented NMPC formulations and further pursue a Lyapunov stability analysis. The system is assumed to have the following property.

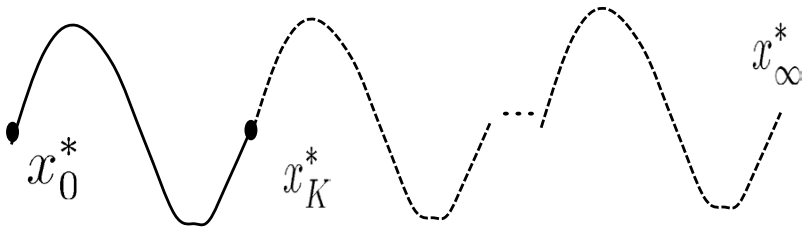

Figure 7.1: Illustration of the optimal cyclic steady state.

An input sequence $\mathbf{u}=(u_0,u_1,u_2,\ldots)$ is termed as feasible for the initial state x if $\mathbf{u}\in\mathbb{U}$, and the corresponding state sequence evolves according to the plant (2.1) with initial condition that satisfies $x_k\in\mathbb{X},\ k=0,1,\ldots,\infty$. Moreover, the admissible set $\mathbb{Z}_N$ can be

defined as the set of $(x, \mathbf{u})$

$$\mathbb{Z}_N = \{(x, \mathbf{u}) | x_k \in \mathbb{X} \text{ and } u_k \in \mathbb{U},\ k = 0, 1, \ldots, \infty\},$$

and the projection of $\mathbb{Z}_N$ onto the space $\mathbb{X}$ can be further defined as the set of admissible states $\mathbb{X}_N$, i.e.

$$\mathbb{X}_N = \{x | \exists \mathbf{u} \text{ such that } (x, \mathbf{u}) \in \mathbb{Z}_N\}. \tag{7.2}$$

We make the following commonly used assumption.

Assumption 3 *$f(\cdot,\cdot)$ and $l(\cdot,\cdot)$ are Lipschitz continuous on the admissible set, and there exist Lipschitz constants l_f and $l_l \geq 0$ such that for all (z_1, v_1), $(z_2, v_2) \in \mathbb{Z}_N$,*

$$\begin{aligned} |f(z_1, v_1) - f(z_2, v_2)| &\leq l_f |(z_1, v_1) - (z_2, v_2)| \\ |l(z_1, v_1) - l(z_2, v_2)| &\leq l_l |(z_1, v_1) - (z_2, v_2)| \end{aligned} \tag{7.3}$$

Moreover, the system is assumed to have some degree of controllability. Here we extend the concept of weak controllability defined at a single steady state by [30] to weak controllability at the optimal cyclic steady state $[(x_0^*, u_0^*), (x_1^*, u_1^*), \ldots (x_{K-1}^*, u_{K-1}^*)]$. Without losing generality, let $N = cK$, where c is a positive integer. Therefore $\sum_{k=0}^{N+K-1}(\cdot) := \sum_{p=0}^{c-1}\sum_{j=0}^{K-1}(\cdot)$.

Assumption 4 *(Weak controllability at the cyclic steady state): There exists a $\mathcal{K}_\infty$ function $\gamma(\cdot)$ such that for every initial condition $x \in \mathbb{X}_N$, there exists $\mathbf{u}$ such that $(x, \mathbf{u}) \in \mathbb{Z}_N$ and*

$$\sum_{p=0}^{c-1}\sum_{j=0}^{K-1} |u_{pK+j} - u_j^*| \leq \sum_{j=0}^{K-1} \gamma(|x_j - x_j^*|). \tag{7.4}$$

This assumption means that starting from the admissible state set, the system can be steered to the cyclic steady state in N steps without requiring large cost for the input sequence, while satisfying the constraints.

Finally, we note that the analysis in the next two sections also applies to conventional NMPC controllers, of the tracking or economic type, where the system evolves to a steady state and $K = 1$.

7.3 Strategies for Economically-Oriented NMPC

There are many strategies to guarantee the nominal stability of a set-point tracking NMPC formulation. For example, it is well known that an infinite-horizon NMPC formulation will yield nominal stability. In addition, it has been shown by Keerthi and Gilbert [61] that an equality constraint at the end of the prediction horizon also generates nominal stability. In this section, motivated by these two strategies, we propose two similar economically-oriented NMPC formulations with nominal stability proof.

7.3.1 Periodic Constraint NMPC

In the first approach, we modify the general NMPC formulation (3.14) by adding a periodic constraint at the end of the horizon:

$$\begin{aligned} & \min && \sum_{i=0}^{N+K-1} l(z_i, v_i) \\ \text{s.t} \quad & z_{i+1} &= & f(z_i, v_i), \quad i = 0, \ldots, N+K-1 \\ & z_0 &= & x_k,\ z_{N+K} = z_N, \\ & z_i &\in & \mathbb{X},\ v_i \in \mathbb{U} \end{aligned} \tag{7.5}$$

where $N+K$ is the horizon length.

In addition, $z_{N+K} = z_N$ is a periodic constraint as shown in Fig. 7.2. If the optimization problem (7.5) is well-posed and the solution of (7.5) is locally unique, then the dy-

namic system $f(\cdot,\cdot)$ will be driven from the initial condition $z_0 = x_k$ to a cyclic steady state $[z_N, z_{N+1}, \ldots, z_{N+K-1}]$, which equals to $[x_0^*, x_1^*, \ldots, x_{K-1}^*]$ according to the principle of optimality. As a result, the periodic constraint in economically-oriented NMPC (7.5) for the cyclic steady state can be viewed as the terminal equality constraint in set-point tracking NMPC (2.9) to mimic the plant dynamic over infinite time at the end of a finite horizon, as described in [61].

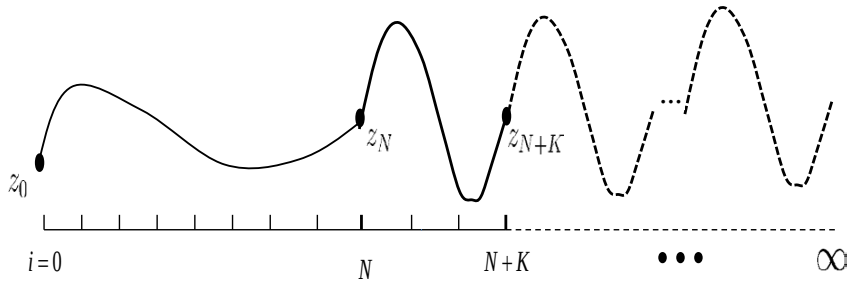

Figure 7.2: Illustration of economically-oriented NMPC with periodic constraint.

For simplicity, we make the following assumption in this section.

Assumption 5 *The optimization problem* (7.5) *satisfies the linear independent constraint qualification (LICQ) [85], sufficient second order condition (SSOC) [85] and strict complementarity (SC) [85] at the solution.*

Assumption 4 states that there exists an N such that the optimization problem (7.5) has a feasible solution with bounded objective, while Assumption 5 indicates that (7.5) is well-posed and its solution is locally unique. Therefore, the plant (2.1) controlled by NMPC (7.5) evolves to the optimal cyclic steady state $[x_0^*, x_1^*, \ldots, x_{K-1}^*]$.

To analyze the stability of NMPC, we consider previous Lyapunov stability results for set-point tracking NMPC as described in [78, 95]. In a recent work, Diehl et al [30] established a Lyapunov function for NMPC with a general economic objective function. It deals with

stability at a single steady state and establishes a Lyapunov function at the steady state. As a single steady state is not present for system (2.1) with cyclic behavior, we introduce a transformed system by subtracting the optimal cyclic steady state from the original system as follows,

$$\begin{aligned} \bar{z}_i &= z_i - x_i^* \\ \bar{v}_i &= v_i - u_i^*, \end{aligned} \tag{7.6}$$

and the transformed state evolves according to

$$\begin{aligned} \bar{z}_{i+1} &= f(\bar{z}_i + x_i^*, \bar{v}_i + u_i^*) - x_{i+1}^* \\ &= f(\bar{z}_i + x_i^*, \bar{v}_i + u_i^*) - x_{i+1-cK}^*. \end{aligned} \tag{7.7}$$

The second equality comes from the fact that the cyclic steady state x^* has a period K. It is worth emphasizing that the cyclic steady state (x_i^*, u_i^*) is assumed known in the transformed system $\bar{z}_{i+1} = \bar{f}(\bar{z}_i, \bar{v}_i)$ for the purpose of the stability analysis, but not for the implementation of the NMPC controller.

From equation (7.7), we see when $(\bar{z}_i, \bar{v}_i) = (0,0)$,

$$\begin{aligned} x_{i+1}^* &= f(x_i^*, u_i^*) = x_{i+1-cK}^* \\ \text{or} \quad z_{i+1} &= f(z_i, v_i) = z_{i+1-cK}, \quad \text{and} \quad z_i = x_i^*. \end{aligned} \tag{7.8}$$

This means that if the transformed system (7.6) is steered from initial state $\bar{z}_0 = x_k - x_0^*$ to 0, then the original system will converge to the optimal cyclic steady state, i.e. $(z_i, v_i) \to (x_i^*, u_i^*)$, when $(\bar{z}_i, \bar{v}_i) \to (0,0)$. In addition, since we consider the nominal system in this study, the plant state x evolves exactly according to the predicted state z. Therefore, the following lemma can be stated.

Lemma 5 *The stability of the transformed system*

$$\bar{z}_{i+1} = \bar{f}(\bar{z}_i, \bar{v}_i) := f(\bar{z}_i + x_i^*, \bar{v}_i + u_i^*) - x_{i+1}^* \tag{7.9}$$

at $(0,0)$ *is equivalent to the stability of the original closed-loop system* $x_{i+1} = f(x_i, u_i)$ *at the cyclic steady state* (x_i^*, u_i^*).

The proof of the Lemma follows the argument that the optimal cyclic steady state (x^*, u^*) is bounded, and both $\bar{z}$, $\bar{v}$ and x, u converge to their targets simultaneously. Therefore, the asymptotic stability of the original system is the same as that of the transformed system. As a result, we can prove the stability of the original system by showing that the transformed system is asymptotically stable at the origin.

For the purpose of stability analysis, we modify the objective function in the NMPC formulation (7.5) by subtracting the optimal cyclic steady state cost $l(x^*, u^*)$, that is

$$\sum_{i=0}^{N+K-1} (l(z_i, v_i) - l(x_i^*, u_i^*)). \tag{7.10}$$

Note that since Assumption 5 implies that the optimal cyclic steady state $[(x_0^*, u_0^*), (x_1^*, u_1^*), \ldots, (x_{K-1}^*, u_{K-1}^*)]$ is a unique solution, and $\sum_{i=0}^{N+K-1} l(x_i^*, u_i^*)$ is a constant. Thus, economically-oriented NMPC formulation (7.5) yields the same control action if the objective function is modified as (7.10). Consequently, stability result of the NMPC (7.5) remains the same even though equation (7.10) is used as the objective function.

For the transformed system (7.6), we further modify the objective function (7.10) as follows,

$$\begin{aligned} V(\bar{x}_k) &= \sum_{i=0}^{N+K-1} \bar{l}(\bar{z}_i, \bar{v}_i) \\ &:= \sum_{i=0}^{N+K-1} \left(l(\bar{z}_i + x_i^*, \bar{v}_i + u_i^*) - l(x_i^*, u_i^*)\right), \end{aligned} \tag{7.11}$$

where $\bar{x}_k = x_k - x_0^*$. It is easy to see

$$\bar{l}(0,0) = 0. \tag{7.12}$$

Therefore in the following, we show the value function (7.11) is a Lyapunov function and the transformed system is asymptotically stable at the origin.

In view of Assumption 3, it is equivalent to state that for all (z_1, v_1), $(z_2, v_2) \in \mathbb{Z}_N$, the transformed system $\bar{f}(\cdot,\cdot)$ and cost function $\bar{l}(\cdot,\cdot)$ are Lipschitz continuous, that is there exist Lipschitz constants $l_{\bar{f}}$ and $l_{\bar{l}} \geq 0$ such that

$$\begin{aligned} |\bar{f}(\bar{z}_1, \bar{v}_1) - \bar{f}(\bar{z}_2, \bar{v}_2)| &\leq l_{\bar{f}} |(\bar{z}_1, \bar{v}_1) - (\bar{z}_2, \bar{v}_2)| \\ |\bar{l}(\bar{z}_1, \bar{v}_1) - \bar{l}(\bar{z}_2, \bar{v}_2)| &\leq l_{\bar{l}} |(\bar{z}_1, \bar{v}_1) - (\bar{z}_2, \bar{v}_2)| \end{aligned} \tag{7.13}$$

Similarly, the weak controllability Assumption 4 and the periodic constraint in (7.5) requires the transformed system (7.6) to be steerable to the origin without large input cost. Hence, there exists a $\mathscr{K}_\infty$ function $\gamma_z(\cdot)$

$$\sum_{i=0}^{N+K-1} |\bar{v}_i - 0| \leq \gamma_z(|\bar{z}_0 - 0|). \tag{7.14}$$

Finally, we make a similar assumption for the transformed system as with the stability analysis for the set-point tracking NMPC.

Assumption 6 *There exists a $\mathscr{K}_\infty$ function $\beta(\cdot)$ such that the stage cost $\bar{l}(\cdot,\cdot)$ satisfies*

$$\bar{l}(\bar{z}, \bar{v}) \geq \beta(|\bar{z} - 0|) \tag{7.15}$$

In practice, a general economic objective function may not satisfy this assumption, but one can add regularization terms to the economic objective function so that Assumption 6 holds.

The main theorem of this section is stated as:

Theorem 4 *Let Assumptions 3, 4, 5 and 6 hold, then $V(\bar{x}_k)$ defined as equation* (7.11) *is a Lyapunov function and the transformed system $(\bar{z},\bar{v})$ is asymptotically stable at $(0,0)$. Consequently, the original closed-loop system controlled by the periodic constraint NMPC* (7.5) *is asymptotically stable at the optimal cyclic steady state (x_i^*,u_i^*).*

Proof: From the definition of a $\mathscr{K}_\infty$ function, Assumption 6 implies that

$$\bar{l}(\bar{z},\bar{v}) \geq 0, \tag{7.16}$$

then

$$V(\bar{x}_k) = \sum_{i=0}^{N+K-1} \bar{l}(\bar{z}_i,\bar{v}_i) \geq \beta(|\bar{x}_k - 0|) \tag{7.17}$$

Moreover, Assumption 4 and periodic constraint in (7.5) imply that for the transformed system, $\bar{z}_i = 0, \forall i \geq N+K-1$. Therefore from the fact that the system is nominal, we have

$$V(\bar{f}(\bar{x}_k,\bar{u}_k)) - V(\bar{x}_k) \leq -\bar{l}(\bar{x}_k,\bar{u}_k) \leq -\beta(|\bar{x}_k - 0|), \tag{7.18}$$

where the second inequality comes from Assumption 6.

Finally from equation (7.12), Assumption 3 and equation (7.13), we see

$$\begin{aligned} V(\bar{x}_k) &= \sum_{i=0}^{N+K-1} \bar{l}(\bar{z}_i,\bar{v}_i) \\ &= \sum_{i=0}^{N+K-1} \big(\bar{l}(\bar{z}_i,\bar{v}_i) - \bar{l}(0,0)\big) \\ &\leq l_{\bar{l}}\Big(\sum_{i=0}^{N+K-1} |\bar{z}_i - 0| + \sum_{i=0}^{N+K-1} |\bar{v}_i - 0|\Big). \end{aligned} \tag{7.19}$$

Moreover, from Lipschitz continuity of $\bar{f}(\cdot,\cdot)$, we have

$$\begin{aligned} |\bar{z}_i - 0| \leq\ & l_{\bar{f}}^i |\bar{z}_0 - 0| + l_{\bar{f}}^i |\bar{v}_0 - 0| \\ & + l_{\bar{f}}^{i-1} |\bar{v}_1 - 0| + \ldots + l_{\bar{f}} |\bar{v}_{i-1} - 0|. \end{aligned} \tag{7.20}$$

Summing this inequality gives

$$\sum_{i=0}^{N+K-1} |\bar{z}_i - 0| \leq L_F \left[|\bar{z}_0 - 0| + \sum_{i=0}^{N+K-1} |\bar{v}_i - 0| \right] \tag{7.21}$$

where $L_F \geq 1 + l_{\bar{f}} + \ldots + l_{\bar{f}}^{N+K-1}$.

In addition, from Assumption 4 and equation (7.14), we have

$$\sum_{i=0}^{N+K-1} |\bar{v}_i - 0| \leq \gamma_z(|\bar{z}_0 - 0|) \tag{7.22}$$

Notice $\bar{z}_0 = \bar{x}_k$. As a result, equation (7.19) turns out to be

$$\begin{aligned} V(\bar{x}_k) &\leq l_{\bar{l}}\Big(\sum_{i=0}^{N+K-1} |\bar{z}_i - 0| + \sum_{i=0}^{N+K-1} |\bar{v}_i - 0| \Big) \\ &\leq l_{\bar{l}} L_F |\bar{x}_k - 0| + l_{\bar{l}}(L_F + 1)\gamma_z(|\bar{x}_k - 0|). \end{aligned} \tag{7.23}$$

Hence

$$V(\bar{x}_k) \leq \alpha(|\bar{x}_k|) \tag{7.24}$$

where $\alpha(\cdot) = l_{\bar{l}} L_F(\cdot) + l_{\bar{l}}(L_F + 1)\gamma_z(\cdot)$ is a $\mathscr{K}_\infty$ function. Therefore, equations (7.17), (7.18) and (7.24) indicate that $V(\bar{x}_k)$ is an Lyapunov function and the transformed system is asymptotically stable. Then in view of Lemma 5, the original closed-loop system is asymptotically stable at the optimal cyclic steady state. ■

7.3.2 Infinite Horizon NMPC with a Discount Factor

In the second approach, we propose an infinite horizon formulation without periodic constraints, which is the counterpart of the infinite horizon formulation for set-point tracking NMPC. The main advantage of using infinite horizon formulation is that the somewhat arbitrary choice of the final time of the optimization problem is avoided. Moreover since the cost function is optimized on the infinite horizon, we also consider a discount factor

in the cost function. The discount factor $\rho > 0$ projects the future profit or cost to the present value and is introduced as in [111]. More discussion on the discount factor and its economic implication can be found in [111]. The infinite horizon NMPC with economic objective function at time step k is formulated as follows:

$$\min_{(z_i,v_i)} \sum_{i=0}^{\infty} \frac{l(z_i,v_i)}{(1+\rho)^{k+i}} + |z_i - z_{K+i}|_Q^2 + |v_i - v_{K+i}|_R^2 \tag{7.25a}$$

$$\text{s.t}: \quad z_{i+1} = f(z_i,v_i), \quad i = 1,\ldots,\infty \tag{7.25b}$$

$$z_0 = x_k \tag{7.25c}$$

$$z_i \in \mathbb{X}, \quad \text{and} \quad v_i \in \mathbb{U} \tag{7.25d}$$

By adding the term $|z_i - z_{K+i}|_Q^2 + |v_i - v_{K+i}|_R^2$, where Q and R are positive definite weighting matrices, one can regularize the objective function to ensure the problem (7.25) is well-posed and its solution is locally unique. Moreover, it forces the system to converge to a cyclic steady state with period K. Otherwise, the objective function will grow infinitely. Since the discount factor $\rho > 0$, and $l(z,v)$ remains bounded for all $z \in \mathbb{X},\ v \in \mathbb{U}$, $\lim_{i\to\infty} \frac{l(z_i,v_i)}{(1+\rho)^{k+i}} \to 0$. Hence, the objective function (7.25a) remains bounded on the infinite horizon.

Similar to Assumption 5, we make the following assumption for the infinite horizon NMPC (7.25).

Assumption 7 *The optimization problem* (7.25) *satisfies linear independent constraint qualification (LICQ) [85], sufficient second order condition (SSOC) [85] and strict complementarity (SC) [85] at the solution.*

In practice, one can adjust Q and R in the regularization terms in the objective function to ensure this assumption is satisfied, which implies that the optimization problem (7.25) is well-posed and its solution is locally unique. As a result, by the principle of optimality, the

system evolves to the optimal cyclic steady state $[x_0^*, x_1^*, \ldots, x_{K-1}^*]$.

For the purpose of stability analysis, we introduce the transformed system (7.6) as in the Section 7.3.1, and Lemma 5 holds true for the infinite horizon formulation as well. Moreover, the objective function in (7.25) is modified by subtracting the optimal cyclic steady state cost,

$$\sum_{i=0}^{\infty} \frac{l(z_i, v_i) - l(x_i^*, u_i^*)}{(1+\rho)^{k+i}} + |z_i - z_{K+i}|_Q^2 + |v_i - v_{K+i}|_R^2. \tag{7.26}$$

Since

$$-\sum_{i=0}^{\infty} \frac{l(x_i^*, u_i^*)}{(1+\rho)^{k+i}}$$

is a constant, the objective function (7.26) only differs from the objective function (7.25a) by a constant, and the infinite horizon formulation (7.25) yields the same control action if (7.26) is used as the objective function. In addition, with $x_i^* = x_{K+i}^*$ and $u_i^* = u_{K+i}^*$, the objective function (7.26) is further modified as

$$\begin{aligned} V_\infty(\bar{x}_k) &= \sum_{i=0}^{\infty} L(\bar{z}_i, \bar{v}_i) \\ &= \sum_{i=0}^{\infty} \frac{\bar{l}(\bar{z}_i, \bar{v}_i)}{(1+\rho)^{k+i}} + |(z_i - x_i^*) - (z_{K+i} - x_{K+i}^*)|_Q^2 + |(v_i - u_i^*) - (v_{K+i} - u_{K+i}^*)|_R^2, \end{aligned} \tag{7.27}$$

where $\bar{x}_k = x_k - x_0^*$ at time step k, and $\bar{l}(\bar{z}_i, \bar{v}_i)$ is defined in equation (7.11). It is clear that $L(0,0) = 0$. Therefore, in the following, we show that $V_\infty(\bar{x}_k)$ is a Lyapunov function at time step k.

In view of Assumption 3 and equation (7.13), it is easy to see that the stage cost $L(\cdot,\cdot)$ is Lipschitz continuous. Thus there exist Lipschitz constants l_L and $l_{\bar{f}}$ such that

$$\begin{aligned} |\bar{f}(\bar{z}_1, \bar{v}_1) - \bar{f}(\bar{z}_2, \bar{v}_2)| &\leq l_{\bar{f}} |(\bar{z}_1, \bar{v}_1) - (\bar{z}_2, \bar{v}_2)| \\ |L(\bar{z}_1, \bar{v}_1) - L(\bar{z}_2, \bar{v}_2)| &\leq l_L |(\bar{z}_1, \bar{v}_1) - (\bar{z}_2, \bar{v}_2)|, \end{aligned} \tag{7.28}$$

where $\bar{f}(\cdot,\cdot)$ is defined in (7.9) and the Lipschitz constant $l_{\bar{f}}$ is defined in (7.13).

In addition, the regularization term $|(z_i - z_{K+i})|_Q^2 + |(v_i - v_{K+i})|_R^2$ allows us to make the following assumption similar to Assumption 6.

Assumption 8 *There exits a K_∞ function $\beta_\infty(\cdot)$ such that the stage cost $L(\cdot,\cdot)$ defined in* (7.27)*, satisfies*

$$L(\bar{z},\bar{v}) \geq \beta_\infty(|\bar{z}-0|). \tag{7.29}$$

Moreover, the weak controllability of Assumption 4 indicates that there exists a sequence of feasible control actions $\tilde{v}_0, \tilde{v}_1, \ldots, \tilde{v}_{N+K-1}$ that steers the plant from the initial condition x_k to the optimal cyclic steady state $[(x_0^*, u_0^*), (x_1^*, u_1^*), \ldots, (x_{K-1}^*, u_{K-1}^*)]$ in N time steps. As a result, $(\tilde{z}_i, \tilde{v}_i) = (x_i^*, u_i^*), \forall i \geq N+K$. For this particular feasible solution, let the transformed system be

$$\begin{aligned} \hat{z}_i &= \tilde{z}_i - x_i^* \\ \hat{v}_i &= \tilde{v}_i - u_i^*,\ i = 0,1,\ldots,\infty, \end{aligned} \tag{7.30}$$

then

$$L(\hat{z}_i, \hat{v}_i) = 0 \quad i \geq N+K. \tag{7.31}$$

Furthermore, for the transformed system, condition (7.4) implies that there exists a $\mathscr{K}_\infty$ function $\gamma_\infty(\cdot)$

$$\sum_{i=0}^{N+K-1} |\hat{v}_i - 0| \leq \gamma_\infty(|\bar{x}_k - 0|). \tag{7.32}$$

Now, we are ready to state the main theorem in this section.

Theorem 5 *Let Assumptions 3, 4, 7 and 8 hold, then at time step k, the value function $V_\infty(\bar{x}_k)$ defined by* (7.27) *is a Lyapunov function, and the transformed system* (7.6) *is asymptotically stable at* $(0,0)$*. Consequently, the original closed-loop system controlled by the*

infinite horizon NMPC (7.25) *is asymptotically stable at the optimal cyclic steady state* (x_i^*, u_i^*).

Proof: Assumption 8 indicates that

$$L(\bar{z}, \bar{v}) \geq 0,$$

then

$$V_\infty(\bar{x}_k) = \sum_{i=0}^{\infty} L(\bar{z}_i, \bar{v}_i) \geq L(\bar{z}_0, \bar{v}_0) \geq \beta_\infty(|\bar{x}_k - 0|). \tag{7.33}$$

From the principle of optimality and the fact that the system is nominal, we have

$$\begin{aligned} V_\infty(\bar{f}(\bar{x}_k, \bar{u}_k)) - V_\infty(\bar{x}_k) &= \sum_{i=1}^{\infty} L(\bar{z}_i, \bar{v}_i) - \sum_{i=0}^{\infty} L(\bar{z}_i, \bar{v}_i) \\ &= -L(\bar{z}_0, \bar{v}_0) \leq -\beta_\infty(|\bar{x}_k - 0|), \end{aligned} \tag{7.34}$$

where the inequality is from Assumption 8 and $\bar{z}_0 = \bar{x}_k$ at the time step k.

Since $(\tilde{z}_i, \tilde{v}_i)$ (and the corresponding transformation $(\hat{z}_i, \hat{v}_i)$) is a feasible solution to problem (7.25), the associated cost is greater or equal than that of the optimal solution, that is

$$\begin{aligned} V_\infty(\bar{x}_k) &= \sum_{i=0}^{\infty} L(\bar{z}_i, \bar{v}_i) \leq \sum_{i=0}^{\infty} L(\hat{z}_i, \hat{v}_i) \\ &= \sum_{i=0}^{N+K-1} L(\hat{z}_i, \hat{v}_i), \end{aligned} \tag{7.35}$$

where the last equality is from equation (7.31). Then taking norms, utilizing the triangle inequality, and Lipschiz continuity of $L(\cdot, \cdot)$ in (7.28) , we have

$$\begin{aligned} V_\infty(\bar{x}_k) &\leq \sum_{i=0}^{N+K-1} (L(\hat{z}_i, \hat{v}_i) - L(0,0)) \\ &\leq \sum_{i=0}^{N+K-1} l_L(|\hat{z}_i - 0| + |\hat{v}_i - 0|). \end{aligned} \tag{7.36}$$

Moreover, repeatedly using Lipschiz continuity of $\bar{f}(\cdot,\cdot)$, we see

$$|\hat{z}_i - 0| \leq l_{\bar{f}}^i |\hat{z}_0 - 0| + l_{\bar{f}}^i |\hat{v}_0 - 0| + l_{\bar{f}}^{i-1} |\hat{v}_1 - 0| + \cdots + l_{\bar{f}} |\hat{v}_{i-1} - 0|. \tag{7.37}$$

Summing this inequality yields

$$\sum_{i=0}^{N+K-1} |\hat{z}_i - 0| \leq L_F \left[|\hat{z}_0 - 0| + \sum_{i=0}^{N+K-1} |\hat{v}_i - 0| \right], \tag{7.38}$$

where $L_F = 1 + l_{\bar{f}} + \cdots + l_{\bar{f}}^{N+K-1}$. In view of Assumption 4, equation (7.32) and $\hat{z}_0 = \bar{x}_k$ at time step k, the value function $V_\infty(\bar{x}_k)$ can be expressed as:

$$\begin{aligned} V_\infty(\bar{x}_k) &\leq \sum_{i=0}^{N+K-1} \left(L(\hat{z}_i, \hat{v}_i) - L(0,0) \right) \\ &\leq l_L L_F |\hat{z}_0 - 0| + l_L (L_F + 1) \gamma_\infty(|\hat{z}_0 - 0|) \end{aligned} \tag{7.39}$$

Hence we can define a $\mathscr{K}_\infty$ function $\alpha_\infty(\cdot) = l_L L_F(\cdot) + l_L(L_F + 1)\gamma_\infty(\cdot)$ so that the value function satisfies,

$$V_\infty(\bar{x}_k) \leq \alpha_\infty(|\bar{x}_k|) \tag{7.40}$$

As a result, equation (7.33), (7.34) and (7.40) indicates that at time step k, $V_\infty(\bar{x}_k)$ is a Lyapunov function and the transformed system is asymptotically stable. Then in view of Lemma 5, the original closed loop system is asymptotically stable at the cyclic steady state. ■

7.4 Simulation Examples

In this section, we consider two simulation systems for the infinite horizon NMPC formulation (7.25) and periodic constraint NMPC (7.5), respectively.

7.4.1 Double-tank System with Infinite Horizon NMPC

First, an interconnected double-tank system as shown in Fig. 7.3 is studied. The liquid inlet flow into the first tank is F_{in}. The liquid outlet flow from the first tank is the liquid inlet flow into the second tank. It is determined by the liquid height in the first tank x_1, i.e. $0.4x_1^{\frac{1}{2}}$. The liquid outlet flow from the second tank is termed as F_{out}. Similarly, F_{out} is a function of the liquid height in the second tank x_2, i.e. $F_{out} = 0.4x_2^{\frac{1}{2}}$. It is required that F_{out} is maintained above a certain level all the time, i.e. $F_{out} \geq 0.16$ using F_{in} as the control variable. In addition, the operational cost is considered as F_{in} multiplied by a sinusoidally varying power price with 10 time steps as the period, which is shown at the bottom of Fig. 4.7. The control objective is to minimize the operational cost while satisfying all the system constraints.

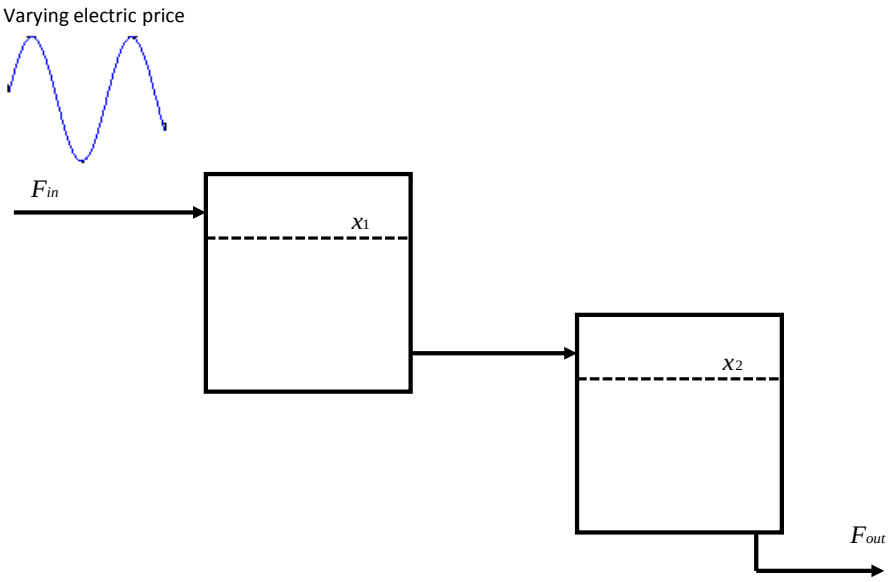

Figure 7.3: Double-tank system.

The mathematical model of the double-tank system can be described by the following ODE

system:

$$\begin{aligned} \frac{dx_1}{dt} &= 0.16F_{in} - 0.4x_1^{\frac{1}{2}} \\ \frac{dx_2}{dt} &= 0.4x_1^{\frac{1}{2}} - F_{out} \\ F_{out} &= 0.4x_2^{\frac{1}{2}}. \end{aligned} \tag{7.41}$$

The infinite horizon NMPC (7.25) is applied to this system. The objective function is to minimize the utility cost, and the period is $K = 10$ time steps, and the horizon is $N = 50$ time steps. The discount factor is $\rho = 0.01$. The tuning matrices are $Q = \text{diag}[1,1]$ and $R = 0$.

The closed-loop responses of this system are shown in Figs. 7.4, 7.5 and 7.6. From Fig. 7.4, we see that both the states in the double-tank system exhibit cyclic steady state behavior with a period of 10 time steps, which is the same as the sinusoidally varying power price profile. Moreover, after a few sampling times, the system asymptotically converges to the cyclic steady state and is stabilized. As a result, the outlet flow F_{out} also changes sinusoidally with the varying power price as shown in Fig. 7.5. In addition, it is interesting to note from Fig. 7.6 that the F_{in} roughly follows the trend of the price profile. This means that most of the liquid inlet flow is pumped into the double-tank system when it is the cheapest to do so.

Moreover, it is worth mentioning that the periodic constraint NMPC (7.5) is also implemented on the double-tank system and a very similar simulation result is observed.

7.4.2 Periodic Constraint NMPC for the ASU

In this section, periodic constraint NMPC (7.5) is used to control the nominal ASU model as described in Section 4.2. The control structure is exactly the same as in Section 4.4

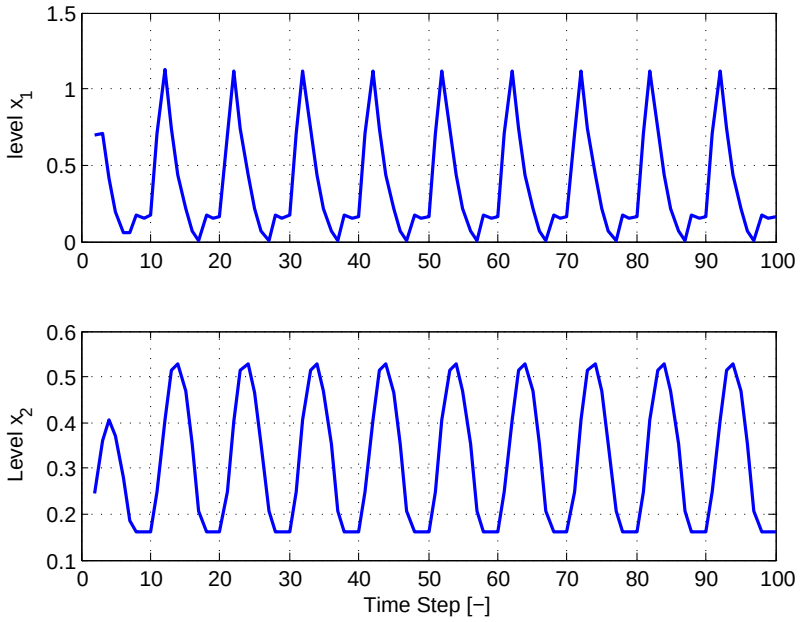

Figure 7.4: State variables (levels) profiles in the tank controlled by economically-oriented NMPC

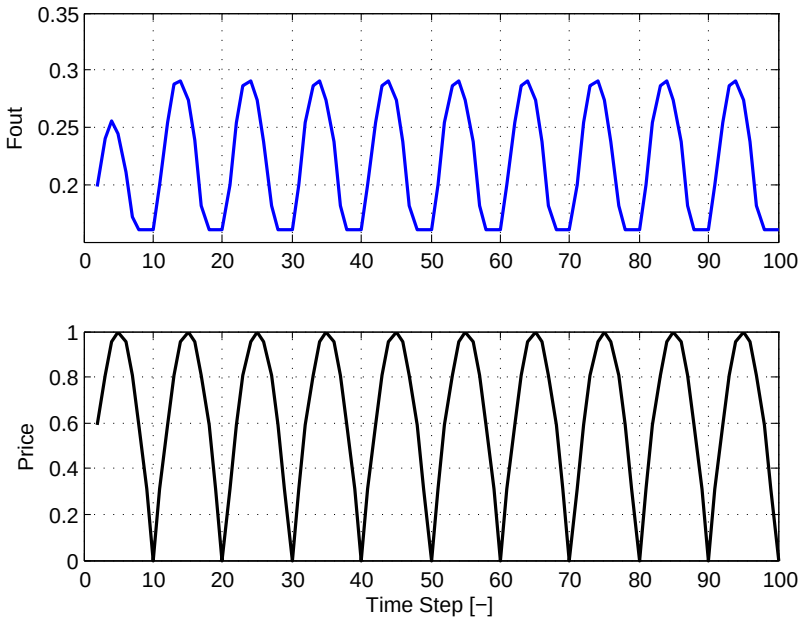

Figure 7.5: Outlet flow profile from the tank controlled by economically-oriented NMPC, F_{out} and power price profile

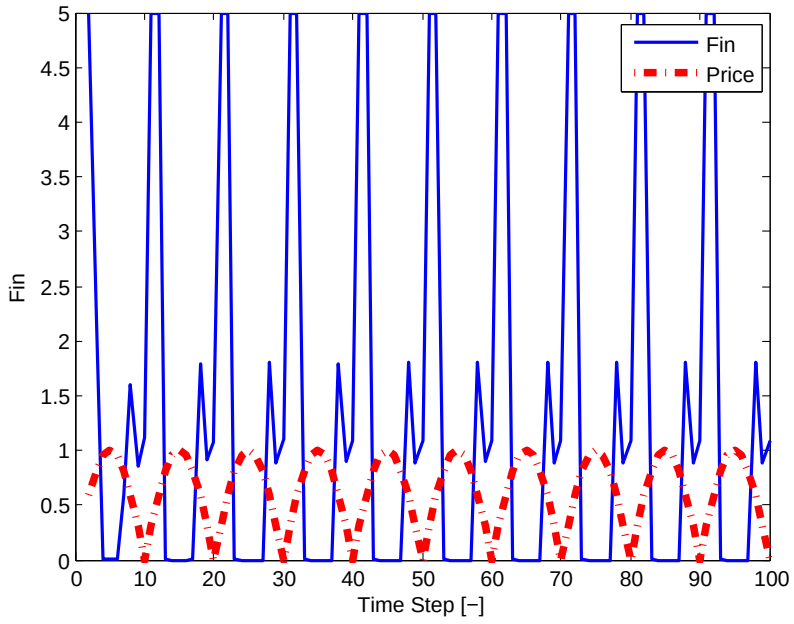

Figure 7.6: Control variable (F_{in} to first tank) profile in economically-oriented NMPC

and the objective function is chosen to be (4.16). The regularization term *reg.* in (4.16) can make sure that the periodic constraint NMPC (7.5) satisfies Assumptions 5 and 6. Moreover, the sinusoidally varying electricity price with period of 60 minutes is shown in Fig. 7.7. This high frequency is chosen to provide a clearer demonstration of cyclic behavior.

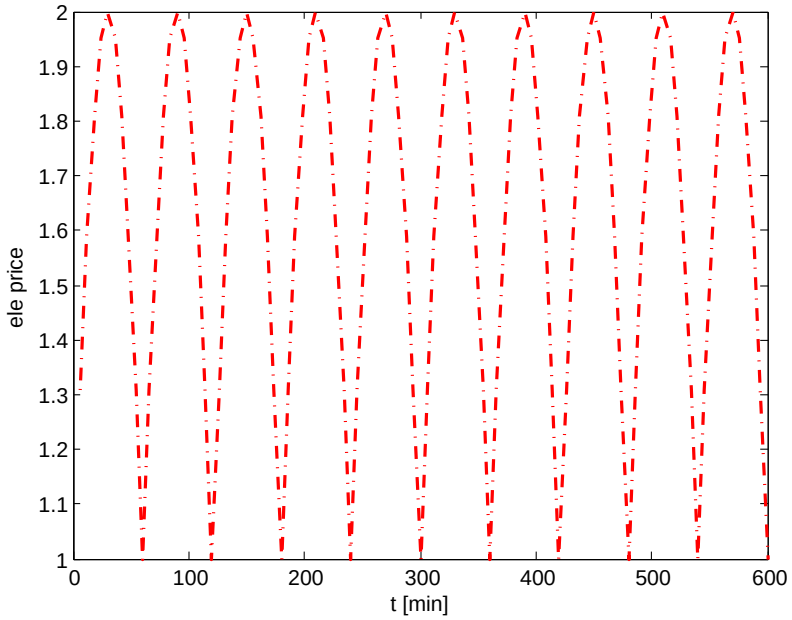

Figure 7.7: Varying power price profile

The closed-loop responses are shown in Fig. 7.8 and 7.9. It is easy to see that both input flowrates (EA and MA) exhibit sinusoidal behavior, and are at their minimum when the electricity price is the highest. Moreover, the economically-oriented periodic constraint NMPC (7.5) reduces the operational cost ((EA+MA)$\times$ ele price) by 29.71%, compared to set-point tracking NMPC.

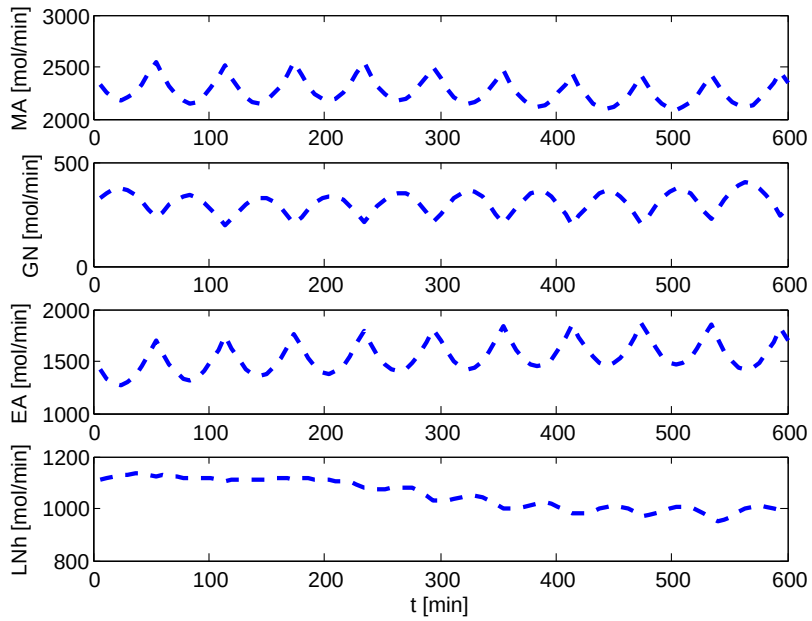

Figure 7.8: Input profile in the ASU controlled by economically-oriented NMPC

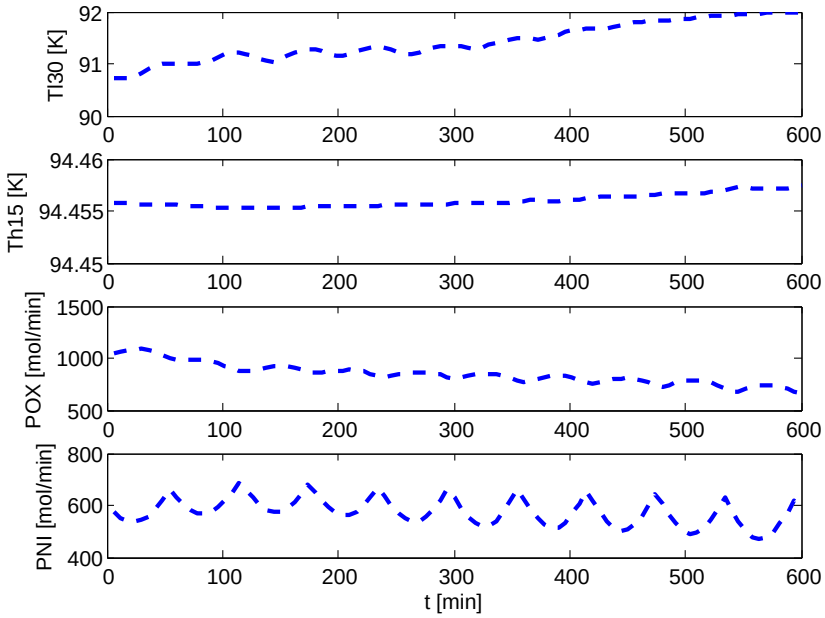

Figure 7.9: Output profile in the ASU controlled by economically-oriented NMPC

7.5 Concluding Remarks

This chapter proposes economically-oriented NMPC formulations with guaranteed nominal stability for systems with cyclic steady state behavior. A periodic constraint NMPC formulation and an infinite horizon NMPC formulation with a discount factor are proposed to solve the economically-oriented problems. However, since the NMPC objective function, which is the most common candidate of a Lyapunov function, is not strictly decreasing at the optimal cyclic steady state, it is difficult to directly apply the widely-used framework for set-point tracking NMPC to prove stability. To overcome this problem, transformed systems that subtract the optimal cyclic steady state from the original systems are introduced. It is easy to establish Lyapunov functions for the transformed systems. Moreover, we show that the transformed systems enjoy the same nominal stability as the original systems. Hence, nominal stability for the original system is also proved. Moreover, we note that the stability analysis for both formulations also applies to conventional NMPC controllers, of the tracking or economic type, where the system evolves to a steady state and $K = 1$.

To demonstrate the performance of these NMPC formulations, we consider two case studies where electricity price varies periodically. Therefore, there is an economic interest to apply the proposed formulations on the systems to take advantage of the varying electricity price. The infinite horizon NMPC formulation is implemented on a double-tank system, while the periodic constraint NMPC is applied to the ASU process. In both cases, the systems are stabilized at optimal cyclic steady states, and the electricity costs are minimized.

Chapter 8

Conclusions

Nonlinear model predictive control (NMPC) has gradually emerged as an important advanced control technique in the process industry. Current advances in dynamic optimization algorithms and software allow us to incorporate first-principle dynamic models and solve them quickly enough online. The incorporation of first-principle dynamic models leads to an economically-oriented formulation that directly optimizes the economic performance of an operation. Despite good practical performance reported by many researchers, there are still open questions regarding the theoretical and practical issues of NMPC. This dissertation aims to address some of these theoretical challenges of NMPC and dynamic real time optimization (D-RTO). In this chapter, we summarize the thesis contributions and present recommendations for future work.

8.1 Thesis Summary and Contributions

Chapter 2 reviews the recent developments in the area of real time NMPC strategies and stability analyses for both set-point tracking and economically-oriented NMPC. It serves as a centralized literature review in the dissertation.

Chapter 3 briefly discusses the advantages and disadvantages of different approaches for solving DAE-constrained optimization problem. Full-discretization strategy based on or-

thogonal collocation is used throughout this dissertation. This strategy will lead to large scale NLP problems. IPOPT, which is an interior point NLP solver is used. However, solving the problem may introduce computational delay especially for online applications such as NMPC and MHE, which are the focus of this dissertation. Hence, the advanced step algorithm based on NLP sensitivity is introduced to reduce the online computational delay.

Chapter 4 makes use of the methods discussed in Chapter 3 and applies them for a large scale air separation unit. Both set-point tracking and economically-oriented NMPC controllers are studied. Our contributions are:

- The derivation of first-principle dynamic model for an ASU process.
- Simulation study of implementing asNMPC on the ASU model shows advantages over linear MPC, which is the common practice in the process industry.
- Proposing economically-oriented NMPC formulations that directly optimize the economical performance of the ASU. Around 6% cost reduction is achieved. In this case, a moving-horizon-based ARIMA modeling strategy is developed to forecast the future electricity prices.

Chapter 5 studies a practical issue in the NMPC formulation, which is to achieve offset-free behavior based on state estimation in the presence of plant-model mismatch. Moreover, the asNMPC and asMHE methods introduced in Chapter 3 are used to reduce the online computational delay with little performance loss. Our contributions are:

- Proposing two variations of offset-free output-feedback NMPC based on MHE. When the uncertainty structure is unknown, we use state and output disturbances to compensate for the uncertainty parameter. On the other hand, if the uncertainty parameter

structure is known, MHE is used to estimate both the state and uncertainty simultaneously to remove the plant-model mismatch.

- The state and output disturbance formulation is shown to have steady state offset-free property. Moreover, the analysis is based on a general state estimation formulation. Therefore, it applies to output-feedback NMPC with a wide class of state estimators, including MHE, EKF and other recursive observers.

Chapter 6 focuses on the closed-loop robust stability of output-feedback NMPC in the presence of plant-model mismatch. Although both nominal and robust stability have been heavily investigated in the literature, there are few contributions devoted to the stability property of output-feedback NMPC. This follows because there is no general separation principle for nonlinear systems. Therefore, we choose EKF as the nonlinear observer in the output-feedback NMPC in this chapter because of its popularity in industry. Our contributions are:

- Analysis of robust stability of EKF in the presence of plant-model mismatch. The estimation error dynamic is shown to have ISS property.
- A separation-principle-like result for the EKF is proven. It is demonstrated that the EKF error dynamics are not affected by the control action.
- The impact of the estimation error on the robust stability of the output-feedback NMPC is studied. It is shown that the robust stability region shrinks and only ISpS property can be established for the closed-loop system.
- An output-feedback NMPC formulation with EKF based on state and output disturbances is proposed and it inherits the offset-free result in Chapter 5. Moreover, it is observed that the proposed OFSC formulation (6.52) has superior performance against the traditional OFOC method (6.51).

Chapter 7 studies the nominal stability of economically-oriented state-feedback NMPC for cyclic processes. Here, the commonly-used Lyapunov framework to analyze the stability can not be applied directly to the economically-oriented NMPC. This is because of the following two reasons: 1) the objective function of economically-oriented NMPC is unbounded on the infinite horizon; 2) the corresponding Lyapunov function is not decreasing when the plant exhibits cyclic behavior. Our contributions are:

- The nominal stability of the economically-oriented NMPC is proven by establishing Lyapunov satiability for a transformed system, which enjoys the same stability as the original system.
- A periodic constraint formulation that forces the system to converge to the optimal cyclic steady state is proposed. The stability result applies to this formulation.
- An infinite-horizon formulation with discount factor is proposed to steer the system to the optimal cyclic steady state. This formulation also inherits the stability result.

The publications resulting from this dissertation are [53, 44, 52, 48, 49, 46, 43, 45, 47, 50, 51, 42].

8.2 Recommendations for Future Work

In this dissertation, we have studied practical and theoretical issues from set-point tracking NMPC to economically-oriented NMPC for large scale processes. Applications of economically-oriented NMPC can achieve better economical performance for energy intensive systems. These applications have helped us to identify many issues to improve this work. Some recommendations for future work are as follows.

8.2.1 Stability of Economically-Oriented NMPC

The stability property of economically-oriented NMPC has drawn a lot of attention recently. It is believed to be a key feature for the future advanced controllers, because an economically-oriented objective can directly optimize the performance. In this dissertation, we have started to work on the stability of economically-oriented NMPC for cyclic processes. However, the obtained result is based on the state-feedback NMPC without any disturbance or plant-model mismatch. We believe it is beneficial to extend the current result to more general cases, including:

- **Robust stability with respect to plant-model mismatch and disturbances:** For set-point tracking NMPC, Limon et al. [72] proposed to use ISS as the unifying framework to analyze the robust stability. We believe this ISS framework can be adapted to analyze the robust stability of the economically-oriented NMPC.

- **Robust stability with respect to the disturbances in the period:** In this dissertation, the obtained stability result is based on the assumption that the period of the cyclic steady state is known exactly. In many operations, the length of the period may suffer some fluctuations. For example, the utility pricing scheme is a result of many complicated factors, including demand, supply, location or even politics. It is very likely that the period is subjected to fluctuation. In addition, the operation disturbances in cyclic processes such as PSA and SMB may also cause the designed period to be shifted. As a result, it is very interesting to study the robust stability of control in these scenarios.

8.2.2 Closed-Loop Stability of Output-Feedback NMPC

In this dissertation, we analyzed the robust stability of output-feedback NMPC based on EKF. It is shown that the EKF has a property similar to the separation principle that helps the analysis of the closed-loop stability. We believe the current result can be extended in the following ways:

- **Output-feedback NMPC based on other observers:** It is well-known that EKF has some practical issues. For example, it is difficult to pose inequality constraint in EKF. In addition, it is necessary to calculate sensitivity at each time step which may be time-consuming for large scale problems. Many different observers have been proposed to improve the estimation performance, like MHE, ensemble Kalman filter EnKF [28, 11], particle filtering [5], unscented Kalman filter [56, 55]. However, they can not be analyzed using the framework in [52] to show the robust stability. Hence, it is required to analyze the robust stability of these observers using different means. More importantly, a general separation principle that shows the stability of these observers in the closed-loop is necessary. Finally, the impact of the estimation error on the output-feedback NMPC should be studied.

- **Output-feedback economically-oriented NMPC:** The current stability result is for set-point tracking NMPC. Nevertheless, we believe the analysis should be able to adapt to the economically-oriented NMPC formulation. Moreover it is very interesting to study the robust stability for output-feedback economically-oriented NMPC.

8.2.3 Robust NMPC Formulation

We have studied robust stability property of the output-feedback NMPC formulation in this work. However, it belongs to the category named *a priori* robust stability, which means that the stability result inherits from the closed-loop system. No special design strategy is used to improve the robustness of the controller. On the other hand, *a posteriori* robust NMPC, which resorts to other strategies to guarantee the robust stability in the presence of a large uncertainty, has been investigated by other researchers. At this stage, the approaches appeared in the literature are still premature and mainly for set-point tracking state-feedback formulation. Contributions in this area particularly for the economically-oriented NMPC are still needed.

- **Robust stability for set-point tracking NMPC:** Currently, the most widely-studied *a posteriori* strategies are min-max formulation [66, 77] which solves a min-max optimization problem and tube-based [71, 91, 22, 69] NMPC which calculates the control actions based on different uncertainty regions. In addition, we proposed an *a posteriori* strategy based on multi-scenario formulation [46]. However, all the methods suffer exponentially-growth computational complexity with respect to the uncertainty region. As a result, it is desirable to have other approaches with lighter computational burdens.

- **Extension to economical NMPC and output-feedback NMPC:** It is expected that the *a posteriori* robust strategy can be extended to the output-feedback NMPC. In this case, it is interesting to design a robust state estimator. Then the output-feedback NMPC formulation is robust with the state estimation error. In addition, this method should be adapted to the economically-oriented NMPC as well.

8.2.4 Applications of Economically-Oriented NMPC

In this dissertation, the proposed economically-oriented NMPC with guaranteed nominal stability is implemented on the ASU with cyclic behavior. In this case, the cyclic behavior is created by introducing cyclicly varying electricity price. Moreover, a regularization term is added to the formulation to ensure the stability. It is interesting to apply the proposed method to other applications, particularly systems with cyclic operational nature.

- **Implementing economically-oriented NMPC for PSA and SMB:** The proposed economically-oriented NMPC needs to be tested on these systems with general cyclic operational nature. It may require longer prediction horizon in order to cover the entire cycle. As a result, the proposed economically-oriented NMPC formulation may be incorporated with the upper-level decision-making process.

- **Improve the formulation of economically-oriented NMPC:** Throughout this dissertation, we have argued that the economically-oriented NMPC formulation needs to be regularized in order to have a unique solution and satisfy the assumptions in the stability analysis. However, to some extent, the regularization term sacrifices optimality. It is interesting to quantify the optimality loss and introduce a better regularization term that offsets the loss of optimality, such as a time-varying regularization term. In addition, it will also be beneficial to study how the robust stability property affects optimality.

Bibliography

[1] Adetola, V. and Guay, M. [2010], 'Integration of real-time optimization and model predictive control', *Journal of Process Control* **20**, 125–133.

[2] Agarwal, A., Biegler, L. and Zitney, S. [2010], 'Superstructure-based optimal synthesis of pressure swing adsorption cycles for precombustion co_2 capture', *Ind. Eng. Chem. Res.* **49**, 5066–5079.

[3] Alessandri, A., Baglietto, M. and Battistelli, G. [2008], 'Moving-horizon state estimation for nonlinear discrete-time systems: new stability results and approximation schemes', *Automatica* **44**, 1753–1765.

[4] Angeli, D. and Rawlings, J. [2010], Receding horizon cost optimization and control for nonlinar plants, *in* 'Proceedings of 8th IFAC Symposium on Nonlinear Control Systems (NOLCOS)', Bologna, Italy.

[5] Arulampalam, M., Maskell, S. and Gordon, N. [2002], 'A tutorial on particle filters for online nonlinear/non-gaussian bayesian tracking', *IEEE Tran. Signal Processing* **50**, 174 – 188.

[6] Ascher, U. and Petzold, L. [1998], *Computer Methods for Ordinary Differentional Equations and Differential-Algebraic Equations*, SIAM, Philadelphia, PA.

[7] Aske, E., Strand, S. and Skogestad, S. [2008], 'Coordinator mpc for maxmizing plant throughput', *Computers & Chemical Engineering* **32**, 195–204f.

[8] Bartusiak, R. [2007], Nlmpc: A platform for optimal control of feed- or product-flexible manufacturing, *in* R. Findeisen, F. Allgöwer and L. Biegler, eds, 'Assessment and Future Directions of Nonlinear Model Predictive Control', Springer, pp. 1–16.

[9] Baumrucker, B. and Biegler, L. [2010], 'Mpec strategies for cost optimization of pipeline operations', *Computers and Chemical Engineering* **34**, 900–913.

[10] Bemporad, A., Morari, M., Dua, V. and Pistikopoulos, E. [2002], 'The explicit linear quadratic regulator for constrained systems', *Automatica* **38**, 3–20.

[11] Bengtsson, T., Snyder, C. and Nychka, D. [2003], 'Toward a nonlinear ensemble filter for high-dimensional systems', *J. of Geophysical Research* **108**, 8775–8784.

[12] Betts, J. [2001], *Practical Methods for Optimal Control Using Nonlinear Programming*, SIAM, Philadelphia, PA.

[13] Bian, S., Khowinij, S., Henson, M., Belanger, P. and Megan, L. [2005], 'Compartmental modeling of high purity air separation columns', *Computer & Chemical Engineering* **29**, 2096–2109.

[14] Biegler, L. [2010], *Nonlinear Programming: Concepts, Algorithms, and Applications to Chemical Processes*, SIAM, Philadelphia, PA.

[15] Biegler, L., Cervantes, A. and Wächter, A. [2002], 'Advances in simultaneous strategies for dynamic process optimization', *Chem. Eng. Sci* **57**, 575–593.

[16] Biegler, L., Grossmann, I. and Westerberg, A. [1997], *Systematic Methods of Chemical Process Design*, Prentice-Hall, Upper Saddle River, NJ.

[17] Bitmead, R., Gevers, M. and Wertz, V. [1990], *Adaptive Optimial Control - The Thinking Man's GPC*, Prentice-Hall, Englewood Cliffs, NJ.

[18] Bloss, K. [2000], Dynamic Process Optimization through Adjoint Formulations and Constraint Aggregation, PhD thesis, Lehigh University.

[19] Bock, H., ed. [1983], *Numerical Treatment of Inverse Problems in Differential and Integral Equations: Proceedings of an International Workshop, Heidelberg, Fed. Rep. of G.*

[20] Boutayed, M. and Aubry, D. [1999], 'A strong tracking extended kalman observer for nonlinear discrete-time systems', *IEEE Transactions on Automatic Control* **44**, 1550–1556.

[21] Box, G., Jenkins, G. and Reinsel, G., eds [1994], *Time Series Analysis: Forecasting and Control*, third edn, Prentice-Hall.

[22] Bravo, J., Alamo, T. and Camacho, E. [2006], 'Robust mpc of constrained discrete-time nonlinear systems based on approximated reachable sets', *Automatica* **42**, 1745–1751.

[23] Bryson, A. and Ho, Y. [1975], *Applied Optimal Control*, Hemisphere.

[24] Büskens, C. and Maurer, H. [2001], Sensitivity analysis and real-time control of parametric control problems using nonlinear programming methods, *in* S. K. M. Grötschel and J. Rambau, eds, 'Online Optimization of Large-scale Systems', Springer-Verlag, pp. 57–68.

[25] Chen, H. and Allgöwer, F. [1998], 'A quasi-infinite horizon nonlinear model predictive control scheme with guaranteed stability', *Automatica* **34**, 1205–1217.

[26] Chen, Z., Henson, M., Belanger, P. and Megan, L. [2007], Nonlinear model predictive control of cryogenic air separation columns, *in* 'Proceedings of AIChE Annual Meeting'.

[27] Cutler, C. and Perry, R. [1983], 'Real-time optimization with multivariable control is required to maximize profits', *Comp. Chem. Eng.* **7**, 663–667.

[28] Daum, F. [2005], 'Nonlinear filters: beyond the kalman filter', *IEEE A & E Systems Magazine* **20**, 57–69.

[29] DeHaan, D. and Guay, M. [1996], 'A new real-time perspective on nonlinear model predictive control', *Journal of Process Control* **16**, 615–624.

[30] Diehl, M., Amrit, R. and Rawlings, J. [2010], A lyapunov function for economic optimizing model predictive control. Accepted for Publication, IEEE Trans. on Auto. Cont.

[31] Diehl, M., Bock, H. and Schlöder, J. [2005], 'A real-time iteration scheme for nonlinear optimization in optimal feedback control', *SIAM Journal on Control and Optimization* **43**, 1714–1736.

[32] Diehl, M., Uslu, I., Findeisen, R., Schwarzkopf, S., Allgöwer, F. and et al [2002], 'Real-time optimization for large scale processes: Nonlinear model predictive control of a high purity distillation column', *Journal of Process Control* **12**, 577–585.

[33] Engell, S. [2007], 'Feedback control for optimal process operation', *J. Proc. Cont.* **17**, 203–219.

[34] Fiacco, A., ed. [1983], *Introduction to Sensitivity and Stability Analysis in Nonlinear Programming*, Academic Press, New York.

[35] Findeisen, R. and Allgöwer, F. [2004], Computational delay in nonlinear model predictive control, *in* 'Proc. Int. Symp. Adv. Control of Chemical Processes', HongKong.

[36] Findeisen, R., Imsland, L., Allgöwer, F. and Foss, B. [2003], 'Output feedback stabilization of constrained systems with nonlinear predictive control', *International Journal of Robust and Nonlinear Control* **13**, 211–228.

[37] Garcia, C. and Morshedi, A. [1986], 'Quadratic programming solution of dynamic matrix control (qdmc)', *Chemical Engineering Communication* **46**, 73–87.

[38] Grancharova, A., Johansen, T. and Tøndel, P. [2007], Computational aspects of approximate explicit nonlinear model predictive control, *in* R. Findeisen, F. Allgöwer and L. Biegler, eds, 'Assessment and Future Directions of Nonlinear Model Predictive Control', Springer, pp. 181–192.

[39] Grimm, G., Messina, M. J., Tuna, S. and Teel, A. [2004], 'Examples when nonlinear model predictive control is nonrobust', *Automatica* **40**, 523–533.

[40] Helbig, A., Abel, O. and Marquardt, W. [2007], Structural concepts for optimization based control of transient processes, *in* F. Allgöwer and A. Zheng, eds, 'Nonlinear Model Predictive Control', Birkhäuser Verlag, Basel-Boston-Berlin, pp. 295–312.

[41] Hicks, G. and Ray, W. [1971], 'Approximation methods for optimal control synthesis', *Can. J. Chem. Eng.* **49**, 522–529.

[42] Huang, R. and Biegler, L. [2009], Robust nonlinear model predictive controller design based on multi-scenario formulation, *in* 'Proc. American Control Conference (ACC) 09', St. Louis, MO.

[43] Huang, R. and Biegler, L. [2011], Stability of economically-oriented nmpc with periodic constraint. Invited to submit to IFAC World Congress.

[44] Huang, R., Biegler, L. and Patwardhan, S. [2010], 'Fast offset-free nonlinear model predictive control based on moving horizon estimation', *Ind. Eng. Cheme. Res* **49**, 7882–7890.

[45] Huang, R., Harinath, E. and Biegler, L. [2010], Lyapunov stability of economically-oriented nmpc for cyclic processes. Submitted for publication.

[46] Huang, R., Patwardhan, S. and Biegler, L. [2009*a*], Multi-scenario-based robust nonlinear model predictive control with first principle models, *in* R. Alves, C. Nascimento and E. B. Jr., eds, 'Computer-Aided Chemical Engineering', Elsevier, pp. 1293–1298.

[47] Huang, R., Patwardhan, S. and Biegler, L. [2009*b*], Robust extended kalman filter based nonlinear model predictive control formulation, *in* 'Proc. 48th Conference on Decision and Control (CDC)', Shanghai, China.

[48] Huang, R., Patwardhan, S. and Biegler, L. [2009*c*], Robust nonlinear model predictive control based on extended recursive filters. Submitted for publication.

[49] Huang, R., Patwardhan, S. and Biegler, L. [2009*d*], Robust stability of nonlinear model predictive control with extended kalman filter and target setting. Submitted for publication.

[50] Huang, R., Patwardhan, S. and Biegler, L. [2010*a*], An adaptive quasi-infinite horizon nmpc scheme based on target setting, *in* 'Proc. 9th DYCOPS', Leuven, Belgium.

[51] Huang, R., Patwardhan, S. and Biegler, L. [2010*b*], Offset-free nonlinear model predictive control based on moving horizon estimation for an air separation unit, *in* 'Proc. 9th DYCOPS', Leuven, Belgium.

[52] Huang, R., Patwardhan, S. and Biegler, L. [2010*c*], 'Stability of a class of discrete-time nonlinear recursive observers', *J. of Process Control* **20**, 1150–1160.

[53] Huang, R., Zavala, V. and Biegler, L. [2009], 'Advanced step nonlinear model predictive control for air separation units', *Journal of Process Control* **19**, 678–685.

[54] Ierapetritou, M., Wu, D., Vin, J., Sweeney, P. and Chigirinskiy, M. [2002], 'Cost minimization in an energy-intensive plant using mathematical programming approaches', *Ind. Eng. Chem. Res* **41**, 5262–5277.

[55] Julier, S. and Uhlmann, J. [2004*a*], 'Corrections to unscented filtering and nonlinear estimation', *Proc. IEEE* **92**, 1958.

[56] Julier, S. and Uhlmann, J. [2004*b*], 'Unscented filtering and nonlinear estimation', *Proc. IEEE* **92**, 401–422.

[57] Kadam, J. and Marquardt, W. [2004], Sensitivity-based solution updates in closed-loop dynamic optimization, *in* 'Proc. th DYCOPS', Camridge, MA.

[58] Kadam, J. V. and Marquardt, W. [2007], Nonlinear model predictive cotnrol of the hashimoto simulated moving bed process, *in* R. Findeisen, F. Allgöwer and L. Biegler, eds, 'Assessment and Future Directions of Nonlinear Model Predictive Control', Springer, pp. 419–434.

[59] Kameswaram, S. and Biegler, L. [2008], 'Convergence rates for direct transcription of optimal control problems using collocation at radau points', *Comput. Optim. Appl.* **41**, 81–126.

[60] Kawajiri, Y. and Biegler, L. [2006], 'A nonlinear programming superstructure for optimal dynamic operations of simulated moving bed processes', *Ind. Eng. Chem. Res.* **45**, 8503–8513.

[61] Keerthi, S. and Gilbert, E. [1988], 'Optimal infinite-horizon feedback laws for a general class of constrained discrete-time systems: stability and moving-horizon approximations', *J. of Optimization Theory and Applications* **57**, 265–293.

[62] Kothare, S. and Morari, M. [2000], 'Contractive model predictive control for constrained nonlinear systems', *IEEE Transactions on Automatic Control* **45**, 1053–1071.

[63] Kronseder, T., Stryk, O., Bulirsch, R. and Kröner, A. [2001], Towards nonlinear model-based predictive optimal control of large-scale process models with application to air separation unit, *in* M. Grötschel and S. Krumke, eds, 'Online optimization of large scale systems: State of the art', Verlag - Springer, pp. 385–412.

[64] Krstić, M. and Wang, H. [2000], 'Stability of extrmum seeking feedback for general nonlinear dynamic systems', *Automatica* **36**, 595–601.

[65] L. Magni, G. N. and Scattolini, R. [2004], 'On the stabilization of nonlinear discrete-time systems with output feedback', *International Journal of Robust and Nonlinear Control* **14**, 1379–1391.

[66] L. Magni, G. N., Scattolini, R. and Allgöwer, F. [2003], 'Robust model predictive control of nonlinear discrete-time systems', *International Journal of Robust and Nonlinear Control* **13**, 229–246.

[67] Lee, J., Natarajan, S. and Lee, K. [2001], 'A model-based predictive control approach to repetitive control of continuous processes with periodic operations', *J. of Proc. Cont.* **11**, 195–207.

[68] Lee, J. and Ricker, N. [1994], 'Extended kalman filter based nonlinear model predictive control', *Ind. Eng. Chem. Res* **33**, 1530–1541.

[69] Lee, J. and Yu, Z. [1997], 'Worst-case formulations of model predictive control for systems with bounded parameters', *Automatica* **33**, 763–781.

[70] Li, W. and Biegler, L. [1988], 'Process control strategies for constrained nonlinear systems', *Industrial & Engineering Chemistry Research* **27**, 1421–1433.

[71] Limon, D., Alamo, T. and Camacho, E. [2002], Input-to-state stable mpc for constrained discrete-time nonlinear systems with bounded additiveuncertainties, *in* 'IEEE CDC', Las Vegas, NV, USA, pp. 4619–4624.

[72] Limon, D., Alamo, T., Raimondo, D., la Peña, D., Bravo, J. and Camacho, E. [2009], Input-to-state stability: a unifying framework for robust model predictive control, *in* L. Magni, D. Raimondo and F. Allgöwer, eds, 'Nonlinear Model Predictive Control: Towards New Challenging Applications', Springer, pp. 1–26.

[73] Luyben, W., Tyreus, B. and Luyben, M. [1999], *Plantwide Process Control*, McGraw-Hill, New York.

[74] Magni, L. and Scattolini, R. [2007], Robustness and robut design of mpc for nonlienar descrete-time systems, *in* R. Findeisen, F. Allgöwer and L. Biegler, eds, 'Assessment and Future Directions of Nonlinear Model Predictive Control', Springer, pp. 239–254.

[75] Marlin, T. [1995], *Process Control*, McGraw-Hill, New York.

[76] Marquis, P. and Broustail, J. [1998], Smoc, abridge between state space and model predictive controllers: Application to automation of a hydrotreating unit, *in* T. McAvoy, Y. Arkun and E. Zafiriou, eds, 'IFAC Workshop on Model based Process Control'.

[77] Mayne, D. [2001], 'Control of constrained dynamic systems', *European Journal of Control* **7**, 87–99.

[78] Mayne, D., Rawlings, J., Rao, C. and Scokaert, P. [2000], 'Constrained model predictive control: stability and optimality', *Automatica* **36**, 789–814.

[79] Meadows, E. and Rawlings, J. [1997], Model predictive control, *in* M. Henson and D. Seborg, eds, 'Nonlinear Process Control', Prentice Hall, pp. 233–310.

[80] Messina, M., Tuna, S. and Teel, A. [2005], 'Discrete-time certainty equivalence output feedback: allowing discontinuous control law including those from model predictive control', *Automatica* **41**, 617–628.

[81] Michalska, H. and Mayne, D. [1993], 'Robust receding horizon control of constrained nonlinear systems', *IEEE Transactions on Automatic Control* **38**, 1623–1633.

[82] Morari, M. and Lee, J. [1999], 'Model predictive control: past, present and future', *Computer & Chemical Engineering* **23**, 667–682.

[83] Morari, M., Stephanopoulos, G. and Arkun, Y. [1980], 'Studies in synthesis of control structures for chemcial processes, part 1', *AIChE J.* **26**, 220–232.

[84] Muske, K. and Badgwell, T. [2002], 'Disturbance modeling for offset-free linear model predictive control', *J. of Process Control* **12**, 617–632.

[85] Nocedal, J. and Wright, S., eds [2006], *Numerical Optimization*, second edn, Springer.

[86] Oliveira, N. and Biegler, L. [1995], 'An extensioni of newtow-type algorithms for nonlienar process control', *Automatica* **31**, 281–286.

[87] Pannocchia, G. and Bemporad, A. [2007], 'Combined design of disturbace model and observer for offset-free model predictive control', *IEEE Transactions on Automatic Control* **52**, 1048–1053.

[88] Pannocchia, G. and Kerrigan, E. [2005], 'Offset-free receding horizon control of constrained linear systems', *AIChE Journal* **51**, 3134–3146.

[89] Qin, S. and Badgwell, T. [2003], 'A survey of industrial model predictive control technology', *Control Engineering Practice* **11**, 733–764.

[90] Raghunathan, A., Diaz, M. and Biegler, L. [2004], 'An mpec formulation for dynamic optimization of distillation operations', *Computer & Chemical Engineering* **28**, 2037–2052.

[91] Raković, S., Teel, A., Mayne, D. and Astolfi, A. [2006], Simple robust control invariant tubes for some classes of nonlinear discrete time systems, *in* 'Proceedings of the 45th IEEE Conference on Decision & Control', San Diego, CA, USA, pp. 6397–6402.

[92] Rao, C., Rawlings, J. and Mayne, D. [2003], 'Constrained state estimatin for nonlinear-discrete-time systems: stability and moving horizon approximations', *IEEE Transactions on Automatic Control* **48**, 246–258.

[93] Rawlings, J. and Amrit, R. [2009], Optimizing process economic performance using model predictive control, *in* L. Magni, D. M. Raimondo and F. Allgöwer, eds, 'Assessment and Future Directions of Nonlinear Model Predictive Control', Springer, pp. 119–138.

[94] Rawlings, J., Bonné, D., Jørgensen, J., Venkat, A. and Jørgensen, S. [2008], 'Unreachable setpoint in model predictive control', *IEEE Trans. on Auto. Cont.* **53**, 2209–2215.

[95] Rawlings, J. and Mayne, D., eds [2009], *Model Predictive Control: Theory and Design*, Nob Hill Publishing.

[96] Reid, R., Prausnitz, J. and Poling, B., eds [1987], *The Properties of Gases and Liquids*, New York : McGraw-Hill.

[97] Reif, K. and Unbehauen, R. [1999], 'The extended kalman filter as an exponential observer for nonlinear systems', *IEEE Transactions on Signal Processing* **47**, 2324–2328.

[98] Roffle, B., Betlem, B. and Ruijter, J. [2000], 'First principles dynamic modeling and multivariable control of a cryogenic distillation process', *Computer & Chemical Engineering* **24**, 111–123.

[99] Roset, B., Heemels, W., Lazar, M. and Nijmeijer, H. [2008], 'On robustness of constrained discrete-time systems to state measurement errors', *Automatica* **44**, 1161–1165.

[100] Santos, L., Afonso, P., Castro, J., Oliveira, N. and Biegler, L. [2001], 'On-line implementation of nonlinear mpc: An experimental case study', *Control Engineering Practice* **9**, 847–857.

[101] Scokaert, P., Mayne, D. and Rawlings, J. [1999], 'Suboptimal model predictive control (feasibility implies stability)', *IEEE Trans. Auto. Contr.* **43**, 1136–1142.

[102] Sequeira, E., Graells, M. and Puigjaner, L. [2002], 'Real-time evolution of online optimization of continuous process', *Ind. Eng. Chem. Res.* **41**, 1815–1825.

[103] Srinivasrao, M., Patwardhan, S. and Gudi, R. [2006], 'From data to nonlinear predictive control. 2. improving regulatory performance using identified observers', *Ind. Eng. Chem. Res.* **45**, 3593–3603.

[104] Srinivasrao, M., Patwardhan, S. and Gudi, R. [2007], 'Nonlinear predictive control of irregularly sampled multirate systems using blackbox observers', *Journal of Process Control* **17**, 17–35.

[105] Tosukhowonga, T., Lee, J., Lee, J. and Lu, J. [2004], 'An introduction to a dynamic plant-wide optimization strategy for an integrated plant', *Comp. Chem. Eng.* **29**, 199–208.

[106] Vassiliadis, V., Sargent, R. and Pantelides, C. [1994*a*], 'Solution of a class of multistage dynamic optimization problems. part one - algorithmic framework', *Ind. Eng. Chem. Res.* **33**, 2115–2123.

[107] Vassiliadis, V., Sargent, R. and Pantelides, C. [1994*b*], 'Solution of a class of multistage dynamic optimization problems. part two - problems with path constraints', *Ind. Eng. Chem. Res.* **33**, 2123–2133.

[108] Vinson, D. [2006], 'Air separation control technology', *Computer & Chemical Engineering* **30**, 1436–1446.

[109] Wächter, A. and Biegler, L. [2006], 'On the implementation of a primal-dual interior point filter line search algorithm for large-scale nonlinear programming', *Math. Program* **106**, 25–27.

[110] White, V., Perkins, J. and Espie, D. [1996], 'Switchability analysis', *Computer & Chemical Engineering* **20**, 469–474.

[111] Würth, L., Rawlings, J. B. and Marquardt, W. [2009], Economic dynamic real-time optimization and nonlinear model predictive control on infinite hoirzons, *in* 'International Symposium on Advanced Control of Chemical Process', Istanbul, Turkey.

[112] Yousfi, C. and Tournier, R. [1991], Steady-state optimization inside model predictive control, *in* 'American Control Conference', Boston, MA, pp. 1866–1870.

[113] Zanin, A., Gouvêa, M. and Odloak, D. [2000], 'Integrating real-time optimization into the model predictive controller of the fcc system', *Cont. Eng. Practice* **10**, 819–831.

[114] Zavala, V. [2010], 'Stability analysis of an approximate scheme for moving horizon estimation', *Computers and Chemical Engineering* **34**, 1662–1670.

[115] Zavala, V. and Biegler, L. [2009*a*], 'The advanced step nmpc controller: Optimality, stability and robustness', *Automatica* **45**, 86–93.

[116] Zavala, V., Laird, C. and Biegler, L. [2008], 'A fast moving horizon estimation algorithm based on nonlinear programming sensitivity', *Journal of Process Control* **18**, 876–884.

[117] Zavala, V. M. and Biegler, L. [2009*b*], 'Optimization-based strategies for the operation of low-density polyethylene tubular reactors: Nonlinear model predictive control', *Computers and Chemical Engineering* **33**, 1735–1746.